

https://dspace.org/

# Characterising the Role of Cholesterol in Hypoxia-induced Epithelial- Mesenchymal Transition in Breast Cancer

**Abdulla, Naaziyah**

**2022**

University of the Witwatersrand, Johannesburg

https://hdl.handle.net/10539/43895

Abdulla, Naaziyah . (2022). Characterising the Role of Cholesterol in Hypoxia-induced Epithelial- Mesenchymal Transition in Breast Cancer [Master's dissertation, University of the Witwatersrand, Johannesburg].WireDSpace.

Downloaded from a DSpace repository. https://dspace.org/

UNIVERSITY OF THE
WITWATERSRAND,
JOHANNESBURG

# Characterising the Role of Cholesterol in Hypoxia-induced Epithelial-Mesenchymal Transition in Breast Cancer

by

**Naaziyah Abdulla**

**(1348887)**

**Masters Dissertation**

Submitted in fulfilment of the requirements for the degree

**Master of Science**

in

**Molecular and Cell Biology**

in the Faculty of Science, University of the Witwatersrand, Johannesburg, South Africa

Supervisor: Professor Mandeep Kaur

February 2022

# Table of Contents

**Declaration** ..... v

**Acknowledgements** ..... vi

**Research Outputs** ..... vii

**List of Figures** ..... viii

**List of Tables** ..... ix

**List of Symbols** ..... x

**List of Abbreviations** ..... x

**Abstract** ..... 1

**1. Introduction** ..... 2

1.1. Breast Cancer Epidemiology ..... 2

1.2. Breast Cancer Heterogeneity Influences Disease Prognosis and Response to Therapy ..... 2

1.3. The Epithelial-Mesenchymal Transition (EMT) ..... 6

1.4. Molecular Mechanisms of EMT ..... 8

1.4.1. Transforming Growth Factor-β Signalling Pathway ..... 8

1.4.2. Wnt Signalling Pathway ..... 8

1.4.3. Sonic Hedgehog (Shh) Signalling ..... 8

1.4.4. SNAIL family of transcription factors ..... 9

1.4.5. Basic helix-loop-helix transcription factors ..... 10

1.4.6. Zinc-finger E-box Binding Homeobox (ZEB) Family ..... 10

1.5. Hypoxia Serves a Crucial Role in the Induction of EMT and Metastasis ..... 11

1.6. Regulation of Cholesterol Homeostasis is Critical for Normal Cellular Functioning ..... 15

1.7. Cholesterol Regulates Key Signal Transduction Pathways of EMT Induction & Maintenance ..... 17

1.7.1. Wnt Signalling Pathway ..... 18

1.7.2. Sonic Hedgehog (Shh) Signalling ..... 18

1.7.3. Transforming Growth Factor – β (TGF-β) Signalling ..... 19

**1.8. Cholesterol Modulates the Multi-Drug Resistant Transporter P-glycoprotein Contributing to Drug Resistance** ..... 20

1.9. Introduction to the Current Study ..... 21

1.9.1. Cholesterol Synthesis Inhibitory Drugs ..... 21

1.9.2. Cholesterol Depletory Agents ..... 22

**2. Aim and Objectives** ..... **24**

2.1. Aim: ..... 24

2.2. Objectives ..... 24

**3. Materials and Methods:** ..... **25**

**Workflow** ..... **25**

**Methods:** ..... **26**

3.1. Cell Culture ..... 26

3.2. Hypoxia-induced EMT ..... 26

3.3. Cell Counting ..... 27

3.4. Immunofluorescent Staining ..... 28

3.5. Growth Curve Using Cell Counts as a Measure of Viability ..... 29

3.6. $RT^2$ Profiler PCR Array – Human Cancer Drug Resistance ..... 30

3.6.1. RNA Extraction and Purification ..... 30

3.6.2. gDNA Elimination and cDNA Synthesis ..... 31

3.6.3. Quantitative Reverse Transcription PCR ..... 32

3.6.4. Gene Expression Network Maps: OmicsNet and Cytoscape ..... 33

3.7. Cholesterol and Lipid Staining ..... 34

3.7.1. Filipin Staining ..... 34

3.7.2. Vybrant Alexa Fluor® Lipid Raft Labelling ..... 34

3.7.3. BODIPY Staining ..... 35

3.8. Transwell® Invasion Assay ..... 36

3.9. Drug Transporter Functionality Assay ..... 37

3.10. Statistical Analysis ..... 38

**4. Results:** ..... 39

4.1. Optimizing Hypoxia Induction in MCF-7 cells ..... 39

4.2. Growth Curve Following $CoCl_2$ Treatment in MCF-7 cells ..... 40

4.3. Analysing Changes in MCF-7 Cell Morphology Following $CoCl_2$ Treatment ..... 41

4.4. Confirming HIF-1α Induction in MCF-7 cells following $CoCl_2$ treatment ..... 42

4.5. Confirming EMT Induction following $CoCl_2$ treatment in MCF-7 ..... 43

4.6. Analysing Expression of Ki-67 in MCF-7 cells as a Marker of Cell Proliferation ..... 44

4.7. Documented changes in pathway dynamics following hypoxia-induced EMT in MCF-7 cells ..... 45

4.8. Delineating the link between hypoxia-induced EMT and cholesterol in MCF-7 cells ..... 49

4.8.1. Filipin Staining ..... 49

4.8.2. Vybrant Alexa Fluor® Lipid Raft Labelling.....51

4.8.3. BODIPY Staining .....53

4.8.4. Analyzing the Effect of Targeting Cellular Cholesterol in EMT.....54

4.9. Assessing the invasive potential of MCF-7 cells post-EMT induction following treatment with cholesterol targeting agents.....57

4.10. Analysing the drug resistant potential of MCF-7 cells post-EMT induction following treatment with cholesterol targeting agents.....58

**5. Discussion: .....60**

5.1. $CoCl_2$ mediated induction of HIF-1α – Mechanism of action and resulting implications on the expression of downstream target proteins.....60

5.2. Effect of $CoCl_2$ on cell viability and proliferation .....62

5.3. Alterations to Cellular Morphology and Resulting Implications following Hypoxia-Induced. EMT .....64

5.4. Molecular Mechanisms facilitating Hypoxia-induced EMT.....65

5.5. Hypoxia-induced EMT potentiates drug resistance in MCF-7 cells.....67

5.6. Hypoxia-induced EMT increases cellular cholesterol content potentiating an aggressive disease phenotype .....73

5.7. Hypoxia mediated MDR potential is efficiently combatted by targeting cholesterol.....77

**6. Conclusions and Future Perspectives.....78**

**7. Successes and Limitations of the Study.....81**

**8. Supplementary Data .....82**

**.....82**

**9. Turnitin Summary Plagiarism Report.....83**

**10. References.....84**

# Declaration

I, Naaziyah Abdulla (1348887), am a student registered for the degree of Master of Science (MSc.) in the academic year 2021.

I hereby declare the following:

❖ I am aware that plagiarism (the use of someone else's work without their permission and/or without acknowledging the original source) is wrong.

❖ I confirm that the work submitted for assessment for the above degree is my own unaided work except where explicitly indicated otherwise.

❖ I have not submitted this work before for any other degree or examination at this or any other University.

❖ I have followed the required conventions in referencing the thoughts and ideas of others.

❖ I understand that the University of the Witwatersrand may take disciplinary action against me if there is a belief that this is not my own unaided work or that I have failed to acknowledge the source of the ideas or words in my writing.

Signed  day of 21st February 2022

## Acknowledgements

This research would not have been possible without the support and assistance of the following people and institutions:

I would like to thank my supervisor Professor Mandeep Kaur for all the guidance, encouragement, assistance and time invested in this project.

Many thanks to all the colleagues in GH527 for the continuous support and insight to the project.

The University of the Witwatersrand (Postgraduate Merit Award) and the National Research Foundation (NRF) for financial assistance during my study period.

Finally, I would like to thank my parents, family and close friends who have supported and encouraged me for the duration of this research project.

# Research Outputs

*i. Publication:*

**Mechanistic Insights Delineating the Role of Cholesterol in Epithelial Mesenchymal Transition and Drug Resistance in Cancer**

**Abdulla, N.,** Vincent, C.T and Kaur, M. (2021) Mechanistic Insights Delineating the Role of Cholesterol in Epithelial Mesenchymal Transition and Drug Resistance in Cancer, *Frontiers in Cell and Developmental Biology***,** 19;9:728325, doi:10.3389/fcell.2021.728325

*ii. Conference:*

**Characterising the Role of Cholesterol in Hypoxia-induced Epithelial-Mesenchymal Transition in Breast Cancer**

**Abdulla, N.** and Kaur, M., presented at: "NZBCS-2021: The Virtual New Zealand Breast Cancer Symposium" – Oral Presentation, 19th November, 2021.

**List of Figures**

Figure 1.1: Metastatic Progression is Dependent on the EMT Process ..... 6
Figure 1.2: Summary of EMT induced changes in cellular physiology ..... 11
Figure 1.3: Molecular Mechanisms Governing HIF-1α Regulation and Cellular Function ..... 14
Figure 1.4: Molecular Mechanisms of Cholesterol Homeostasis ..... 17
Figure 3: Summary Workflow ..... 25
Figure 4.1: Optimising $CoCl_2$ mediated Hypoxia Induction in MCF-7 cells ..... 40
Figure 4.2: Effect of $CoCl_2$ treatment on the growth of MCF-7 cells ..... 41
Figure 4.3: Effect of $CoCl_2$ treatment on MCF-7 cell morphology ..... 41
Figure 4.4: Effect of $CoCl_2$ on the expression of HIF-1α target gene VEGF ..... 43
Figure 4.5: Effect of $CoCl_2$ on Molecular Markers of EMT ..... 44
Figure 4.6: Effect of $CoCl_2$ on Ki-67 expression ..... 45
Figure 4.7: Network map of genes involved in cancer drug resistance pathways following hypoxia-induced EMT ..... 48
Figure 4.8: Quantifying free cholesterol levels following cholesterol depletion in MCF-7 cells pre- and post-EMT induction ..... 50
Figure 4.9: Quantifying membrane cholesterol levels following cholesterol depletion in MCF-7 cells pre- and post-EMT induction ..... 52
Figure 4.10: Quantifying cholesteryl ester levels in lipid droplets following cholesterol depletion in MCF-7 cells pre- and post-EMT induction ..... 54
Figure 4.11: Quantifying E-cadherin expression in MCF-7 cells following treatment with cholesterol targeting agents ..... 55
Figure 4.12: Quantifying vimentin expression in MCF-7 cells following treatment with cholesterol targeting agents ..... 56
Figure 4.13: Assessing the invasive potential of MCF-7 cells following treatment with cholesterol targeting agents ..... 57
Figure 4.14: Evaluating the effect of targeting cholesterol on the functionality of the MDR1 transporter ..... 58
Figure S1.1: Effect of $CoCl_2$ on the expression of cholesterol efflux protein ABCA1 ..... 82

**List of Tables**

Table 3.1: Genomic DNA Elimination Mix ..... 31
Table 3.2: Reverse Transcription Mix ..... 31
Table 3.3: PCR Components Mix ..... 32
Table 3.4: Cycling conditions ..... 33

## List of Symbols

| | |
|---|---|
| α | alpha |
| β | beta |
| *xg* | Centrifugal Force |
| °C | Degrees Celsius |
| g | Grams |
| µ | Micro |
| mg | Milligram |
| ml | Millilitre |
| µm | Micrometre |
| µM | Micromolar |
| µl | Microlitre |
| nm | Nanometre |
| % | Percentage |
| ® | Registered |
| ™ | Trademark |

## List of Abbreviations

| | |
|---|---|
| ABCA1 | ATP-binding cassette subfamily A member 1 |
| ABCB1 | ATP-binding cassette, sub-family B (MDR/TAP), member 1 |
| ABCC3 | ATP-binding cassette, sub-family C (MDR/TAP), member 3 |
| ABCC5 | ATP-binding cassette, sub-family C (MDR/TAP), member 5 |
| ABCG1 | ATP-binding cassette subfamily C member 1 |
| ACAT | Acyl-CoA Cholesterol Acyltransferase |
| ANOVA | Analysis of Variance |
| AP1S1 | Adaptor-related protein complex 1, sigma 1 subunit |
| APC | Adenomatous Polyposis Coli |
| AR | Androgen Receptor |
| AXIN | Axis Inhibition Protein |
| BAX | BCL2-associated X protein |
| BC | Breast Cancer |

| | |
|---|---|
| BCL2 | B-cell CLL/lymphoma 2 |
| BCL2L1 | BCL2 Like 1 |
| bHLH | Basic helix-loop-helix |
| BLMH | Bleomycin Hydrolase |
| BODIPY | 4,4-difluoro-1,3,5,7,8-pentamethyl-4-bora-3a,4a-diaza-s-indacene |
| BRCA1 | Breast cancer 1, early onset |
| Calcein AM | Calcein Acetoxymethyl Ester |
| CBP | Creb binding protein |
| CCND1 | Cyclin D1 |
| CDK2 | Cyclin-dependent kinase 2 |
| CDKN1B | Cyclin Dependent Kinase Inhibitor 1B |
| CDKN2D | Cyclin Dependent Kinase Inhibitor 2D |
| cDNA | Complementary DNA |
| CDs | Cyclodextrins |
| CEs | Cholesteryl Esters |
| CETP | Cholesteryl Ester Transfer Protein |
| CLPTM1L | CLPTM1-like |
| $CoCl_2$ | Cobalt Chloride |
| CRD | Cysteine-rich Domain |
| CSC | Cancer Stem Cell |
| CT-B | Cholera Toxin Subunit B |
| CYP1A1 | Cytochrome p450 Family 1 Subfamily A Member 1 |
| CYP2B6 | Cytochrome p450 Family 2 Subfamily B Member 6 |
| CYP450 | Cytochrome p450 |
| DHFR | Dihydrofolate Reductase |
| DMEM | Dulbecco's Modified Eagle's Medium |
| Dvl | Dishevelled |
| ECM | Extracellular Matrix |
| EDTA | Ethylenediaminetetraacetic Acid |
| EMT | Epithelial-Mesenchymal Transition |
| EPHX1 | Epoxide hydrolase 1, microsomal (xenobiotic) |
| ER | Estrogen Receptor |
| ERAD | ER associated Protein Degradation |
| ERBB2 | V-erb-b2 erythroblastic leukemia viral oncogene homolog 2, neuro/glioblastoma derived oncogene homolog (avian) |
| ERBB3 | V-erb-b2 erythroblastic leukemia viral oncogene homolog 3 (avian) |

| | |
|---|---|
| EREs | Estrogen Response Elements |
| ESR1 | Estrogen receptor 1 |
| FBS | Foetal Bovine Serum |
| FGF2 | Fibroblast Growth Factor 2 (basic) |
| FIH | Factor Inhibiting Hypoxia |
| FOS | FBJ murine osteosarcoma viral oncogene homolog |
| Fz | Frizzled |
| gDNA | Genomic DNA |
| GSK3 | Glycogen Synthase Kinase-3 |
| GSK3A | Glycogen Synthase Kinase 3 Alpha |
| GSK3β | Glycogen Synthase Kinase 3-Beta |
| HDLs | High-density Lipoproteins |
| Hh | Hedgehog |
| HIF | Hypoxia-inducible Factor |
| HIF1A | Hypoxia Inducible Factor 1-Alpha |
| HMG-CoA | 3-hydroxy-3-methylglutaryl-coenzyme A |
| HMGCR | 3-hydroxy-3-methylglutaryl-coenzyme A reductase |
| HREs | Hypoxia-responsive Elements |
| IGF1R | Insulin-like growth factor 1 receptor |
| IL | Interleukin |
| LCAT | Lecithin-cholesterol Acyltransferase |
| LDL | Low-density Lipoprotein |
| LDLR | Low Density Lipoprotein Receptor |
| LEF | Lymphoid-enhancer Factor |
| lncRNAs | Long non-coding RNA |
| LRP | Low-density Lipoprotein receptor-related Protein |
| LXR | Liver-X-Receptor |
| MDR1 | Multidrug Resistance Protein 1 |
| MET | MET Proto-Oncogene, Receptor Tyrosine Kinase |
| mins | minutes |
| miRNAs | micro RNAs |
| MMP | Matrix Metalloproteinase |
| MMPs | Matrix Metalloproteinases |
| MSH2 | MutS homolog 2, colon cancer, nonpolyposis type 1 (E. coli) |
| MYC | V-myc myelocytomatosis viral oncogene homolog (avian) |
| MβCD | Methyl-beta-Cyclodextrin |

| | |
|---|---|
| ncRNAs | non-coding RNA |
| ODD | Oxygen Dependent Degradation |
| PAS | PER/ARNT/SIM |
| PBS | Phosphate Buffered Saline |
| PCR | Polymerase Chain Reaction |
| PCSK-9 | Proprotein Convertase Subtilisin/Kexin type-9 |
| P-gp | Permeability-glycoprotein |
| PHD | Prolyl Hydroxylases |
| PPARG | Peroxisome Proliferator Activated Receptor Gamma |
| PR | Progesterone Receptor |
| PTCH1 | Patched 1 |
| RARA | Retinoic Acid Receptor, Alpha |
| RB1 | RB Transcriptional Corepressor 1 |
| RELB | RELB Proto-Oncogene, NF-KB Subunit |
| ROS | Reactive Oxygen Species |
| RT | Reverse Transcriptase |
| RT-qPCR | Reverse-Transcriptase Quantitative Polymerase Chain Reaction |
| RXR | Retinoid-X-Receptor |
| RXRB | Retinoid X Receptor Beta |
| SERDs | Selective Estrogen Receptor Downregulators |
| SERMs | Selective Estrogen Receptor Modulators |
| Shh | Sonic Hedgehog |
| Smo | Smoothened |
| SOD1 | Superoxide dismutase 1, soluble |
| SR-B1 | Scavenger Receptor B1 |
| SREBP2 | Sterol Regulatory Element Binding Protein-2 |
| SSD | Sterol-sensing Domain |
| TAM | Tamoxifen |
| TCA | Tricarboxylic Acid |
| TCF | T-cell factor |
| TF | Transcription Factor |
| TGF-β | Transforming Growth Factor β |
| TNBC | Triple Negative Breast Cancer |
| TNF-α | Tumour-necrosis Factor α |
| TOP1 | DNA Topoisomerase I |
| TP53 | Tumour Protein P53 |

| | |
|---|---|
| TβR-I | TGF-β type I receptor |
| TβR-II | TGF-β type II receptor |
| UGCG | UDP-glucose ceramide glucosyltransferase |
| VEGF | Vascular Endothelial Growth Facor |
| Wnt | Wingless-related integration site |

**Abstract**

The cellular epithelial-mesenchymal transition (EMT) process is a complex labyrinth dependent on subversion of critical cellular signalling pathways, which crosstalk extensively to confer cancer cells with characteristics that mediate metastasis. Based on the pleotropic role of cholesterol in the cell, it is not surprising that cancer cells have evolved several mechanisms to facilitate cholesterol dyshomeostasis. In addition to meeting the increased metabolic demands of cancer cells, deregulated cholesterol metabolism also facilitates increased cellular cholesterol availability which is crucial to regulating the activity of protein intermediates in EMT-related signalling pathways. Despite evidence indicating that cholesterol directly regulates signalling pathways related to EMT, no publication to date has attempted to address the effect of EMT induction on cellular cholesterol levels in cancer. To shed light on the dynamics of cholesterol in the relationship between hypoxia and EMT, cholesterol content in MCF-7 cells pre- and post-hypoxia induced EMT was assessed. This dissertation presents findings indicating increased levels of free cholesterol, cholesteryl esters as well as lipid raft cholesterol in MCF-7 cells following hypoxia-induced EMT. Interestingly, MCF-7 cells post-EMT induction displayed increased sensitivity to treatment with cholesterol targeting agents and presented with reversion to an epithelial state as evidenced by the increased expression of epithelial markers, decreased expression of mesenchymal markers and also reduced invasive potential. Importantly, treatment with cholesterol targeting agents is also seen to abrogate the drug resistant potential following hypoxia-induced EMT. Based on these observations, it is proposed that targeting cellular cholesterol could be a promising area to invest in the search for novel therapeutics effective in combatting cancer metastasis.

# 1. Introduction

## 1.1. Breast Cancer Epidemiology

The majority of global deaths can be attributed to non-communicable diseases, predicting that cancer will constitute the primary cause of mortality in the 21st century (Bray et al., 2018). In 2020, an estimated 10 million deaths were accredited to cancer with a predicted 70% of these deaths being documented in low- and middle-income countries (World Health Organisation). Data provided by the International Agency for Research on Cancer predict a 78% increase in cancer cases in South Africa by the year 2030 (GLOBOCAN). In terms of breast cancer (BC), this cancer has been classified as the most frequently diagnosed cancer in females in 159 out of the 185 countries analysed, where in 2020, more than two million cases of BC were documented in females with 684 996 BC deaths reported worldwide (Sung et al., 2021). This consequently highlights the importance of improving current therapies or developing novel therapeutic strategies to facilitate eradication of this disease.

## 1.2. Breast Cancer Heterogeneity Influences Disease Prognosis and Response to Therapy

Principally BC is defined as an abnormal growth of cells attributed to uncontrolled cell division which develops in various glands, ducts, and tissues in the breast (American Cancer Society, 2017). Carcinomas, classified as BCs arising from the epithelium constitute the most significant number of BC cases (Feng et al., 2018).

Interestingly, the heterogeneous nature of BC is evidenced by the identification of numerous biological subtypes each known to manifest distinct clinical behaviour and response to treatment (Feng et al., 2018). Importantly, the advent of gene expression profiling techniques has facilitated classification based on the presence or absence of intrinsic genes that encode cellular receptors which include the estrogen receptor (ER), progesterone receptor (PR) as well as overexpression of the human epidermal growth factor receptor 2 (Feng et al., 2018). It is worth noting, despite all the subtypes that do exist, approximately 75% of all BC cases are dependent on the ER (Spring et al., 2016). The importance of this steroid hormone receptor in promoting pathogenesis stems from its function as a transcription factor (TF) upon appropriate ligand binding. Once estrogen binds to receptors in the nucleus, conformational changes that occur, mediate receptor dimerization and subsequent translocation to specific estrogen response elements (EREs) that are located at the promoter region of target genes (Fuentes and Silveyra, 2019). Alternatively, ERs are able to modulate gene expression without direct

interaction with DNA, which is achieved by protein-protein interaction with other transcription factors (TFs) and response elements in the cell nucleus (Fuentes and Silveyra, 2019). This consequently activates oncogenic signalling pathways in BC cells (Waks and Winer, 2019). Interestingly, increasing experimental evidence have identified a role for ERα as well as its co-regulators in the regulation of genes involved in each step of the metastatic cascade (Nair and Sachdeva, 2018).

The estrogen dependent nature of BC was identified more than 100 years ago classifying endocrine-based therapies as one of the earliest forms of targeted therapy (AlFakeeh and Brezden-Masley, 2018). This form of therapy has subsequently evolved to become the most effective and least toxic systemic therapy for ER-positive BC. This is attained by employing one of two strategies. The first strategy includes impeding the production of estrogen (the ligand required for ER functioning) thereby reducing ligand availability and abrogating receptor function (Spring et al., 2016). This can be achieved by employing aromatase inhibitors which restrain the functioning of the aromatase enzyme (responsible for the conversion of androgens to estrogens). Luteinizing hormone agonists can also be utilised to lower the production of estrogen by the ovaries (Spring et al., 2016).

An alternative means of endocrine therapy is facilitated by targeting the ER directly (Spring et al., 2016). In this instance the receptor itself can be targeted by employing selective estrogen receptor modulators (SERMs). In BC, SERMs function predominantly as estrogen antagonists and compete with estrogen to bind to the ER, consequently modulating the co-factors with which the ER interacts with, thereby modulating ER activity (Patel and Bihani, 2018). Moreover, a distinct class of anti-estrogens termed the selective estrogen receptor downregulators (SERDs) achieve their function by binding to and destabilising the ER, leading to ER degradation, consequently abrogating receptor dimerization and repressing ER signalling (Patel and Bihani, 2018). Interestingly, despite the extensive studies conducted in endocrine based therapy, the nonsteroidal anti-estrogen tamoxifen (TAM) since its inception in the early 1970's currently remains the "gold standard treatment" for $ER^+$ BCs (Krauss and Stickeler, 2020).

The efficacy of TAM is dictated by its metabolism to the active metabolites, endoxifen and 4-hydroxytamoxifen, facilitated by the group of cytochrome p450 (*CYP450)* enzymes (Cronin-Fenton et al., 2014). While both 4-hydroxytamoxifen and estrogen bind in a similar fashion to

the ER, the sidechain of 4-hydroxytamoxifen projects out of the ligand binding domain pocket, inducing repositioning of helix-12, consequently resulting in the adoption of an antagonistic conformation (Patel and Bihani, 2018, Traboulsi et al., 2017). This further results in the recruitment of transcriptional co-repressors, impeding ER transcriptional activity at EREs (Patel and Bihani, 2018).

Studies conducted have identified that administration of TAM in the adjuvant setting proved effective in decreasing both BC relapse and mortality by 39% and 31% respectively (De Marchi et al., 2016). Unfortunately, treatment with TAM also leads to severe side effects which include but is by no means restricted to, early onset of menopause, atrophic vaginitis, uterine endometrial cancer and non-alcoholic fatty liver disease (An, 2016, Gu et al., 2017). Additionally, only 50% of the patient population manifest a complete or partial response to therapy which concurrently halts tumour progression, where the remaining patient population either maintain intrinsic resistance or acquire resistance to TAM treatment (AlFakeeh and Brezden-Masley, 2018). Attempts at deciphering the molecular mechanisms governing TAM resistance is thus pivotal to improve clinical therapeutic outcome.

Additionally, BC may also be treated by administering conventional chemo or radiotherapy. In terms of radiotherapy, the administration of high energy radiation damages genetic material and in some instances also affects the integrity of DNA by introducing double stranded breaks (Baskar et al., 2014). With regards to chemotherapy, a combination of cytotoxic agents is administered employing numerous mechanisms which serve to interfere with the process of DNA replication. In both instances the replicative potential of cells is impeded, and cell death is subsequently induced (Pan et al., 2016).

It is important to note that possibility of recurrence of a secondary tumour years after chemo/radio/endocrine- therapy does exist, and the incidence of relapse is often dictated by several criteria namely the primary organ site, tumour grade and stage, in addition to the lifestyle choices adopted by the individual post-treatment (Riggio et al., 2021). The secondary tumour could occur at either the same location or even at a distant site. In this light, the dissemination of cancer cells is achieved by activating various cell signalling pathways in a process termed metastasis (Riggio et al., 2021). Importantly, two different models of metastatic dissemination have been proposed namely the linear model and the parallel model. The linear model is based on the premise that cancer progresses in a stepwise manner, consequently

positing that only advanced neoplasms possess sufficient molecular aberrations to mediate metastasis (Riggio et al., 2021). Conversely the parallel model proposes that metastatic dissemination is a preliminary event occurring in tumorigenesis, where primary tumour cells can potentiate deadly metastases in parallel with each other as well as the primary tumour (Riggio et al., 2021). Interestingly, emerging scientific evidence proposes that the parallel model of cancer cell dissemination occurs more frequently than expected (Riggio et al., 2021). Importantly, the invasion and metastasis facilitated by malignant cancer cells accounts for 90% of BC patient deaths (Riggio et al., 2021).

In general, the metastatic cascade is facilitated by cancer cells in the primary tumour that has attained invasive capabilities (Eslami-S et al., 2020). This step necessitates breaching of the basement membrane together with extracellular matrix (ECM) remodelling. Subsequently, through the process of intravasation, tumour cells gain access to the lumina of blood and lymphatic vessels. Following this, tumour cells must attempt to survive within circulation by avoiding anoikis, immune system evasion as well as resisting haemodynamic sheer forces (Riggio et al., 2021). Upon appropriate signalling, tumour cells extravasate from vasculature and colonise a new tissue thereby forming a micrometastases (Figure 1.1) (Eslami-S et al., 2020). Successful colonisation is dependent on both cell-intrinsic and extrinsic factors namely cellular plasticity, chromosomal instability, and self-renewal potential as well as the tumour microenvironment (Riggio et al., 2021). Interestingly experimental evidence highlights a cellular reprogramming process termed the epithelial-mesenchymal transition (EMT) as playing a pivotal role in successful establishment of the invasion and metastasis cascade implicating EMT in most if not all steps of metastatic dissemination (Lambert et al., 2017). (Figure 1.1)

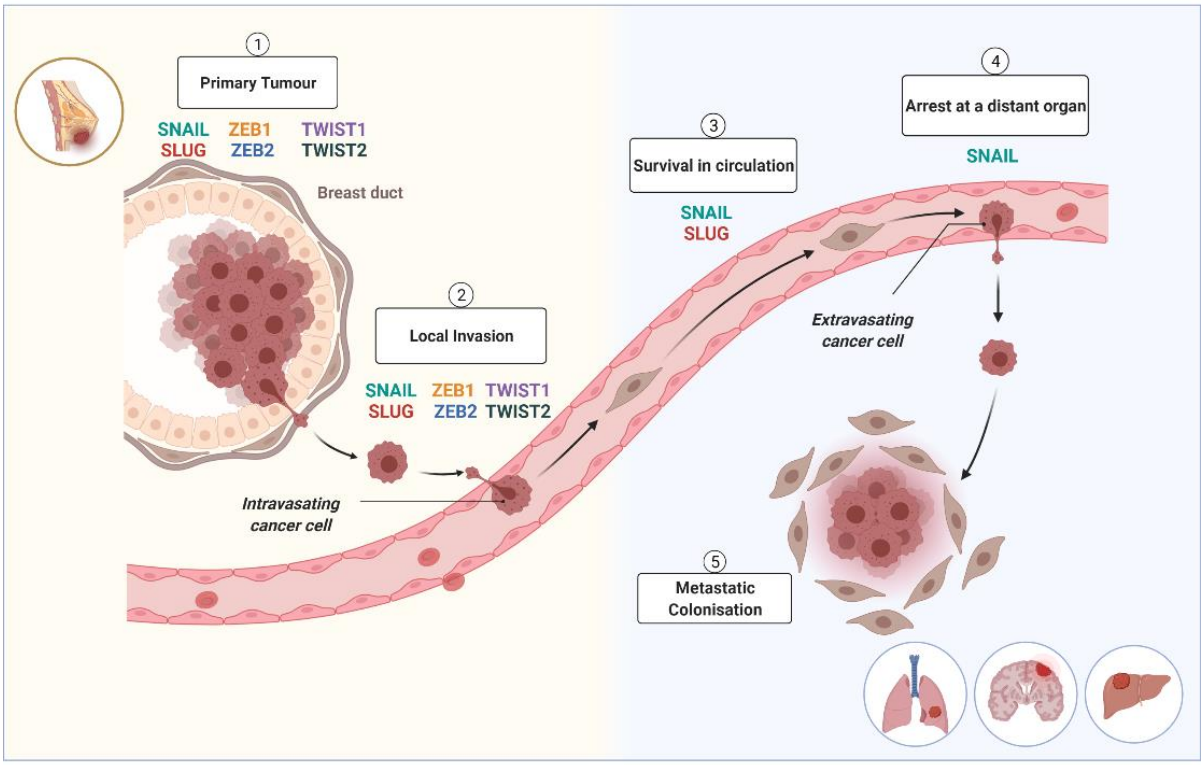



**Figure 1.1: Metastatic Progression is Dependent on the EMT Process**

*Each step in the metastatic cascade is regulated by the master transcription factors governing EMT (discussed in further detail below). In the initial stage of tumorigenesis EMT impedes oncogene-induced senescence and apoptosis facilitating development of the primary tumour. Subsequent processes such as local invasion and survival in circulation are all dependent on EMT. Following this, suppression of EMT and activation of MET (mesenchymal-epithelial transition) in the final step is crucial to facilitate colonisation. (Image created using Biorender.com)*

## 1.3. The Epithelial-Mesenchymal Transition (EMT)

EMT is classified as a cell plasticity program. Initially documented to play a role in the context of embryonic development, additional scientific evidence currently exists implicating EMT in various pathological processes including wound healing, fibrosis, inflammation and cancer (Yeung and Yang, 2017). Previously the EMT program was thought to operate as a binary switch describing a shift between two alternative states, epithelial or mesenchymal (Nieto et al., 2016, Zhang and Weinberg, 2018). In tissues, epithelial cells are often arranged as either a single layer or exist as multi-layered sheets (Serrano-Gomez et al., 2016). These cells are characterised by the presence of specialised contacts called cell junctions that facilitate cell-cell interaction (cadherin based adherens junctions, tight junctions and desmosomes) as well as cell-matrix interactions (hemidesmosomes) that maintain structural integrity and apical-basal polarity (Serrano-Gomez et al., 2016). In terms of cytoskeletal composition, Type I

intermediate filaments such as cytokeratins are expressed and adherens junctions serve to indirectly connect cortical actin filaments of two adjacent cells (Alberts et al., 2002, Shibue and Weinberg, 2017). On the contrary, mesenchymal cells are characterised by minimal cell junctions and detached stromal arrangements promoting front-rear polarity (Cho et al., 2019, Shibue and Weinberg, 2017). In terms of cytoskeletal composition, vimentin is predominantly expressed to enhance cytoskeletal strength contributing to cell flexibility, and actin fibres arrange to form stress fibres (Dongre and Weinberg, 2019, Shibue and Weinberg, 2017). Additionally, the formation of actin-rich membrane projections facilitates cellular movement as well as sensory reception (Singh et al., 2018). Characteristic surface markers utilised to identify epithelial cells include E-cadherin, cytokeratins, occludins as well as claudins while mesenchymal cells are identified based on the presence of N-cadherin, fibronectin and vimentin (Georgakopoulos-Soares et al., 2020). Following activation of the EMT program, master EMT TFs (SNAIL, SLUG, TWIST and ZEB) facilitate the loss of several of the epithelial characteristics, promote cytoskeletal remodelling and initiate a concomitant gain of mesenchymal traits. This transition consequently facilitates a change in cell morphology from squamous, cuboidal, columnar to a fibroblast/spindle-like morphology conferring upon cancer cells migratory and invasive potential (Serrano-Gomez et al., 2016, Shibue and Weinberg, 2017).

Notably, experimental evidence highlights a significant degree of plasticity where instead of transitioning between full epithelial to full mesenchymal, cells traverse through a spectrum of intermediate states along the epithelial-mesenchymal axis expressing varying levels of epithelial and mesenchymal markers (Nieto et al., 2016). Interestingly, completion of the EMT program resulting in cells adopting an extreme mesenchymal phenotype has been documented as an infrequent event in both neoplastic and non-neoplastic human tissue (Derynck and Weinberg, 2019). Predominantly, the stable existence of cells in this hybrid state has been linked with increased metastatic potential as opposed to when cells adopt a complete epithelial/mesenchymal state since the hybrid EMT state facilitates collective cell migration and reinforces ECM attachment (Saitoh, 2018). Furthermore, the plasticity associated with the hybrid phenotype is seen to facilitate the acquisition of stemness as well as drug resistance and correlates with poor survival in several cancer types (Liao and Yang, 2020, Pastushenko and Blanpain, 2019). Even though studies have elucidated a link between EMT and the acquisition of a cancer stem cell (CSC) state, future studies should seek to delineate the precise molecular mechanisms governing this process (Dongre and Weinberg, 2019). Additionally, studies

should also seek to identify whether existence in different hybrid states confer differential response to chemotherapeutic agents, in an attempt to elucidate mechanisms governing drug resistance (Thankamony et al., 2020).

## 1.4. Molecular Mechanisms of EMT

Under conditions of cellular stress such as hypoxia, nutrient deficiency, inflammation, or oxidative stresses activation of intracellular signalling events coincide to facilitate induction of the EMT program. The most well-established pathways include the transforming growth factor-β (TGF-β), Wingless-related integration site (Wnt) and Sonic Hedgehog (Shh) pathways which are further elaborated on below (Kuşoğlu and Biray Avcı, 2019).

### *1.4.1. Transforming Growth Factor-β Signalling Pathway*

Transmembrane signalling by TGF-β is initiated upon ligand binding to membrane bound serine/threonine kinase receptor, termed TGF-β type II receptor (TβR-II) (Heldin and Moustakas, 2016). This leads to recruitment of membrane bound TGF-β type I receptor (TβR-I) resulting in the formation of a heterotetrameric complex (Heldin et al., 2012). The main mechanism of intracellular TGF-β signalling is mediated through the Smad family of TFs which serve to activate or repress TGFβ responsive genes (Derynck and Budi, 2019).

### *1.4.2. Wnt Signalling Pathway*

Canonical Wnt signalling is initiated following the binding of a Wnt ligand to Frizzled receptor which consequently mediates the release of β-catenin from the glycogen synthase kinase 3-β (GSK3β), axis inhibition protein (AXIN), adenomatous polyposis coli (APC) protein destruction complex (Duchartre et al., 2016). This allows for increased stability of β-catenin where it enters the nucleus and subsequently binds to the TFs T-cell factor (TCF) and lymphoid-enhancer factor (LEF). Recruitment of transcriptional co-activators Creb binding protein (CBP) or p300 leads to the formation of an active complex that promotes expression of Wnt target genes (Duchartre et al., 2016, Sebio et al., 2014).

### *1.4.3. Sonic Hedgehog (Shh) Signalling*

Activation of canonical hedgehog (Hh) signalling occurs through binding of the Hh ligand, Shh to the transmembrane receptor patched which leads to de-repression and subsequent release of the bound transmembrane protein Smoothened (Smo) (Wu et al., 2017). Release of Smo allows

for the activation and nuclear localisation of the downstream transcription factor GLI's which promotes transcription of target genes (Zhang et al., 2016).

In terms of EMT, the afore-mentioned intracellular pathways together with many others converge to facilitate transcriptional activation of the master EMT TFs (Dongre and Weinberg, 2019). This consists of the zinc-finger E-box-binding homeobox factors ZEB1/2 and SNAIL 1/2 as well as the basic helix-loop-helix (bHLH) factors TWIST 1/2 which are the most comprehensively studied (Nieto et al., 2016). These pathways further induce post-translational modifications on the master TFs thereby regulating their activity (Lamouille et al., 2014). Additionally, an emerging role of these signalling pathways in regulating micro RNAs (miRNAs) and long non-coding RNAs (lnRNAs) that promote EMT has been documented (Dongre and Weinberg, 2019). It can thus be stated, the presence of signalling cooperation between these pathways is crucial to mediate cellular changes characteristic of EMT. Interestingly, scientific evidence exists indicating that the master EMT-TFs function co-operatively to modulate the expression of target genes as well as each other (Dongre and Weinberg, 2019, Shibue and Weinberg, 2017). In this way, the reciprocal interactions induce comprehensive EMT associated changes even in the event that only one of the TFs are activated (Shibue and Weinberg, 2017). The role of each of the master TFs in facilitating EMT induction will be briefly elucidated and is illustrated in Figure 1.2.

### *1.4.4. SNAIL family of transcription factors*

The SNAIL subfamily of zinc-finger TFs is represented by three members in vertebrates namely Snail (Snail 1), Slug (Snail 2) and Smuc (Snail 3). Seeing that Snail and Slug are implicated in the induction of EMT they will further be elaborated on below.

Earlier studies conducted document that transcriptional repression of E-cadherin was achieved through direct binding of Snail and Slug to E-box regions in the proximal promoter region (Batlle et al., 2000, Hajra et al., 2002), while emerging scientific evidences continue to illustrate the recruitment of epigenetic regulators that affect both DNA and chromatin accessibility and consequently E-cadherin expression (Peinado et al., 2004, Dong et al., 2012, Herranz et al., 2008, Hou et al., 2008, Tong et al., 2012, Lin et al., 2010, Wu et al., 2012). Additionally, Snail and Slug are also implicated in repressing the expression of occludins and claudins which are present in tight junctions, crucial to maintaining cell polarity (Ikenouchi et al., 2003, Martínez-Estrada et al., 2006, Wang et al., 2007). Interestingly, in addition to

functioning as a transcriptional repressor, scientific evidence exists implicating Snail and Slug in transcriptional activation and consequently contributing to EMT. In particular, Snail and Slug are shown to upregulate key mesenchymal markers, namely vimentin and fibronectin (Cano et al., 2000, Jethwa et al., 2008). While mechanisms governing the repressive activity of Snail and Slug has been comprehensively investigated, the activator function is not well elucidated. It is hence crucial that additional studies are conducted to delineate the conditions under which these transcription factors act as transcriptional activators or transcriptional repressors and the resulting implications this has on the induction of EMT.

### *1.4.5. Basic helix-loop-helix transcription factors*

While several members of this family have been identified, Twist1 has been documented to play a pivotal role in EMT and will be further elaborated on below. In addition to the above-mentioned domains, Twist 1 is also identified to possess a WR (tryptophan and arginine) motif, termed the TWIST box which has been implicated in facilitating Twist1 protein folding and also functioning as either an activation or repressive domain (Castanon and Baylies, 2002, Franco et al., 2010). Like Snail, Twist has also been documented to repress expression of epithelial related proteins and promote the expression of mesenchymal related proteins, by directly binding to E-cadherin promoter regions, recruiting epigenetic regulators that influence DNA and chromatin accessibility as well as modulating expression of non-coding RNAs (ncRNA's) that play a role in EMT-induction (Yang et al., 2004, Fu et al., 2011, Yang et al., 2012, Meng et al., 2018).

### *1.4.6. Zinc-finger E-box Binding Homeobox (ZEB) Family*

The ZEB family of TFs in humans comprises both ZEB1 and ZEB2. They are classified as zinc finger/homeodomain TFs (Georgakopoulos-Soares et al., 2020, Abba et al., 2016). These TFs possess characteristic protein-binding domains which facilitate the recruitment protein-binding domains facilitate the recruitment of co-repressors as well as co-activators leading to gene repression or gene activation, respectively (Zhang et al., 2015a). Based on this dual function, they can induce EMT by employing both repression of epithelial proteins and activation of mesenchymal proteins (Bindels et al., 2006).

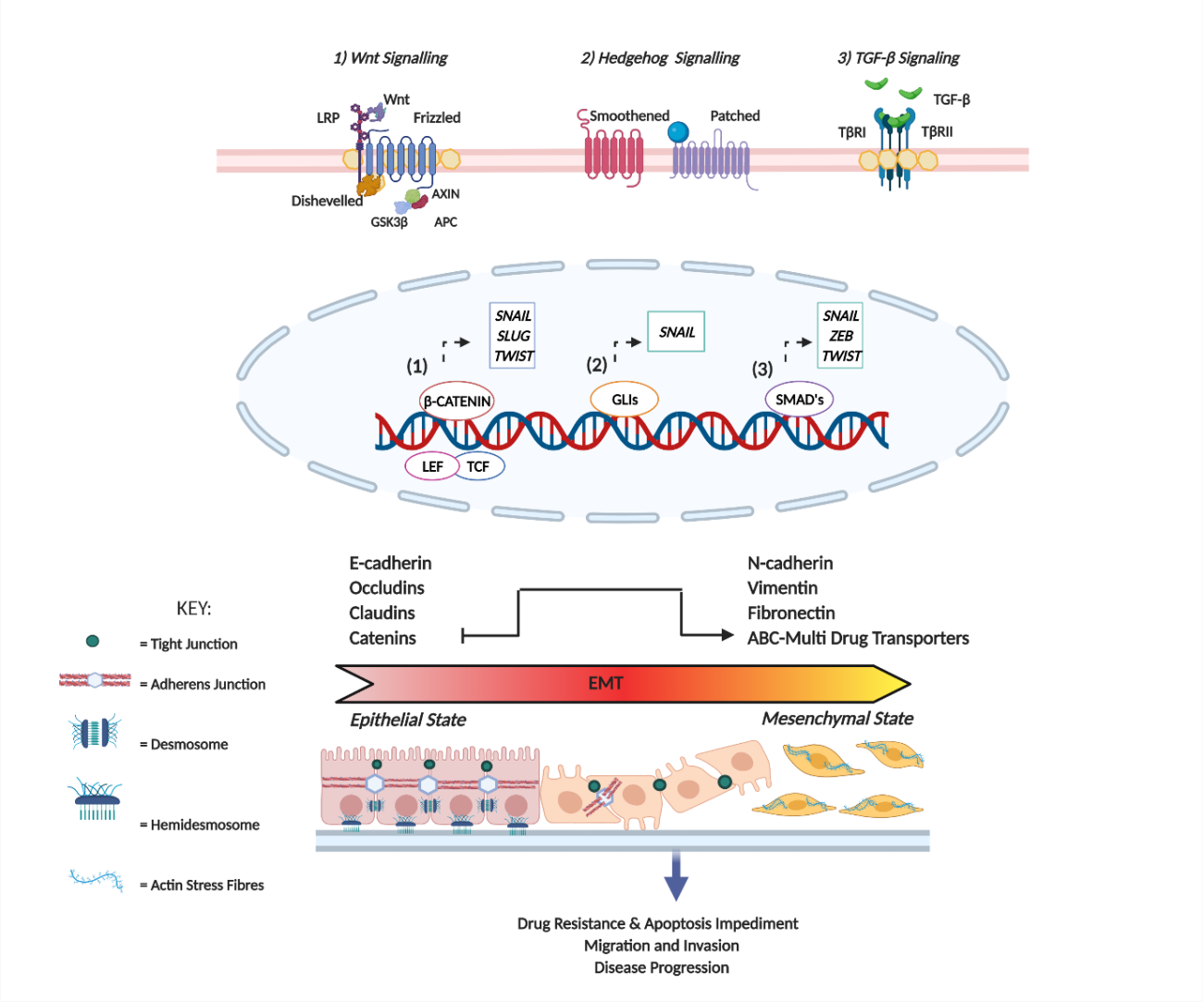



**Figure 1.2: Summary of EMT induced changes in cellular physiology**

*The induction of EMT is characterised by significant alterations to cellular physiology including altered cell-cell junctions, differences in the proteins constituting the cytoskeleton, altered cell-ECM interactions as well as cell polarity. (Image Source: Abdulla et al., 2021)*

## 1.5. Hypoxia Serves a Crucial Role in the Induction of EMT and Metastasis

As a tumour progresses, efficient vascularisation is crucial. Consequently, cancer cells have evolved to synthesise blood vessels from pre-existing vessels through a process termed angiogenesis (Nurwidya et al., 2012). Under physiological conditions oxygen level in a tissue is maintained between 4.6% - 9.4% (Saxena and Jolly, 2019). Importantly, activation of angiogenesis in cancer leads to the formation of vasculature often displaying abnormal characteristics such as distended capillaries, leaky walls and irregular blood flow (Nurwidya et al., 2012). Additionally, as the cancer progresses, the rate of cell proliferation exceeds the rate

of neoangiogenesis consequently leading to a mismatch between the supply of oxygen and its consumption by the tumour (Challapalli et al., 2017). This in turn results in decreased oxygen levels (≤ 2%) leading to a condition termed hypoxia (Chee et al., 2019).

Hypoxia has been implicated in altering the behaviour of cancer cells by manipulating various oxygen-sensitive pathways. The most comprehensively studied, is that mediated by the hypoxia-inducible factor (HIF) family of TFs (Nurwidya *et al*., 2012). These HIFs occur as heterodimers containing an oxygen sensitive subunit (α) and a constitutively expressed β subunit. Both subunits possess a bHLH as well as PER/ARNT/SIM (PAS) domain that is required for DNA binding and dimerization. The oxygen dependent degradation domain (ODD) of HIF-1α mediates oxygen dependent degradation (Butturini et al., 2019). Under normoxic conditions, prolyl hydroxylase enzymes, hydroxylate HIF-1α on conserved Pro residues within the ODD facilitating von-Hippel-Lindau mediated ubiquitination and subsequent proteasomal degradation (Choudhry and Harris, 2018). Additionally, Asn-hydroxylation mediated by factor-inhibiting HIF-1α impedes interaction with the co-activators p300/CBP co-activator (Muñoz-Sánchez and Chánez-Cárdenas, 2019). Both mechanisms are documented to abrogate HIF transcriptional activation under normoxic conditions. Under conditions of hypoxia, the hydroxylases lose their activity, leading to HIF-1α stabilisation. HIF-1α subsequently translocates to the nucleus and binds to HIF-1β as well as the p300/CBP co-activator forming a complex (Chee et al., 2019). The activated complex binds to multiple hypoxia-responsive elements (HREs) in the promoter regions to activate transcription of target genes (Jing et al., 2019).

Interestingly scientific evidence now links the induction of hypoxia with the activation of EMT program subsequently giving rise to cells with cancer stem cell properties (Shibue and Weinberg, 2017). In particular, HIF-1α is implicated in contributing to EMT based on its ability to increase the expression of EMT drivers namely SNAIL, ZEB1 and TWIST (master TFs). Additionally, various signalling pathways are activated by hypoxia which are critical to EMT induction including the Notch, Wnt/ β-catenin, Sonic Hedgehog as well as the TGF-β pathways (Tirpe et al., 2019). Furthermore, hypoxic conditions increase the production of EMT-induced inflammatory cytokines such as tumour-necrosis factor α (TNF-α), interleukin (IL)-6 as well as IL-1β (Bao et al., 2012). Interestingly, hypoxia also contributes to the acquisition of the EMT phenotype by regulating DNA methylation, histone modification as well as the expression of ncRNAs required for EMT induction (Choudhry and Harris, 2018).

With regards to the role hypoxia plays in metastasis, several studies provide further evidence implicating hypoxia in mediating principal steps in the metastatic cascade (Figure 1.3). Apart from inducing EMT consequently conferring on these cells an invasive phenotype, exposure to hypoxic conditions can also directly facilitate cancer cell invasion. Scientific findings describe a potential role of HIF-1α in the regulation of gelatinase activity of matrix metalloproteinase (MMP)-9 and also in the transcriptional regulation of MMP-15 by binding to HRE at the promoter region (Gupta et al., 2014). Additional proteases that are regulated by hypoxia to mediate matrix remodelling include cathepsins, lysyl oxidases as well as prolyl-hydroxylase 4 (Rankin et al., 2016). HIFs are further implicated in mediating intravasation and extravasation by disrupting the interaction between adjacent endothelial cells lining vasculature through the secretion of angiopoietin-like 4 and further promote the interaction of tumour cells with endothelial cells through the production of L1 cell adhesion molecule (Rankin et al., 2016). Hypoxia is also documented to mediate immune evasion by repressing the cytolytic ability of T- and natural killer cells as well as the phagocytic function of macrophages (Krzywinska and Stockmann, 2018). Interestingly, the release of chemokines and cytokines by hypoxic cancer cells further influence the polarisation and promote the recruitment of immune-suppressive cell types such as the alternatively activated M2 macrophages and the T-regulatory cells (Krzywinska and Stockmann, 2018).

In terms of the role hypoxia plays in drug resistance, studies conducted indicate a binding site for HIF-1α in the promoter region of multidrug resistance protein 1 (MDR1) leading to increased expression of this principal drug efflux pump, whereas in other instances hypoxic conditions is seen to enhance the activity of MDR1 (Chen et al., 2014). Interestingly, sustained activation of pro-survival pathways namely the PI3K/Akt pathway is shown to mediate hypoxia induced drug resistance (Jiao and Nan, 2012) (Figure 1.3). Hypoxic conditions also protect cells from drug-induced senescence and is shown to impede apoptotic induction by increasing the expression of anti-apoptotic proteins while reducing the expression of pro-apoptotic proteins (Kim et al., 2018a, Jing et al., 2019). Additionally, seeing that chemotherapeutic agents are reliant on the presence of cellular oxygen to mediate cellular cytotoxicity, hypoxic conditions is seen to reduce the efficacy of chemotherapeutic administration (Qiu et al., 2017a). Interestingly, emerging evidence is pointing to a role for hypoxia in promoting the enrichment of dormant cancer cells with stem cell properties that are resistant to therapy (Qiu et al., 2017a) (Figure 1.3).

Based on the above findings it is evident that hypoxia mediated induction of EMT facilitates a more aggressive cancer phenotype. It is thus imperative that novel therapeutics targeting HIF-1 and related signalling pathways are developed to combat cancer progression.

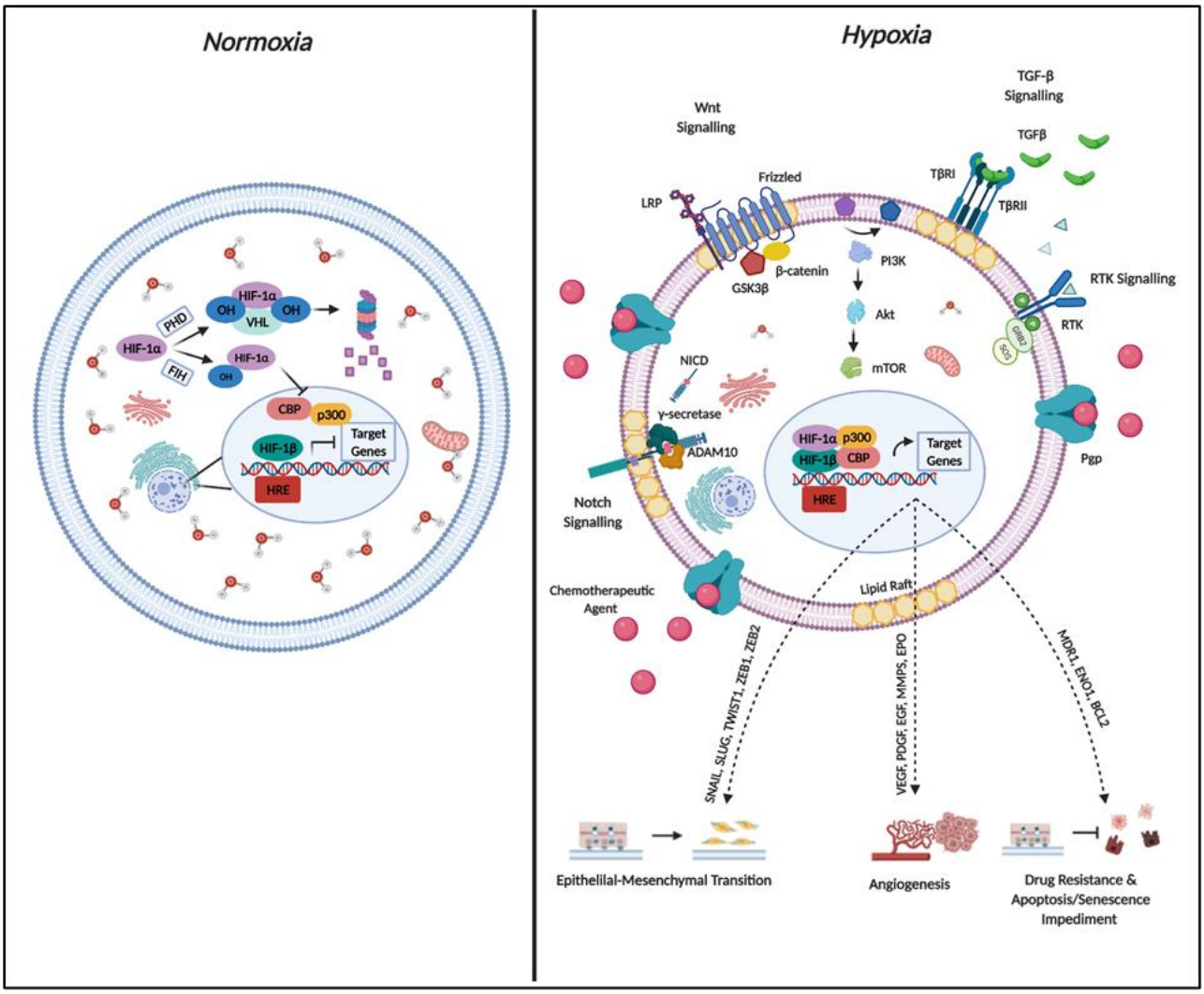



**Figure 1.3: Molecular Mechanisms Governing HIF-1α Regulation and Cellular Function**

*Hypoxic conditions induce HIF-1α mediated signalling which facilitates the induction of signalling pathways characteristic of EMT namely the Wnt pathway, Notch pathway, RTK signalling as well as the TGF-β pathway. Activation of the stem-cell related pathways in turn facilitate transcription of the master TFs required for EMT induction, angiogenesis as well as drug resistance consequently contributing to cancer aggressiveness (Image Source: Abdulla et al., 2021).*

## 1.6. Regulation of Cholesterol Homeostasis is Critical for Normal Cellular Functioning

Cholesterol is a crucial lipid known to maintain cellular homeostasis by regulating the survival and growth of cells (Kuzu et al., 2016). It also serves as the key sterol component in the plasma membrane constituting approximately 30% of the lipid bilayer (Zhang et al., 2019). Structural integrity and fluidity of the cell membrane is thus consequently dictated by membrane cholesterol content. As a result, cholesterol is implicated in modulating the homeodynamics of a vast majority of cell surface related proteins (Zhang et al., 2019). Additionally, cholesterol serves as a crucial component in the formation of microdomains termed lipid rafts which house several proteins (Murai, 2015). It is the protein presence within these domains that will ultimately dictate functional capabilities including signalling, proliferation, differentiation, adhesion and apoptosis (Zalba and ten Hagen, 2017).

The synthesis of cholesterol is carried it out in a highly conserved process that is regulated by 21 enzymatic reactions (Silvente-Poirot and Poirot, 2014). In the mitochondria the tricarboxylic acid (TCA) cycle generates a metabolite termed citrate. Cholesterol synthesis is initiated when citrate is converted to acetyl-coenzyme A (Murai, 2015). Subsequently, through the mevalonate pathway acetyl-coenzyme A is converted to lanosterol in a series of enzymatic reactions that takes place in the endoplasmic reticulum (Murai, 2015). 3-hydroxy-3-methylglutaryl-coenzyme A (HMG-CoA) reductase (HMGCR) is the pivotal enzyme in this process as it catalyses the conversion of HMG-CoA to mevalonate in a rate-limiting step (Murai, 2015). Cholesterol is subsequently formed when the lanosterol is converted to cholesterol either by the Bloch pathway or the Kandutsch-Russell pathway (Murai, 2015).

Based on the pivotal role of cholesterol in cells, complex cholesterol homeostatic mechanisms have evolved to facilitate efficient regulation. Under healthy homeostatic conditions, cholesterol level in the cell is modulated by an appropriate balance between cholesterol synthesis, dietary intake and the removal of excess cholesterol from peripheral tissue (Luu et al., 2013a). These processes are facilitated by the presence of several important signalling molecules and enzymes that function at various stages of cholesterol metabolism and are summarised in Figure 1.4.

Intracellular regulation of cholesterol levels is principally mediated by TFs. With regards to cholesterol biosynthesis and uptake, a pivotal group of TFs termed the sterol regulatory element binding proteins (SREBPs) have been implicated in regulation (Nelson et al., 2014b). SREBP2

serves as a sensor for cholesterol in which excess free cholesterol facilitates the maintenance of an inactive state (Nelson et al., 2014b). On the contrary a decrease in the intracellular cholesterol levels induces proteolytic processing of SREBP2 thereby facilitating binding of the nuclear isoform of SREBP (nSREBP2) to sterol response elements to facilitate expression of lipogenesis target genes namely HMGCR, low density lipoprotein receptor (LDLR) and proprotein convertase subtilisin/kexin type-9 (PCSK-9) (Luu et al., 2013b, Nelson et al., 2014a). HMGCR catalyses the rate limiting step in cholesterol biosynthesis, whereas the LDLR imports cholesterol from the cellular milieu through endocytosis and hydrolysis of low-density lipoprotein (LDL) particles (Luu et al., 2013b). Collectively, this will lead to increased sterol levels within the cell. PCSK-9 regulates LDLR by either degrading LDLR by recruiting it to lysosome, or by prohibiting the endocytic recycling of LDLR by binding to the epidermal like growth factor repeat of LDLR (Poirier et al., 2009). To prevent the excess accumulation of cholesterol in the cell, acyl-CoA cholesterol acyltransferase (ACAT) converts free cholesterol to cholesteryl esters (CEs) which are subsequently transported by cholesteryl ester transfer protein (CETP) from the site of synthesis to sites of storage in lipid droplets (Izem and Morton, 2007). Excess cellular cholesterol and cholesterol-derived oxysterols promotes the Liver-X-Receptor (LXR)-Retinoid-X-Receptor (RXR) mediated transcription of the two principal transporters ATP-binding cassette subfamily A member 1 (ABCA1) and subfamily C member 1 (ABCG1) (Nelson et al., 2014a). ABCA1 will subsequently transfer the excess cholesterol to apolipoproteins to form discoidal HDL (Luu et al., 2013b). Mature spherical high-density lipoproteins (HDLs) are formed by an esterification process facilitated by lecithin-cholesterol acyltransferase (LCAT) in which a fatty-acyl group is transferred to the 3-β hydroxyl moiety of cholesterol thereby converting it to a CE (Luu et al., 2013b). Thereafter scavenger receptor B1 (SR-B1) is responsible for transporting the HDL particles containing CEs to the liver in a direct pathway. In the indirect reverse cholesterol transport pathway, CETP facilitates the transfer of cholesterol from HDL to LDL particles through the formation of a ternary complex (Zhang et al., 2017a). LDL particles can then be endocytosed by LDLR on the liver (Zhang et al., 2017a). Following this, cholesterol has two fates; it can either be excreted or transformed into bile acids to allow for elimination or reabsorption (Luu et al., 2013b).

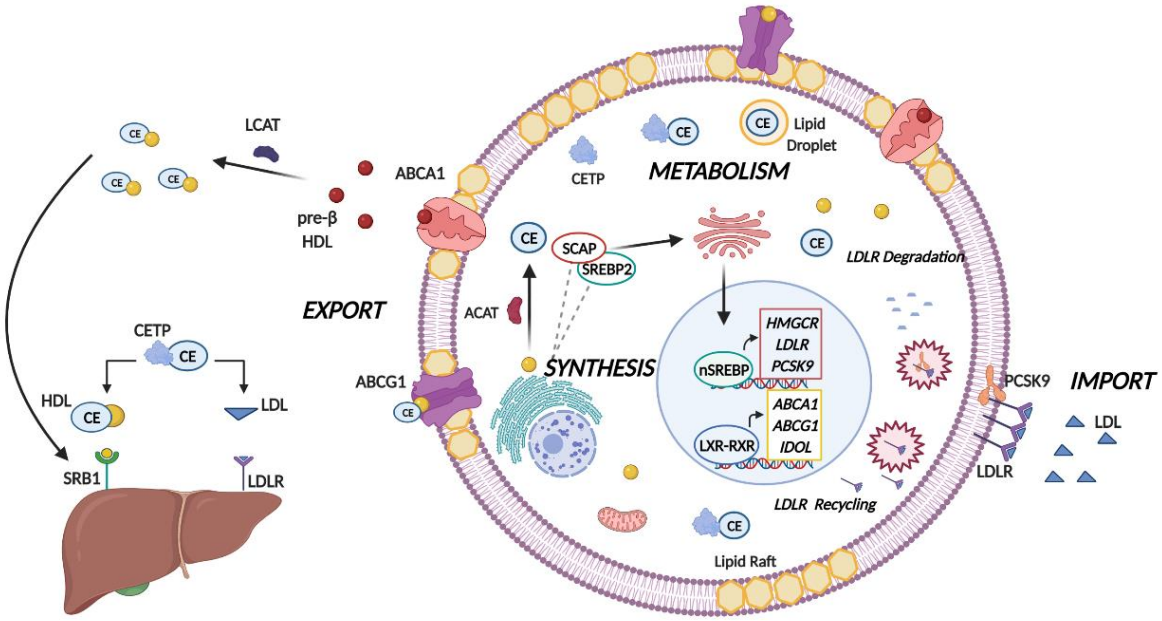



**Figure 1.4: Molecular Mechanisms of Cholesterol Homeostasis**

*Cholesterol homeostasis is maintained by balancing the levels of cholesterol uptake, synthesis and efflux. Extracellular free cholesterol is delivered via LDL particles to LDLR and enters the cell through receptor-mediated endocytosis. The free cholesterol dissociates from the receptor and the receptor is recycled to the cell membrane. Alternatively, binding of PCSK-9 to LDLR induces degradation of LDLR. Once in the cell, free cholesterol is converted to CEs by the enzyme ACAT and is transported by CETP to sites of storage in lipid droplets. In addition to uptake, cellular cholesterol availability is also mediated by SREBP which regulates intracellular cholesterol synthesis. Conversely, excess cellular cholesterol promotes the LXR-RXR mediated transcription of principal cholesterol efflux transporters ABCA1 and ABCG1 leading to elimination of cholesterol carried in HDL particles. Mature HDL particles bind to SR-B1 on the liver resulting in elimination. Alternatively, CETP mediates transfer of cholesterol from HDL to LDL particles and subsequent uptake by LDLR on the liver. (Image Source: Abdulla et al., 2021)*

## 1.7. Cholesterol Regulates Key Signal Transduction Pathways of EMT Induction & Maintenance

The cellular EMT process is a complex labyrinth dependent on subversion of critical cellular signalling pathways, which crosstalk extensively to mediate the initiation and regulation of the EMT program (Fuxe et al., 2010). Based on the pleotropic role of cholesterol in the cell, it is not surprising that cancer cells have evolved several mechanisms to facilitate cholesterol dyshomeostasis (Mandal and Rahman, 2014). In addition to meeting the increased metabolic demands of cancer cells, deregulated cholesterol metabolism also facilitates increased cellular cholesterol availability which is crucial to regulating the activity of protein intermediates in EMT-related signalling pathways (Li et al., 2020). Furthermore, an increase in cholesterol

content corresponds to an increase in lipid raft presence. Since lipid rafts contain several cell signalling proteins, alteration to lipid raft domains may therefore influence cell signalling pathways that ultimately augment neoplastic transformation (Zalba and ten Hagen, 2017). These rafts in turn regulate crucial processes that cancer cells subvert such as proliferation, migration, invasion, and apoptosis (Zalba and ten Hagen, 2017). Intra- or extracellular stimuli mediate alterations in lipid raft size and protein composition facilitating receptor-ligand and protein-protein interactions leading to downstream activation of signal transduction cascades crucial for cancer cell signalling (Mollinedo and Gajate, 2015). The role of cholesterol in regulating some of the most well studied EMT-related signalling pathways will be further delineated below.

### *1.7.1. Wnt Signalling Pathway*

In canonical Wnt signalling, binding of Wnt ligands to Frizzled (Fz) receptors in conjunction with low-density lipoprotein receptor-related protein (LRP) facilitates recruitment of Dishevelled (Dvl) protein to the plasma membrane (Zhong and Virshup, 2020). This recruitment is facilitated by cholesterol (Sheng et al., 2014), which in turn supports activation of canonical/β-catenin dependent Wnt signalling (Sezgin et al., 2017). Additionally, Wnt binding to the receptor complex occurs exclusively in the plasma membrane ordered compartments termed lipid rafts (Sezgin et al., 2017). Consequently, administering enzymes/drugs that disrupt key constituents in ordered plasma membrane significantly decreased Wnt/β-catenin signalling when cholesterol was disrupted following the administration of cholesterol oxidase (Sezgin et al., 2017). Lipid rafts play a pivotal role in maintaining the integrity of LRP6 and β-catenin in triple negative breast cancer (TNBC) (Badana et al., 2018). This suggests that lipid raft integrity is crucial to dictating the functionality of the Wnt/β catenin signalling which plays a key role in facilitating TNBC aggressiveness (Badana et al., 2018).

### *1.7.2. Sonic Hedgehog (Shh) Signalling*

Shh signalling is essential for embryonic development but has also been documented to play a pivotal role in tumorigenesis and CSC maintenance (Wu et al., 2017). Hedgehog (Hh) signal transduction can be linked with cholesterol through the post-translational modification on the Hh ligands where covalent modification is initiated at the c-terminal end of the ligand through cholesterolysis (Blassberg and Jacob, 2017, Callahan and Wang, 2015). The translocation of cholesterolysis-defective Hh precursors is impeded from the ER to the Golgi. As they are

sequestered in the ER, ER associated protein degradation (ERAD) mediated polyubiquitination and proteasomal degradation is induced which abrogates translocation of the protein out of the ER and hence Hh signalling (Hampton, 2002). In addition to this, the Hh receptor patched 1 (PTCH1) is also documented to possess a sterol-sensing domain (SSD) which is typically present in proteins regulating cholesterol synthesis and transport (Luchetti et al., 2016). A study conducted by Bidet *et al*. proposes that the SSD of PTCH1 allows for cholesterol efflux from the cell when a Shh ligand is absent, this consequently results in a decrease in the intracellular concentration of cholesterol and impedes the activity of the membrane transducer Smo (Bidet et al., 2011). Conversely, binding of a ligand to PTCH1 facilitates the uptake of PTCH1 and impedes the efflux of cholesterol. The increased intracellular concentration of cholesterol mediates increased abundance of Smo at the membrane (Bidet et al., 2011). Importantly, cholesterol is also seen to directly regulate the activity of Smo by binding to its extracellular cysteine-rich domain (CRD). Mutations found in the CRD impedes cholesterol mediated Smo activation and consequently Shh mediated signalling hence indicating the important role of cholesterol in endogenous Hh signalling (Luchetti et al., 2016).

### *1.7.3. Transforming Growth Factor – β (TGF-β) Signalling*

The formation of TβRI/TβRII/TGβ-1 complex is dependent on lipid raft integrity and disruption of lipid rafts impede canonical TGF-β signalling (Zuo and Chen, 2009). Importantly, the localization of TGF-β receptors in lipid rafts is crucial to mediating TGF-β induced activation of MAPK signalling and promoting EMT and cell migration. Contrary to the afore-mentioned studies, a study conducted by Zhao *et al*. suggests that down-regulation of cholesterol may be a consequence of EMT (Zhao et al., 2019). It was recently identified that TGF-β promotes the enrichment of ZEB1 and CtBP at the promoter region of SREBF2 leading to repression of SREBF2 and its downstream target genes. Interestingly the reduction in membrane-bound cholesterol was implicated in enhancing the stability of TGFβRI (Zhao et al., 2019). Additionally, studies conducted by Shapira *et al*. elucidated that cholesterol depletion facilitates a PKR-dependent phosphorylation of eIF2α which enhances the translation of c-Jun (Shapira et al., 2018). An increase in JNK-mediated c-Jun phosphorylation is also reported which enhances the activation of c-Jun and consequently increases the transcription of Smad 2/3. This ultimately allows for enhanced TGF-β mediated signalling (Shapira et al., 2018). These studies elucidate the complex role that cholesterol plays in regulating the expression and activity of TGF-β signalling module. This consequently necessitates additional investigations

into the role of cholesterol in the regulation of TGF-β signalling in a cancer setting to identify whether targeting cellular cholesterol is a feasible means to halt cancer progression.

### 1.8. Cholesterol Modulates the Multi-Drug Resistant Transporter P-glycoprotein Contributing to Drug Resistance

Deregulated cholesterol metabolism is seen to directly contribute to drug resistance by conferring cells with chemoresistant traits. This is achieved either by the influence of cholesterol on cell signaling pathways that contribute to resistance or alternatively through the direct effects on the expression and activity of the ATP binding cassette (ABC) multi-drug transporters. These transporter proteins have a well-established role in facilitating multidrug resistance in cancer cells. They confer cells with a multidrug-resistant (MDR) phenotype by regulating the transport of a broad range of structurally and mechanistically distinct chemotherapeutics across the cell membrane (Assaraf et al., 2019).

*ABCB1* encodes for the multi-drug resistance protein 1 (MDR1) conventionally referred to as permeability glycoprotein (P-gp) and is the most comprehensively studied of all MDR transporters. Studies indicate that cells may either present with inherent resistance to chemotherapeutics through overexpression of ABCB1 or following chemotherapeutic exposure may increase the expression of ABCB1 and in this way acquire resistance (Wang et al., 2019).

Importantly, several studies conducted document the multifaceted role cholesterol plays in modulating the expression as well as the activity of MDR transporters including MDR1. This is elucidated by the observation that cholesterol serves as a transcriptional regulator of MDR efflux transporters where a positive correlation between LXRα/β protein expression and MDR1 expression has been documented. (Kim et al., 2018b). In terms of MDR transporter activity, plasma membrane cholesterol content alters membrane fluidity thereby regulating their activity (Kopecka et al., 2020). Interestingly, the lipid environment surrounding these transporters modulate their conformation, maintaining transporters in a low-energy stable conformation (Kopecka et al., 2020). In terms of cholesterol, this molecule surrounds MDR1 adopting an asymmetrical distribution together with phospholipids (Alam et al., 2019). The outer leaflet is characterised by an ordered ring of cholesterol whereas the inner leaflet presents with both phospholipids and cholesterol. Importantly, the lipid-transporter interactions mediate structural modifications of MDR1 consequently regulating its catalytic activity (Alam et al., 2019). Additionally, studies conducted document that MDR1 substrates accumulate in cholesterol-

rich regions of the membrane thereby enhancing the activity of the pump (Subramanian et al., 2016). Interestingly, evidence exists highlighting the role of cholesterol in altering MDR1 substrate $K_M$ values thereby implying that cholesterol directly interacts with substrate binding sites (Hegedüs et al., 2015). This is illustrated mechanistically, by studies conducted by Clouser *et al.* proposing that plasma membrane cholesterol modulates MDR1- transmembrane helix-membrane interactions, which consequently promotes long-range conformational changes in the nucleotide-binding domain of MDR1 promoting a drastic increase in the rate of ATP hydrolysis (Clouser et al., 2021). This consequently justifies the crucial role cholesterol plays in supporting the activity of MDR1 housed within lipid rafts.

## 1.9. Introduction to the Current Study

Despite evidence indicating that cholesterol directly regulates signalling pathways related to EMT, no publication to date has attempted to address the effect of EMT induction on cellular cholesterol levels in cancer. To shed light on the dynamics of cholesterol in the relationship between hypoxia and EMT, cholesterol content in MCF-7 cells pre- and post-hypoxia induced EMT was assessed. Based on the critical role of cholesterol in cellular signalling pathways concerned with EMT induction and maintenance, this study proposed that cellular cholesterol levels may be directly affected following hypoxia induced EMT to facilitate the acquisition of traits that promote tumour aggressiveness and drug resistance. To explore this concept *in-vitro* two approaches were employed to target cellular cholesterol. This included impeding cholesterol synthesis by treating with a statin. Additionally, excess membrane cholesterol and intracellular cholesterol was depleted through the administration of cholesterol depleting agents namely methyl-beta-cyclodextrin (MβCD) or KS-01 (a novel patented cholesterol depletor), respectively.

### *1.9.1. Cholesterol Synthesis Inhibitory Drugs*

Inhibiting cholesterol synthesis has predominantly been achieved by employing the most widely used lipid lowering agents on the market, i.e. statins (Kuo et al., 2020). These drugs serve as competitive inhibitors of HMGCR, by directly blocking the enzyme's active site and impeding the conversion of HMG-CoA to mevalonate which serves as the proximal and rate-limiting step of cholesterol biosynthesis (Ahmadi et al., 2020). Since the early 1990s the anti-neoplastic properties of statins have been gaining increasing interest but the extent to which statin administration proves effective in cancer treatment remains a point of contention (Matusewicz et al., 2020). Results of several studies indicate that statins possess anti-neoplastic

properties, however contrary to this, scientific evidence also exists potentiating increased risk of cancer following statin therapy (Ahmadi et al., 2020). The variable efficacy of statin treatment is often attributed to inherent differences in tumour subtypes which confer cells with varying levels of vulnerability to statin treatment (Ahmadi et al., 2020, Longo et al., 2020). Additionally, the type of statin administered, the dose and delivery route as well as the duration of statin usage all contribute to the heterogenous response (Ahmadi et al., 2020).

It is important to note, while employing cholesterol synthesis inhibition to reduce cellular cholesterol levels has proven effective in a laboratory setting, the debilitating side effects associated with statin therapy is seen as a major limitation in a clinical setting. Common side effects include and is not limited to: muscle pains, hepato- and renal-toxicity, neurocognitive decline, myopathy as well as idiopathic polyneuropathy (Gu et al., 2019). Importantly, 30% of patient population display non-responsiveness to statin therapy (Ward et al., 2019). This could be attributed to the long-term impediment of cholesterol synthesis in cells where cholesterol plays an integral role in regulating essential cellular processes. Consequently, the discovery of alternative cholesterol lowering agents is pivotal to facilitate advances in targeting cellular cholesterol to combat tumorigenesis.

### *1.9.2. Cholesterol Depletory Agents*

Seeing that cancer cells display increased levels of cholesterol, with studies conducted in BC documenting 6-8x higher levels than normal counterparts (Sagar et al., 2014), it is rational to propose that employing depletion of excess cholesterol could serve as a better alternative to targeting tumorigenesis. The most comprehensively studied means of achieving this is through the administration of a class of molecules termed cyclodextrins (CDs). CDs extract cholesterol from both raft and non-raft domains, consequently affecting the distribution of cholesterol between the plasma and intracellular membranes (Zidovetzki and Levitan, 2007). The chemical structure of CDs results in the arrangement of a cone-like cavity possessing a hydrophobic internal space with accompanying hydrophilic external faces (Coisne et al., 2016). Through a process referred to as the inclusion phenomenon, lipophilic insoluble molecules (like cholesterol) complex with these CDs to form water-soluble complexes (Coisne et al., 2016). Molecular modelling illustrates that two β-CD molecules complex with cholesterol in a perpendicular orientation to the air/water interface when cholesterol is present at the interface of the cholesterol/phospholipid monolayer (Szente and Fenyvesi, 2017).

Methyl-β-cyclodextrin (MβCD) and the associated cyclodextrin derivatives have been employed in various studies and is proven to work effectively in the removal of plasma membrane and lipid raft cholesterol in human cells (Mohammad et al., 2014, Yokoo et al., 2015). Importantly, the decrease in cellular cholesterol content is directly proportional to the concentration of the cyclodextrin administered (Yokoo et al., 2015). Whereas MβCD is seen to extract membrane cholesterol and proves more toxic to the healthy cells, KS-01 displays a more significant effect on intracellular cholesterol as opposed to membrane cholesterol and is hence more toxicologically benign (Qiu et al., 2017b). With respect to cancer cells, the decrease in membrane cholesterol leads to lipid raft disruption which consequently affects cell signalling intermediates that cells subvert to promote tumorigenesis (Coisne et al., 2016). Additionally, a decrease in membrane cholesterol levels is associated with increased drug permeability and consequently enhanced sensitivity in cancer cells (Coisne et al., 2016, Mohammad et al., 2014).

It is important to emphasize, while most of the studies conducted to date target cholesterol synthesis to reduce cellular cholesterol levels, and consequently combat tumorigenesis, studies conducted employing direct membrane cholesterol depletion are lacking. Consequently, the current study seeks to delineate the effects of direct membrane cholesterol depletion as a means to target cellular cholesterol and combat tumorigenesis and compare this approach with cholesterol synthesis inhibition strategies. By conducting this study, a better understanding of cholesterol depletion as a strategy to restore sensitivity is portrayed, which will further assist in addressing whether membrane cholesterol depletion rather than cholesterol synthesis inhibition could serve as a better approach to combat cancer progression.

## 2. Aim and Objectives

### 2.1. Aim:

Utilizing MCF-7 cells, this study aims to investigate the role of cholesterol in hypoxia-induced epithelial-mesenchymal transition (EMT) with the intention of elucidating the role cholesterol plays in mediating cancer progression and drug resistance.

### 2.2. Objectives

#### *2.2.1. EMT Induction and Mechanisms of Drug Resistance*

2.2.1.1. To optimize and confirm hypoxia induction in MCF-7 cells as means to induce EMT.
2.2.1.2. To characterize EMT in MCF-7 cells by analyzing cell morphology.
2.2.1.3. To confirm that cells have undergone EMT by utilizing immunofluorescent staining.
2.2.1.4. To determine the effect on cell proliferation pre- and post-EMT induction by utilizing immunofluorescent staining.
2.2.1.5. To analyze pathway specific gene changes in cancer drug resistance pre- and post-EMT induction.

#### *2.2.2. Delineating the role of cholesterol in EMT*

2.2.2.1. To document the effect of targeting cholesterol on EMT induction through immunofluorescent staining.
2.2.2.2. To determine the invasive potential of cells that have undergone EMT following treatment with various cholesterol targeting agents.
2.2.2.3. To assess the multi-drug resistant potential of cells post-EMT induction following treatment with cholesterol-targeting agents.

## 3. Materials and Methods:

Each of the experimental techniques outlined below were completed to achieve the objectives of this study. Experiments were conducted on MCF-7 cells prior to as well as post-EMT induction unless stated otherwise. Experiments were performed in triplicates employing both biological (n=3) and technical replicates (n=3) validating reproducibility of the results obtained and also facilitating statistical analyses.

### Workflow

To investigate the role of cholesterol in hypoxia-induced EMT in and cancer drug resistance, a summary of the methodology utilised is presented in Figure 3. Initially, EMT was induced by treatment with a hypoxia mimetic (150 µM $CoCl_2$ for 48 hours) and subsequently characterised. Human cancer drug resistance pathway specific gene changes following hypoxia-induced EMT was thereafter determined. Several cholesterol-related assays were employed to assess changes in the cellular cholesterol profile. This was followed by assays delineating the effect of targeting cholesterol on EMT induction and consequently drug resistance.

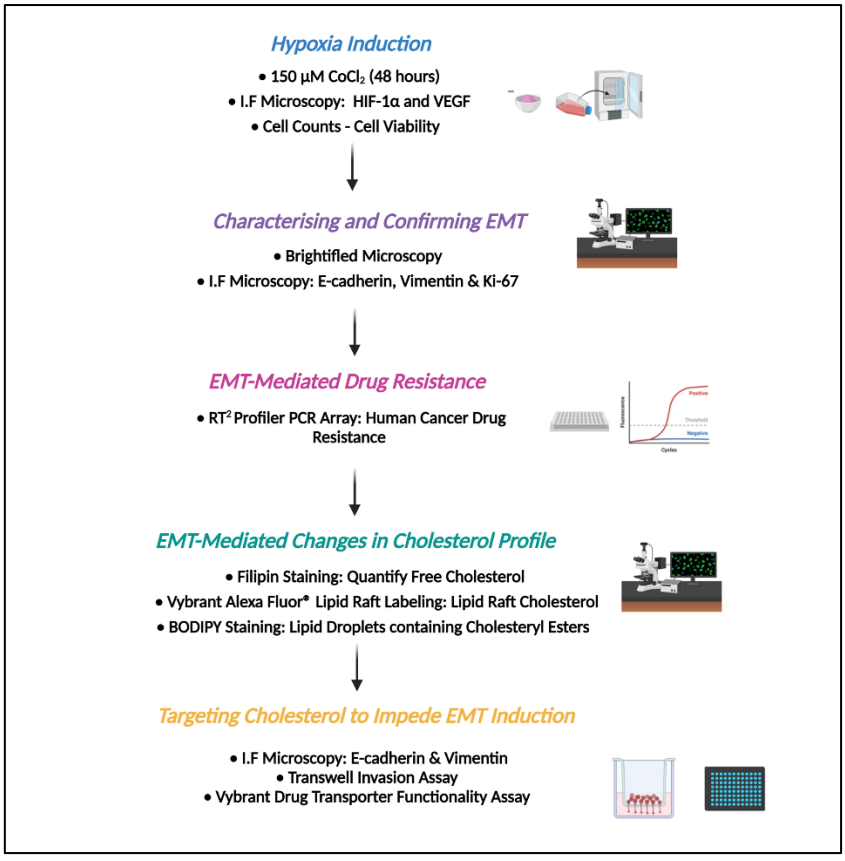



**Figure 3: Summary Workflow**

**Methods:**

### 3.1. Cell Culture

In the current study a human breast adenocarcinoma (MCF-7) cell line procured from The European Collection of Authenticated Cell Cultures (UK) was utilised. These cells were cultured in Dulbecco's Modified Eagle's Medium (DMEM) (Sigma Aldrich, UK) supplemented with 10% foetal bovine serum (FBS) (Celtic Molecular Diagnostics, SA) and 1% Penicillin-Streptomycin (Sigma Aldrich, UK) and incubated at 37 °C in the presence of 5% $CO_2$. It should be noted that passage number did not exceed P20 when culturing.

The constituents in DMEM provided the required nutrients and growth factors to facilitate cell survival and proliferation. The antibiotics prevented the growth of any contaminating bacteria and fungi. Furthermore, incubation at 37 °C in the presence of 5% $CO_2$ facilitated the maintenance of a constant pH through the carbon dioxide-bicarbonate buffer system. By mimicking *in-vivo* conditions so closely, optimal cell growth was ensured.

### 3.2. Hypoxia-induced EMT

Chemical induction of hypoxia is enabled by administering compounds broadly classified as hypoxia mimetics, with the most well studied being cobalt chloride ($CoCl_2$). The $Co^{2+}$ ions function in multiple ways to maintain the availability of HIF-1α in a standard cell culture environment. The proposed hypothesis is the substitution of $Fe^{2+}$ ions with $Co^{2+}$ in the active site of regulatory dioxygenases, namely the prolyl hydroxylases leading to inactivation of this enzyme. This will in turn impede HIF-1α degradation (Muñoz-Sánchez and Chánez-Cárdenas, 2018). HIF-1α activity is consequently maintained in the cell and continues to function in transcriptional activation of key target genes (Pavlacky and Polak, 2020a). Seeing that HIF-1α plays a key role in EMT induction, $CoCl_2$ was employed as a means of mimicking hypoxia-induced EMT.

Initially a working stock solution of 2500 µM $CoCl_2$ was prepared by dilution in distilled or DI water. The resulting solution was further diluted upon administration to cells contained in media. The following concentrations (50 µM,100 µM, 150 µM and 200 µM) and incubation times (12, 24 or 72 hours) were tested to identify which concentration optimally induced hypoxia in MCF-7 cells at 37 ºC. Treating MCF-7 cells with 150 µM of $CoCl_2$ for 48 hours

was seen to optimally induce hypoxia and this concentration was maintained for all further experiments conducted.

### 3.3. Cell Counting

Cell density and viability analysis was performed by employing the Neubauer haemocytometer and selective staining with trypan blue.

Initially media was removed, and cells were washed twice using 1 ml of 1× Phosphate Buffered Saline (PBS) (Sigma Aldrich, UK). Subsequently cells were washed with 1× Trypsin-EDTA (ethylenediaminetetraacetic acid) (Sigma Aldrich, UK; Celtic Molecular Diagnostics, SA), and thereafter harvested by administering 1× Trypsin-EDTA (1.5 ml in a 25 $cm^3$ flask) for approximately 5 minutes (mins) at 37 ºC. Trypsin functions as a serine protease cleaving peptide bonds in cell surface proteins such as fibronectin and collagen IV, whereas EDTA serves as a divalent cation chelator thereby enhancing trypsin activity (Tsuji et al., 2017). Following detachment, trypsin was neutralised by the addition of the appropriate volume of media.

To carry out cell counting, 10 µl of cells was mixed in 10 µl of trypan blue (Sigma Aldrich, UK). The trypan blue stain relies on cell membrane integrity. In terms of viable cells, these cells contain intact membranes that do not take up dye and hence remain unstained. With regards to non-viable cells, membrane integrity is compromised, and cells have leaky membranes that facilitate entry of the dye. In this way viable cells can be differentiated from non-viable cells based on dye uptake. Following this, 10 µl of the mixture was added onto a haemocytometer and both the number of viable and dead cells in all four quadrants (containing 16 mini squares) were ascertained under a Nikon Phase Contrast microscope. The precise dimension of the haemocytometer facilitates administration of a defined volume of cells allowing for the number of cells to be counted. This is possible due to the Neubauer factor ($10^4$) which considers the volume and dimensions of the respective chamber. Percentage cell viability was calculated as follows:

$$Cell\ Viability(\%) = \frac{No.of\ viable\ cells}{Total\ no.of\ cells} \times 100$$

Percentage cell viability had to exceed 95% in order to be utilised for experimentation.

The total number of cells to be plated was determined using the following calculation:

*Calculation 1*:

$$Volume\ to\ be\ plated\ per\ well\ \times No.of\ wells = Volume\ of\ media\ required\ (\boldsymbol{a})$$

*Calculation 2*:

$$\frac{(Total\ volume\ in\ flask\ (\mu l) \times No.of\ cells \times No.of\ wells)}{Total\ no.of\ cells\ in\ the\ flask} = Volume\ of\ cells\ required\ from\ the\ flask\ (\boldsymbol{b})$$

*Calculation 3*:

$$\boldsymbol{a} - \boldsymbol{b} = Volume\ of\ media\ to\ be\ added\ to\ the\ cells$$

It should be noted that plating for all assays were completed in triplicate.

### 3.4. Immunofluorescent Staining

Immunofluorescent staining is based on the specificity of antibody-antigen interaction. In this technique the antibody is conjugated to a fluorochrome thereby facilitating fluorescent detection of a specific antigen (protein) when excited by light of the appropriate wavelength (Donaldson, 2015).

Immunofluorescent staining was utilised at multiple points in the research project. Initially to validate hypoxia induction, the expression of HIF-1α and VEGF was detected. Following this, to characterise hypoxia induced EMT, the expression of specific proteins namely E-cadherin and vimentin was detected. Immunofluorescence was also employed to analyse Ki-67 protein as an indicator of cell proliferation and the expression of the cholesterol efflux protein ABCA1 was also detected pre- and post-EMT induction.

To complete this assay, cells were seeded in a 24-well plate at a density of 20 000 cells/well and subsequently incubated at 37 °C for a period of 24 hours. Following hypoxia induction and appropriate treatments, media was removed followed by 3× PBS washes. Thereafter 500 µl of 4% paraformaldehyde (Sigma Aldrich, UK) was added per well and cells were incubated at room temperature for 15 mins. This step was completed to fix cells which maintained cellular integrity by preserving native conformations (Ireka et al., 2019). Cells were subsequently permeabilised by incubating in 0.1% Triton-X (Sigma Aldrich, UK) for 15 mins. Triton-X-100

achieves this based on its role as a non-ionic detergent thereby disrupting lipid membranes allowing for antibody access to the cell interior (Im et al., 2019). Thereafter a one-hour blocking step was complete by incubating cells with 1% bovine serum albumin (BSA) (VWR Life Sciences, US) made up in 0.1% PBS-Tween 20 (PBST). Blocking is done to impede non-specific binding of the primary antibody. Following this, primary antibody was added [(Mouse Anti-Human HIF-1α (Novus Biologicals- NB100-105), Rabbit Anti-Human VEGF (Novus Biologicals-NB100-664), Mouse Anti-Human E-cadherin (BD Pharmingen – 610182), Rabbit Anti-Human Vimentin (Abcam - ab45939), Rabbit Anti Human -Ki-67 (Novus Biologicals-NB500-170) - 1:250 dilution], and cells were incubated at 4 ºC overnight. The primary antibody bound to the specific target antigen. Once the incubation was complete, the secondary antibody was subsequently added [Goat Anti-Rabbit Texas Red (ThermoFischer Scientific, T-2767), Goat Anti-Mouse Alexa Flour 488 (ThermoFischer Scientific, A-11029)- 1:1000 dilution]. Cells were incubated in secondary antibody for a duration of 45 mins. The fluorochrome conjugated secondary antibody recognised an epitope on the primary antibody, and subsequently bound to it. Each subsequent step listed above was followed by two PBS washes. For nuclear staining, DAPI (Sigma Aldrich, UK) was administered. DAPI permeates the nuclear membrane and intercalates with DNA and in this way facilitated staining (Im et al., 2019). Cells were incubated with 0.0001 mg/ml DAPI for 10 mins at room temperature followed by two PBS-wash steps post incubation. Following the addition of ProLong™ Gold Antifade mounting media (ThermoFischer Scientific) to the slides, cells were subsequently visualised by using the Floid™ Cell Imaging System (Thermo Fischer Scientific, US). Immunofluorescence intensity was quantified by utilising the ImageJ software (NIH, USA). Cells of interest and background fluorescence was analysed by considering the following parameters including area, integrated density and mean grey value. Corrected total cellular fluorescence was calculated as follows: CTCF = Integrated Density – (Area of selected cell × Mean fluorescence of background readings).

### 3.5. Growth Curve Using Cell Counts as a Measure of Viability

The growth of MCF-7 cells was analysed following treatment with 150 µM and 200 µM of $CoCl_2$ over time. This was carried out to ascertain the effect of $CoCl_2$ on MCF-7 cell viability. 80 000 cells were seeded per well in a 6-well plate and incubated at 37 ºC to allow for cell attachment. Following this, cells were treated with the afore-mentioned concentrations of $CoCl_2$ for a period of 4 days, where cells were detached and counted daily utilising a Neubauer

haemocytometer. GraphPad Prism5® was utilised to produce the relevant graphs indicating cell number/ml for each respective concentration over a period of time.

### 3.6. $RT^2$ Profiler PCR Array – Human Cancer Drug Resistance

To elucidate the effect of hypoxia, on pathway specific gene expression of genes involved in cancer drug resistance, a $RT^2$ Profiler PCR Array (QIAGEN, Germany) ($RT^2$ Profiler™ PCR Array Human Cancer Drug Resistance: PAHS-004Z) was completed. This assay was completed with two biological replicates based on the expensive nature of the assay. Arrays were conducted on cells cultured under both normoxic and hypoxic conditions, and a total of 84 genes were analysed. Housekeeping genes included *ACTB* (β-actin), *B2M* (β2-microglobulin), *GAPDH* (glyceraldehyde-3-phosphate dehydrogenase), *HPRT1* (hypoxanthine phosphoribosyltransferase-1) and *RPLP0* (ribosomal protein, large, P0). Fold changes indicating either upregulated or downregulated expression was evaluated under both culture conditions. Results of the most significant genes are reported.

#### *3.6.1. RNA Extraction and Purification*

The Direct-zol™ RNA MiniPrep kit (Zymo Research, Inqaba Biotec™, SA) was utilised for RNA extraction. Initially, cell pellets (~ $1\times10^6$ cells) were resuspended in 300 µl of TRIzol® reagent (Ambion®, Life Technologies, USA). TRIzol® is classified as a monophasic solution composed of phenol and guanidinium isothiocyanate that function to solubilise biological material resulting in the isolation of DNA, RNA and protein (Vorreiter et al., 2016). Following this, an equal volume of ethanol (99,9%) was added to mediate nucleic acid precipitation. Samples were subsequently transferred to a Zymo-Spin™ IICR $Column^2$ placed in a collection tube and centrifuged at 16 000 *xg* for 30 seconds, and the flow through was discarded. These parameters were maintained for subsequent centrifugation steps. To eliminate DNA in the sample, a DNase digestion step was completed, by mixing 5 µl of DNase I to 75 µl of DNA digestion buffer and incubated at room temperature for 15 mins. Subsequently, two wash steps were performed using 400 µl of Direct-zol™ RNA PreWash and 700 µl of RNA wash buffer, respectively. Wash steps were completed to ensure that samples were free from DNA contamination. Lastly, RNA was eluted, and the sample resuspended in 50 µl of DNase/RNase-Free water (Zymo Research, Inqaba Biotec™, SA).

RNA quality (purity and integrity) was assessed prior to cDNA synthesis and RT-qPCR. Quantification of RNA concentration (ng/µl) and purity ($A_{260/280}$ and $A_{260/230}$ ratios, respectively) was performed using the Nanodrop 1000 spectrophotometer (ThermoFischer

Scientific, USA). Nucleic acids display an absorbance maximum at 260 nm due to the aromatic bases in their structure whereas proteins all absorb maximally at 280 nm. Furthermore, organic contaminants such as chaotropic salts, phenols absorb maximally at 230 nm (Gandhi et al., 2020). An $A_{260/280}$ ratio of ~ 2.0 and $A_{260/230}$ ratio of ~ 2.0-2.2 is indicative of pure RNA. Extracted RNA with an $A_{260/A280}$ and $A_{260/230}$ ratio of ~ 2.0 was utilised for cDNA synthesis.

To assess integrity of the extracted RNA, 500 ng of RNA was mixed with 2 µl of 2× RNA loading dye and samples were loaded onto a 1% agarose gel and subsequently electrophoresed at 80 V for 1 hour. The ChemiDoc™ MP system was utilised to visualise 18S and 28S rRNA as a means to infer RNA integrity.

### *3.6.2. gDNA Elimination and cDNA Synthesis*

The RT$^2$ First Strand Kit (Qiagen, Germany) was utilised for complementary DNA (cDNA) synthesis. Initially, contaminating genomic DNA (gDNA) was eliminated by mixing the required reagents (*Table 3.1*) of the DNA elimination mix. Components were mixed and centrifuged, incubated for 5 min at 42 ºC followed by a 1 min incubation on ice. The reverse transcription mix was subsequently prepared according to reagents in *Table 3.2.* and 10 µl of the reverse transcription mix was mixed with 10 µl of gDNA elimination mix. Components were incubated at 42 ºC for 15 mins and the reaction was stopped by incubating at 95 ºC for 5 mins. Lastly, 91 µl of RNase-free water was added to each reaction and components were mixed gently and placed on ice prior to real-time PCR.

***Table 3.1: Genomic DNA Elimination Mix***

| **Component** | **Amount** |
|---|---|
| RNA | 500 ng |
| Buffer GE | 2 µl |
| RNase-free Water | Variable |
| **Total Volume** | **10 µl** |

***Table 3.2: Reverse Transcription Mix***

| **Component** | **Volume (µl)** |
|---|---|
| 5 × Buffer BC3 | 4 |

| | |
|---|---|
| Control P2 | 1 |
| RE3 Reverse Transcriptase Mix | 2 |
| RNase-free water | 3 |
| **Total Volume** | **10** |

### *3.6.3. Quantitative Reverse Transcription PCR*

To quantify the expression of cancer drug resistance genes pre- and post-hypoxia induction, the RT$^2$ SYBR® Green Mastermix (Qiagen, Germany) was utilised to conduct real time polymerase chain reaction (PCR). This is achieved based on the DNA-binding properties of SYBR Green, where fluorescence intensity is significantly increased following intercalation of the dye in the minor groove of double stranded DNA during the extension step. Fluorescence measurements obtained at the end of each amplification cycle can thus be utilised to ascertain the amount of DNA that has been amplified. The real time PCR reaction mix was prepared as outlined in *Table 3.3.* Following this, 25 µl of the PCR component mix was dispensed to each well of the RT$^2$ Profiler PCR Array (Qiagen, Germany), where each well represented a different gene. Wells were tightly sealed with Optical Thin-Wall 8-Cap Strips and subsequently centrifuged for 1 min at 1000 ×g to eliminate air bubbles. The Bio-Rad CFX96 system (Bio-Rad, USA) was utilised for real-time PCR, employing a two-step cycling parameters as outlined in *Table 3.4.* Cq/Ct values were ascertained through the CFX Maestro software (Bio-Rad, USA). Raw Ct values obtained for all genes were exported to an Excel spreadsheet, and fold change between hypoxic and normoxic MCF-7 cells was calculated by using the SABiosciences PCR Array Analysis Template (www.SABiosciences.com/pcrarraydatanalysis.php). Log2 was used to normalise the expression of the genes of each array, allowing to model proportional changes.

***Table 3.3: PCR Components Mix***

| **Component** | **Volume (µl)** |
|---|---|
| 2 × RT$^2$ SYBR® Green Mastermix | 1350 |
| cDNA synthesis reaction | 102 |
| RNase-free water | 1248 |
| **Total Volume** | **2700** |

***Table 3.4: Cycling conditions***

| Cycles | Duration | Temperature | Comments |
|---|---|---|---|
| 1 | 10 min | 95 ºC | HotStart DNA Taq Polymerase is activated by this heating step. |
| 40 | 15 sec | 95 ºC | Perform fluorescence data collection. |
| | 1 min | 60 ºC | |

### *3.6.4. Gene Expression Network Maps: OmicsNet and Cytoscape*

OmicsNet (http://www.omicsnet.ca/faces/home.xhtml) was used to identify target genes and model interactions between target genes in the cancer drug resistance array on the basis of protein-protein interactions. The output generated was subsequently filtered to solely include differentially expressed genes with their direct targets and the resulting network was imported as a network on the Cytoscape interface. Cytoscape is a bioinformatics platform that integrates biomolecular interaction networks with gene expression data generating molecular interaction networks (Shannon et al., 2003). For further network and molecular profiling analysis, the GeneMANIA plugin was utilised. GeneMANIA extends the query list of genes, with genes that are functionally similar to model relationships among genes within a given data set. The GeneMANIA plugin through Cytoscape (http://cytoscape.org, version 3.8.2) was employed to generate gene expression networks, where each gene (node) was coloured according to Log2 fold change (hypoxic/normoxic MCF-7 cells), and interactive genes were connected by grey lines. The program implements a weighted composite functional interaction network, where each network is assigned a weight based primarily on how well-connected genes are to each other relative to the non-query genes. Mapped interactions were considered statistically significant when $q < 0.05$.

## 3.7. Cholesterol and Lipid Staining

### *3.7.1. Filipin Staining*

Filipin is derived naturally from a fluorescent polyene antibiotic with the ability to bind to free cholesterol but not to esterified sterols. As a result, it is efficient in detecting free (i.e., unesterified) cholesterol housed in biological membranes (Maxfield and Wüstner, 2012). Filipin is known to form a tight complex with sterols possessing a planar steroid nucleus, an unesterified 3β hydroxyl group, as well as an apolar side chain at the C-17 position (Maxfield and Wüstner, 2012). The observed excitation for filipin is approximately 360 nm while fluorescence emission is around 480 nm (Maxfield and Wüstner, 2012).

To complete this assay, cells were seeded in a 24-well plate at a density of 20 000 cells/well and subsequently incubated at 37 °C for a period of 24 hours. Cells pre- and post-EMT induction were subject to appropriate treatments with cholesterol inhibitory/depletory agents (1 mM MβCD, 10 mM KS-01 or 10 μM Simvastatin) in the final 2 hours of EMT induction These concentrations were selected based on usage in previously published studies (Mundhara et al., 2019, Wu et al., 2020, Xie et al., 2016). Media was subsequently removed followed by 3× PBS washes. Thereafter 1 ml of 4% formaldehyde (Sigma Aldrich, UK) was added to each well and incubated for 15 mins at room temperature to fix the cells. Cells were subsequently stained with 0.05 mg/ml of filipin (Sigma Aldrich, UK) (reconstituted in PBS) to stain free cholesterol. NucRed™ Dead (ThermoFischer Scientific, USA) was utilised to stain cell nuclei by incubating for 3 mins at room temperature. Each subsequent step listed above was followed by three PBS washes. Following the last wash, cells were mounted and subsequently viewed using the Floid™ Cell Imaging System (ThermoFischer Scientific, US). Immunofluorescence intensity was quantified by utilising the ImageJ software (NIH, USA).

### *3.7.2. Vybrant Alexa Fluor® Lipid Raft Labelling*

Vybrant Alexa Fluor® facilitates the fluorescent labelling of lipid rafts present in cells. The assay utilises a cholera toxin subunit B (CT-B) which is conjugated to a fluorescent probe (Alexa Fluor 594). As the CT-B binds to the pentasaccharide chain of plasma membrane ganglioside $G_{M1}$ the localization, and visualization of lipid raft cholesterol content in cells can be completed (Palmer et al., 2007).

To complete this assay, cells were seeded in a 24-well plate at a density of 20 000 cells/well and subsequently incubated at 37 °C for a period of 24 hours. Cells pre- and post-EMT

induction were subject to appropriate treatments with cholesterol inhibitory/depletory agents (1 mM MβCD, 10 mM KS-01 or 10 µM Simvastatin) in the final 2 hours of EMT induction, after which media was removed followed by 3× PBS washes. Thereafter 1 ml of 4% formaldehyde (Sigma Aldrich, UK) was added to each well and incubated for 15 mins at room temperature to fix the cells. Cells were then incubated with 0.1% Triton-X-100 (Sigma Aldrich, UK) for 15 mins. Subsequently 1 µl/well (made up in 1 ml of PBS) of Alexa Fluor® [Subunit A- cholera toxin subunit B] (ThermoFischer Scientific, USA) was added to the cells and incubated for 30 mins at 37 ºC. Thereafter 1 µl/well (made up in 1 ml of PBS) of Alexa Fluor® [Subunit B- Anti-cholera toxin subunit B antibody] (ThermoFischer Scientific, USA) was added to cells and incubated for 30 mins at 37 ºC. Following this, 0.0001 mg/ml DAPI was utilised to stain nuclei by incubating for 10 mins at room temperature. Each subsequent step listed above was followed by three PBS washes. Following the last wash, cells were mounted and subsequently viewed using the Floid™ Cell Imaging System. Immunofluorescence intensity was quantified by utilising the ImageJ software (NIH, USA).

### *3.7.3. BODIPY Staining*

4,4-difluoro-1,3,5,7,8-pentamethyl-4-bora-3a,4a-diaza-s-indacene (BODIPY) is a neutral lipophilic fluorophore that stains neutral lipid droplets containing CEs and fatty acids. This can be attributed to its non-polar nature allowing for efficient diffusion into the hydrophobic interior of cell membranes. The BODIPY fluorophore is known to conjugate to C-24 of the sterol ring (Chaudhuri and Anand, 2017). When excited by blue light, BODIPY emits light of a wavelength corresponding to a green colour.

To complete this assay, cells were seeded in a 24-well plate at a density of 20 000 cells/well and subsequently incubated at 37 °C for a period of 24 hours. Cells pre- and post-EMT induction were subject to appropriate treatments with cholesterol inhibitory/depletory agents (1 mM MβCD, 10 mM KS-01 or 10 µM Simvastatin) in the final 2 hours of EMT induction, after which media was removed followed by 3× PBS washes. Thereafter 1 ml of 4% formaldehyde (Sigma Aldrich, UK) was added to each well and incubated for 15 mins at room temperature to fix the cells. Cells were subsequently permeabilised by administering 0.1% Triton-X-100 (Sigma Aldrich, UK) for 15 mins at room temperature. Following this 1 ml of BODIPY (ThermoFischer Scientific, USA) working solution was added to each well and incubated for 15 mins at 37 ºC. Nuclear staining was achieved by administering 0.0001 mg/ml DAPI and subsequently incubating for 10 mins at room temperature. Each subsequent step listed above was followed by three PBS washes. Following the last wash, cells were mounted

and thereafter viewed using the Floid™ Cell Imaging System (ThermoFischer Scientific, US). Immunofluorescence intensity was quantified by utilising the ImageJ software (NIH, USA).

### 3.8. Transwell® Invasion Assay

Cell invasion is a pivotal feature of advanced cancers and often facilitates the generation of secondary tumours at distant sites. To mimic this process *in-vitro*, migration and invasion assays are conventionally used. To assay invasive potential, the Transwell® Invasion assay was completed. The assay set up is dependent on a porous filter membrane insert (coated with extracellular matrix) that is placed in each well of the respective plate. Initially cells are seeded on one side of the membrane in the presence of a chemotactic gradient (Marshall J., 2011). Cells are subsequently incubated for the specified period of time (dependent on the cell line) after which the membrane is fixed and stained. Following this, the number of cells on the underside of the membrane is visualised through microscopy to quantify the invasive capacity.

The Transwell® invasion assay was completed on MCF-7 cells pre- and post-EMT induction following treatment with cholesterol targeting agents in the final 2 hours of EMT induction. To complete this assay 100 000 cells/ml (maintained in serum-free media for 24 hours at 37 ºC) were seeded in a transwell chamber containing 0.8 µm pores (ThermoFischer Scientific, UK) coated with GelTrex (ThermoFischer Scientific, UK). The lower chamber contained 500 µl of media supplemented with 10% FBS to set up a chemotactic gradient. Following a 24-hour incubation period, non-invasive cells on the top chamber were removed using a cotton swab. Cells that had invaded the Matrigel and migrated to the underside of the membrane were fixed with 4% formaldehyde for 10 mins and subsequently stained using 0.0001 mg/ml DAPI for 10 mins at room temperature. Following this incubation period, the membrane was gently dipped in PBS to remove excess DAPI. The membrane was subsequently cut using a sterile blade and mounted to glass coverslips. Cell counting was completed in different fields of view to obtain an average number of cells that had invaded the GelTrex (ThermoFischer Scientific, UK). The result was presented as a percentage increase or decrease in the number of invasive cells relative to the control.

### 3.9. Drug Transporter Functionality Assay

The Vybrant® MDR Assay Kit (Thermo Fischer Scientific, USA) was utilised with the aim of assessing the functionality of the key drug transporter MDR1 post-EMT induction. This assay relies on the administration of an appropriate MDR1 substrate, calcein acetoxymethyl ester (calcein AM) to assess the efflux activity. In healthy cells, exposure to the non-fluorescent calcein AM results in dye penetration through the plasma membrane due to its lipophilic nature (Oncul and Ercan, 2017). Following penetration, cytoplasmic esterases within the cell cleave ester bonds resulting in the formation of fluorescent calcein. The fluorescent calcein is subsequently retained in the cytoplasm based on its acidic nature. Under conditions of multi-drug resistance, increased expression of drug efflux pumps facilitate increased rates of expulsion of non-fluorescent calcein AM from the cell interior (Oncul and Ercan, 2017). This subsequently impedes the accumulation of fluorescent calcein in the cytoplasm. On this basis, drug-efflux potential is assessed by measuring the levels of intracellular calcein fluorescence (Oncul and Ercan, 2017).

To complete this assay, MCF-7 cells pre- and post-EMT induction was seeded in a 96 well plate at a density of 10 000 cells/well and incubated for 24 hours at 37 °C. Cells post-EMT induction were subject to appropriate treatments with cholesterol inhibitory/depletory agents (1 mM MβCD, 10 mM KS-01 or 10 µM Simvastatin) in the final 2 hours of EMT induction. Post-EMT cells were treated with 1 µM of Verapamil (a known MDR1 inhibitor) for the same time period which served as a positive control based on knowledge from previous studies elucidating the efficiency of this compound in reducing drug efflux pump activity. Following this, 50 µl of calcein-AM (0.25 µM) was administered to each well and subsequently incubated at 37 °C for a duration of 30 mins in the dark. MDR activity was consequently assessed based on calcein retention in cells. Subsequently, two washes using PBS were completed followed by the administration of 200 µl of PBS to each well. In order to determine fluorescence intensity, the Victor Nivo multi-mode microplate reader (Perkin Elmer, USA) was utilised with the excitation maximum set to 494 nm and the emission maximum set to 517 nm. The percentage of calcein retention in cells was calculated using Microsoft Office Excel© and the corresponding graphs were plotted using GraphPad Prism5®.

### 3.10. Statistical Analysis

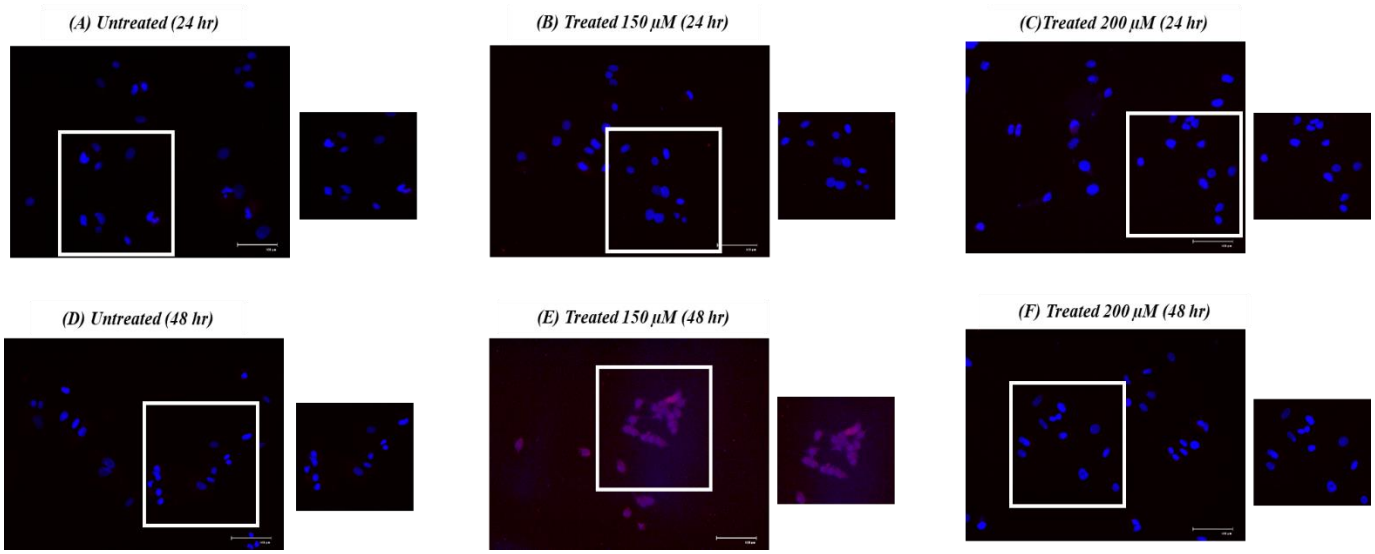
All assays were performed employing three technical replicates (n=3) and an average of the data was obtained. To ensure reproducible data, experiments were performed employing three biological replicates (n=3). For comparisons between two groups a paired Student's t-test was utilised as data is continuous and assumed to be normally distributed. The one-way analysis of variance (ANOVA) test was employed for comparisons between more than two groups with a single independent variable. A two-way ANOVA was conducted for comparisons between more than two groups with two independent variables. For additional pairwise analysis a Bonferroni post-hoc test was completed and is specified for each result. The Student's t-test and ANOVA are parametric tests. Therefore prior to statistical analysis of each data set, a Shapiro-Wilk test of normality was performed to confirm a normal distribution of data. A p-value $\leq 0.05$ was statistically significant. In addition, GraphPad Prism5® was utilised to perform all statistical calculations and to generate the respective graphs.

## 4. Results:

### 4.1. Optimizing Hypoxia Induction in MCF-7 cells

In an attempt to optimize hypoxia induction in MCF-7 cells, cells were cultured with concentrations of cobalt chloride ($CoCl_2$) ranging from 50 – 250 µM for 24, 48, and 72 hours based on previous parameters employed in published literature. While cell viability was not affected following 24- and 48-hour incubation periods, incubating cells for 72 hours affected cell viability and hence 24 and 48 hours were chosen for further optimization *(data not shown)*. Immunofluorescence microscopy was utilized to confirm optimal conditions for hypoxia induction, by staining with Alexa Fluor 680 (measuring HIF-1α protein expression) and DAPI (nuclei stain) *(Figure 4.1a)*. Treatment with 150 µM $CoCl_2$ for 48 hours was determined to work best for hypoxia induction as evidenced by the increased fluorescence intensity as well as nuclear localization of HIF-1α in MCF-7 cells following this treatment condition *(Figure 4.1a – Panel E)*. Image J analysis further confirmed the observed result indicating an approximate 92.91% increase in the corrected total cell fluorescence (CTCF) for HIF-1α expression in $CoCl_2$ treated cells relative to the untreated cells following a 48-hour incubation *(Figure 4.1b)*.

***a)***



***b)***

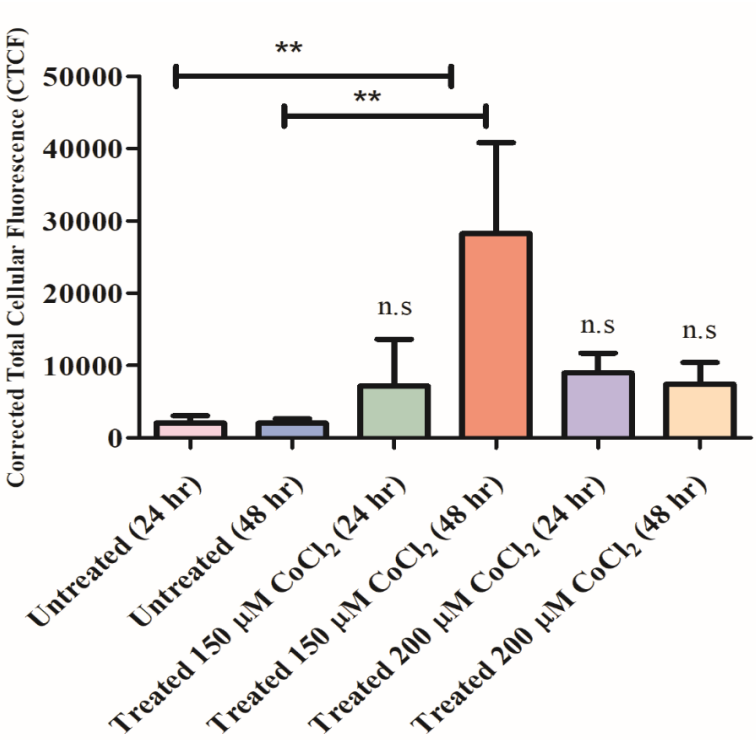



**Figure 4.1: Optimising $CoCl_2$ mediated Hypoxia Induction in MCF-7 cells**

***(a)*** *MCF-7 cells were treated with various concentrations of $CoCl_2$ employing either 24-hour (hr) or 48-hour (hr) incubation time and protein expression and localisation of HIF-1α was evaluated through indirect immunofluorescence staining using the FLoid® Cell Imaging system. HIF-1α expression is indicated by Alexa Fluor 680 staining (red) while nuclei are stained with DAPI (blue). (A) Untreated (24hr), (B) Treated 150 µM (24 hr), (C) Treated 200 µM (24 hr), (D) Untreated (48hr), (E) Treated 150 µM (48 hr), (F) Treated 200 µM (48 hr).* ***(b)*** *Analysis was subsequently performed utilising the ImageJ software. Calculated CTCF values indicate a 92.91% increase in HIF-1α protein expression following $CoCl_2$ treatment relative to the untreated cells following a 48-hour incubation period. Images were captured using the Floid™ Cell Imaging System followed by analysis using the Image J software. The scale bar on each of the images represents 100 µm. A one-way ANOVA test was employed for statistical analysis where data represent the mean ± standard deviation (SD). n=3. * $P < 0.05$, ** $P < 0.01$, *** $P < 0.001$.*

## 4.2. Growth Curve Following $CoCl_2$ Treatment in MCF-7 cells

A cell counting assay was performed to identify the effects of varying concentrations of $CoCl_2$ treatment under different incubation times on MCF-7 cell growth and viability. This was conducted over a 4-day period. It is evident that treatment with 150 µM of $CoCl_2$ for a period of 3 days does not drastically affect cell viability as evidenced by the close correlation of cell number between untreated and treated cells, where cell number only drastically decreases on day 4 of treatment *(Figure 4.2)*. Contrary to this, treatment with 200 µM of $CoCl_2$ displayed a progressive decrease in cell growth as the days progressed with cell growth being significantly retarded from day 2 of treatment *(Figure 4.2)*.

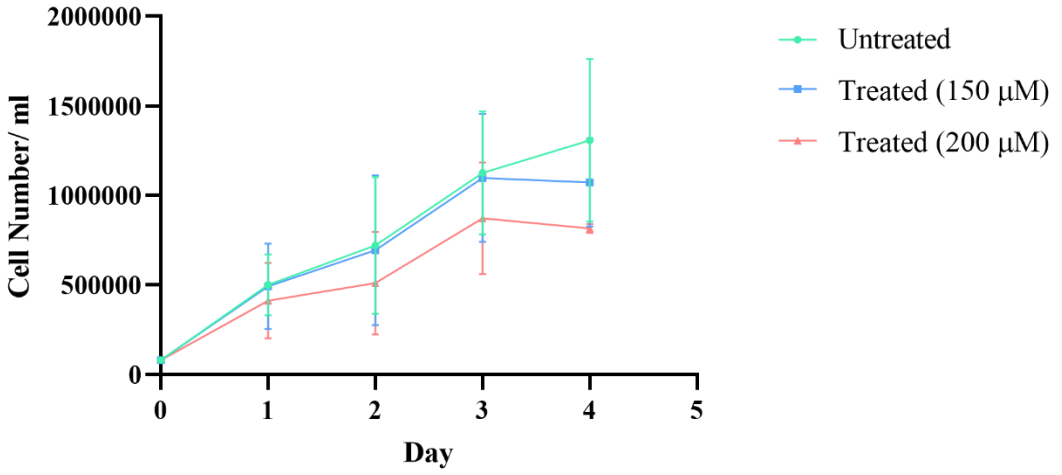
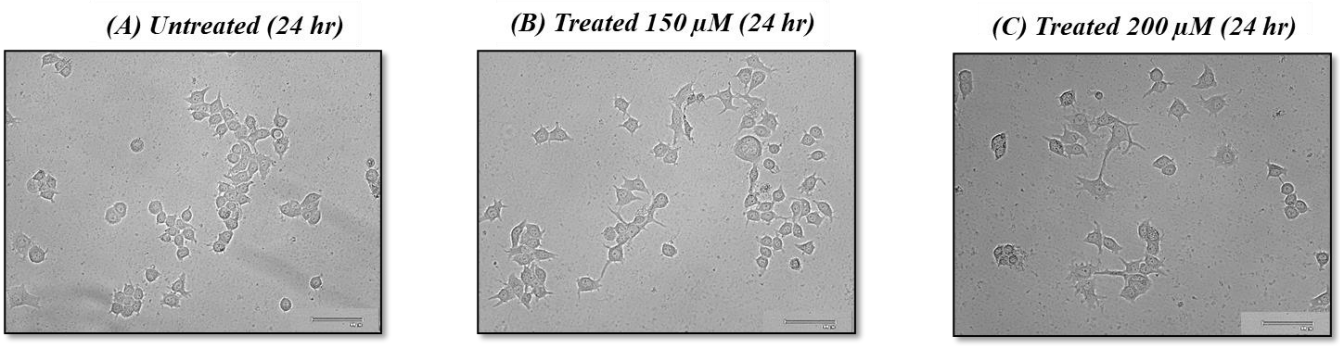



**Figure 4.2: Effect of $CoCl_2$ treatment on the growth of MCF-7 cells**

*Representative graph indicating the effect of $CoCl_2$ on MCF-7 cell number. Cells were seeded under normoxic conditions and allowed to attach. Following this, various concentrations of $CoCl_2$ were administered and cell counts conducted over a 4-day period. Cell number was ascertained through cell counts conducted on a Neubauer Haemocytometer. Data represent the mean ± standard deviation (S.D) (n=3) from raw data.*

## 4.3. Analysing Changes in MCF-7 Cell Morphology Following $CoCl_2$ Treatment

The MCF-7 cell line is an adherent human BC epithelial luminal cell line, displaying characteristic cobble stone-like morphology when cultured under normoxic conditions *(Figure 4.3- Panel A and D)*. Following treatment with 150 µM and 200 µM of $CoCl_2$ for 24- and 48-hour incubation periods, cells display features associated with the mesenchymal phenotype, as indicated by the loss of cell-cell contact and the elongated spindle-like appearance possessing abundant cellular protrusions *(Figure 4.3- Panel B, C, E and F)*.



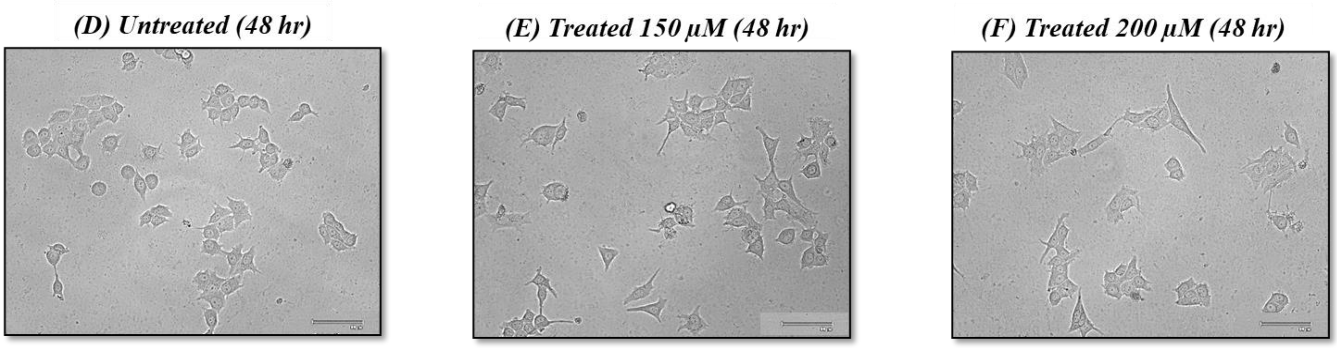



**Figure 4.3: Effect of $CoCl_2$ treatment on MCF-7 cell morphology**

*MCF-7 cells were treated with various concentrations of $CoCl_2$ employing either 24-hour (hr) or 48-hour (hr) incubation time and brightfield images were obtained by using the Floid Cell Imaging system. (A) Untreated (24hr), (B) Treated 150 µM (24 hr), (C) Treated 200 µM (24 hr), (D) Untreated (48hr), (E) Treated 150 µM (48 hr), (F) Treated 200 µM (48 hr). It is evident that cells treated with either 150 µM or 200 µM of $CoCl_2$ at both 24- and 48- hour incubation periods display altered cellular morphology transforming from the characteristic epithelial cobblestone-like morphology to adopt a mesenchymal spindle-like morphology. Images were captured using the Floid™ Cell Imaging System followed by analysis using the Image J software. The scale bar on each of the images represents 100 µm.*

Based on the evidence that administering 150 µM $CoCl_2$ to MCF-7 cells for 48 hours induced a significant increase in the expression of HIF-1α without significantly affecting cell viability and further mediated transformation of cell morphology from an epithelial cobblestone-like appearance to adopt a more mesenchymal phenotype, this treatment condition was maintained for all the subsequent experimental assays conducted.

### 4.4. Confirming HIF-1α Induction in MCF-7 cells following $CoCl_2$ treatment

Seeing that $CoCl_2$ proved effective in stabilizing HIF-1α following a 48-hour treatment, to evaluate HIF-1α activity, the expression of a HIF-1α target gene, vascular endothelial growth factor (VEGF) was analyzed. It was observed that the $CoCl_2$-mediated induction of HIF-1α consequently upregulated the expression of VEGF by 56.15% as evidenced by the increased staining of Alexa Fluor 488 *(green)* which binds to VEGF *(Figure 4.4)* in $CoCl_2$ treated cells relative to untreated cells.

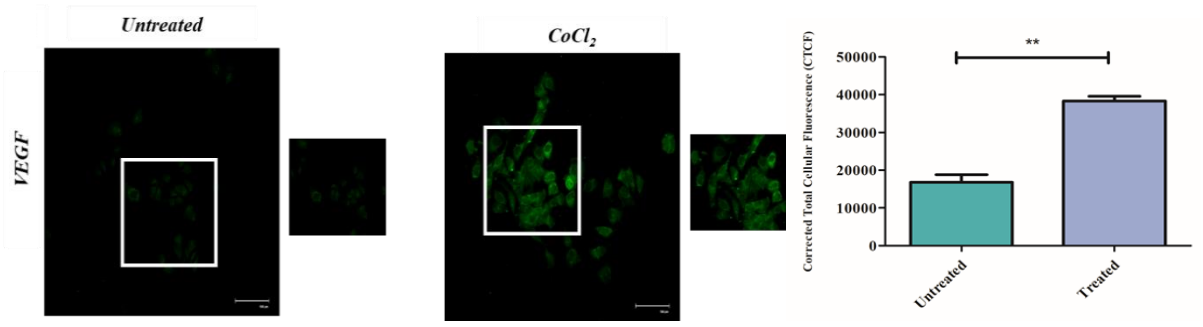



**Figure 4.4: Effect of $CoCl_2$ on the expression of HIF-1α target gene VEGF**

*Protein expression of VEGF in untreated and $CoCl_2$ treated MCF-7 cells for a duration of 48 hours was detected by employing immunofluorescent microscopy. VEGF expression is indicated by Alexa Fluor 488 staining (green). It is evident that VEGF is significantly increased following treatment with $CoCl_2$ where further analysis by Image J, document a 56.15% increase in VEGF expression of $CoCl_2$ treated cells relative to untreated cells. Images were captured using the Floid™ Cell Imaging System followed by analysis using the Image J software. The scale bar on each of the images represents 100 µm. A paired two-tailed t-test was employed for statistical analysis where data represent the mean ± standard deviation. n=3. *P < 0.05, ** P < 0.01, *** P < 0.001.*

## 4.5. Confirming EMT Induction following $CoCl_2$ treatment in MCF-7

To confirm EMT induction in MCF-7 cells, immunofluorescence microscopy was utilized to study the expression of key EMT markers following $CoCl_2$ administration. The epithelial cell junction protein E-cadherin is used as a molecular marker to indicate cells that possess an epithelial phenotype, whereas the intermediate filament vimentin is used as a molecular marker to indicate cells that possess a mesenchymal phenotype. Immunofluorescent images clearly present a significant decrease in the expression of E-cadherin in MCF-7 cells following treatment with $CoCl_2$ as evidenced by the reduced binding Alexa Fluor 488 *(green)* conjugated to E-cadherin where the nuclei are stained with DAPI *(blue)* (*Figure 4.5a*). Contrary to this, treatment with $CoCl_2$ mediated an upregulation of vimentin in MCF-7 cells relative to cells that were untreated. This can be justified by the increased binding of Texas Red *(red)* conjugated to vimentin where the nuclei are stained with DAPI *(blue)* (*Figure 4.5b*). Additional analysis conducted using Image J highlight a 67.89% decrease in the expression of E-cadherin and a 56.42% increase in the expression of vimentin following $CoCl_2$ treatment (*Figure 4.5*).

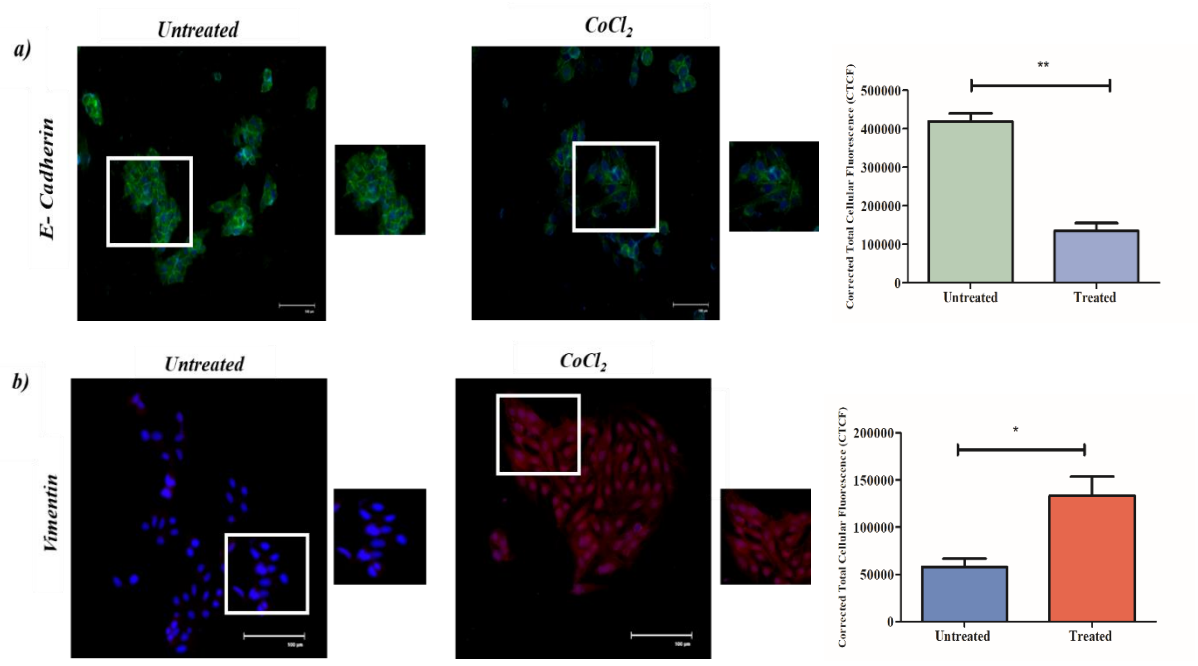



**Figure 4.5: Effect of $CoCl_2$ on Molecular Markers of EMT**

*Protein expression of EMT molecular markers in untreated and $CoCl_2$ treated MCF-7 cells for a duration of 48 hours was detected by employing immunofluorescent microscopy.* ***(a)*** *E-cadherin expression is indicated by Alexa Fluor 488 staining (green) while nuclei are stained with DAPI (blue). It is evident that E-cadherin expression is significantly decreased following treatment with $CoCl_2$ where further analysis by Image J, document a 67.89% decrease in E-cadherin expression of $CoCl_2$ treated cells relative to untreated cells.* ***(b)*** *Vimentin expression is indicated by Texas Red staining (red) while nuclei are stained with DAPI (blue). Vimentin expression is significantly increased following treatment with $CoCl_2$ where further analysis by Image J, document a 56.42% increase in vimentin expression of $CoCl_2$ treated cells relative to untreated cells. Images were captured using the Floid™ Cell Imaging System followed by analysis using the Image J software. The scale bar on each of the images represents 100 µm. A paired two-tailed t-test was employed for statistical analysis where data represent the mean ± standard deviation. n=3. * $P < 0.05$, ** $P < 0.01$, *** $P < 0.001$.*

## 4.6. Analysing Expression of Ki-67 in MCF-7 cells as a Marker of Cell Proliferation

The Ki-67 protein is a nuclear antigen present in cells in all active phases of the cell cycle namely $G_1$, S, $G_2$ as well as the M-phase of the cell cycle and is absent in the resting phases of the cell cycle. The expression of Ki-67 can thus be utilised as an indicator of proliferative activity. Following $CoCl_2$ treatment, MCF-7 cells displayed a 49.35% reduction in Ki-67 staining relative to the untreated cells *(Figure 4.6)*.

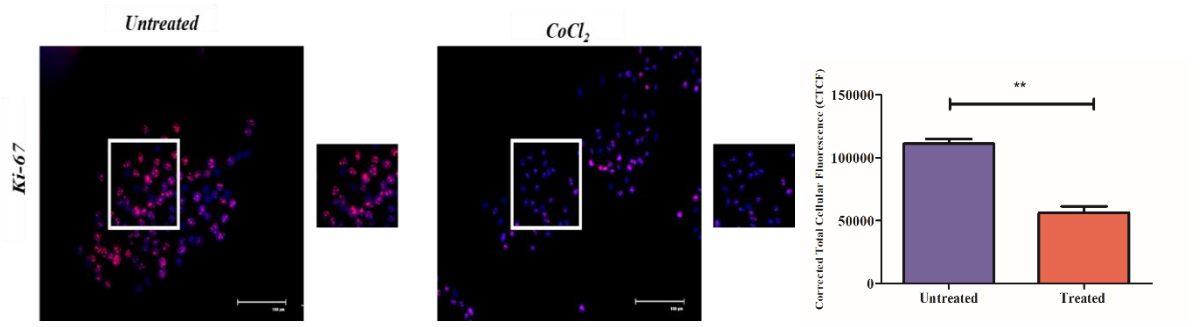



**Figure 4.6: Effect of $CoCl_2$ on Ki-67 expression**

*Ki-67 staining in MCF-7 cells. Ki-67 expression is indicated by Texas Red staining (red) while nuclei are stained with DAPI (blue). Ki-67 expression is significantly decreased following treatment with $CoCl_2$ where further analysis by Image J, document a 49.35% decrease in Ki-67 expression of $CoCl_2$ treated cells relative to untreated cells. Images were captured using the Floid™ Cell Imaging System followed by analysis using the Image J software. The scale bar on each of the images represents 100 µm. A paired two-tailed t-test was employed for statistical analysis where data represent the mean ± standard deviation. n=3. * P < 0.05, ** P < 0.01, *** P < 0.001.*

## 4.7. Documented changes in pathway dynamics following hypoxia-induced EMT in MCF-7 cells

RT-qPCR analysis was conducted on a panel of 84 genes that have well established roles in mediating cancer drug resistance. The effect on gene expression was studied in MCF-7 cells following culturing of cells under hypoxic conditions, and the resulting fold change values were calculated by using the untreated MCF-7 cells as baseline. Gene expression analysis documented an overall upregulation of thirty-seven genes implicated in cancer drug resistance following hypoxia-induced EMT (*Table 4.1*). Interestingly three genes were downregulated following hypoxia-induced EMT, namely *CDKN2D* (Fold change = -9,91), *FOS* (Fold change = -4,75) and *RARA* (Fold change = -3,10). In terms of the upregulated genes, culturing cells under hypoxic conditions led to a significant increase in the expression of multidrug resistance transporters including *ABCB1* (Fold Change = 3,63), *ABCC3* (Fold Change = 587,72) and *ABCC5* (Fold Change = 38,18). While both pro- and anti-apoptotic genes displayed increased expression, the expression of anti-apoptotic genes were significantly higher, *BCL2* (Fold Change = 19,21) *BCL2L1* (Fold Change = 82,26). Hypoxic conditions also led to an upregulation of all genes involved in drug metabolism with the most significant changes being documented in *CYP1A1* (Fold Change = 16,52), *CYP2B6* (Fold Change = 82,26), *DHFR* (Fold Change = 26,61) and *SOD1* (Fold Change = 311,00). Genes involved in DNA damage and repair were also upregulated following hypoxic induction namely *BRCA1* (Fold Change = 7,01) and *MSH2* (Fold Change = 506,19). Interestingly, growth factor receptors were also

upregulated with the most significant changes documented in *ERBB2* (Fold Change = 506,19), *ERRB3* (Fold Change = 506,19) and *IGF1R* (Fold Change = 506,19). Furthermore, cell cycle related genes including *CCND1* (Fold Change = 10,16), *CDK2* (Fold Change = 7,57) and *CDKN1B* (Fold Change = 3,65) were also upregulated following hypoxia-induced EMT. Complete gene expression analysis is summarised in *Table 4.1.* and *Figure 4.7.*

**Table 4.1: Gene expression analysis of genes related to cancer drug resistance in MCF-7 cells subjected to hypoxia-induced EMT relative to untreated MCF-7 cells**

| Gene Symbol | Description | Mode of Action | Fold Change | Log2 Fold Change |
|---|---|---|---|---|
| CDKN2D | Cyclin Dependent Kinase Inhibitor 2D | Cell Cycle | -9,906392459 | -3,308359777 |
| FOS | FBJ murine osteosarcoma viral oncogene homolog | Transcription Factors | -4,751827369 | -2,248482425 |
| RARA | Retinoic acid receptor, alpha | Hormone Receptors | -3,10015711 | -1,63234133 |
| BAX | BCL2-associated X protein | Drug Resistance | 1,500134325 | 0,585091688 |
| CLPTM1L | CLPTM1-like | Drug Metabolism | 2,050389802 | 1,035898209 |
| ESR1 | Estrogen receptor 1 | Hormone Receptors | 2,20003849 | 1,137528764 |
| RELB | RELB Proto-Oncogene, NF-KB Subunit | Transcription Factors | 2,256811987 | 1,174286234 |
| GSK3A | Glycogen synthase kinase 3 alpha | Drug Metabolism | 2,310298557 | 1,208079302 |
| ERBB2 | V-erb-b2 erythroblastic leukemia viral oncogene homolog 2, neuro/glioblastoma derived oncogene homolog (avian) | Growth Factor Receptors | 2,461958547 | 1,299806471 |
| AP1S1 | Adaptor-related protein complex 1, sigma 1 subunit | Transcription Factors | 2,99859012 | 1,584284332 |
| ABCB1 | ATP-binding cassette, sub-family B (MDR/TAP), member 1 | Drug Resistance | 3,63 | 1,859969548 |
| CDKN1B | Cyclin Dependent Kinase Inhibitor 1B | Cell Cycle | 3,653731935 | 1,869370791 |
| FGF2 | Fibroblast growth factor 2 (basic) | Growth Factor Receptors | 3,653731935 | 1,869370791 |
| RXRB | Retinoid X Receptor Beta | Hormone Receptors | 3,653731935 | 1,869370791 |

| | | | | |
|---|---|---|---|---|
| HIF1A | Hypoxia Inducible Factor 1 -Alpha | Transcription Factors | **3,778787028** | **1,917923211** |
| TOP1 | DNA Topoisomerase I | Drug Resistance | **4,124086513** | **2,044074597** |
| EPHX1 | Epoxide hydrolase 1, microsomal (xenobiotic) | Drug Metabolism | **5,304225204** | **2,40714203** |
| PPARG | Peroxisome Proliferator Activated Receptor Gamma | Hormone Receptors | **5,395709813** | **2,431812761** |
| AR | Androgen Receptor | Hormone Receptors | **5,894866583** | **2,559459161** |
| MET | MET Proto-Oncogene, Receptor Tyrosine Kinase | Growth Factor Receptors | **7,004772213** | **2,808338137** |
| BRCA1 | Breast cancer 1, early onset | DNA Damage and Repair | **7,014628528** | **2,810366705** |
| UGCG | UDP-glucose ceramide glucosyltransferase | Drug Metabolism | **7,16637111** | **2,841242755** |
| CDK2 | Cyclin-dependent kinase 2 | Cell Cycle | **7,574225696** | **2,921098411** |
| CCND1 | Cyclin D1 | Cell Cycle | **10,15795614** | **3,344538245** |
| IGF1R | Insulin-like growth factor 1 receptor | Growth Factor Receptors | **10,65697596** | **3,413726209** |
| RB1 | RB Transcriptional Corepressor 1 | Drug Resistance | **14,49136118** | **3,857121209** |
| CYP1A1 | Cytochrome P450 Family 1 Subfamily A Member 1 | Drug Metabolism | **16,52288853** | **4,046394016** |
| BCL2 | B-cell CLL/lymphoma 2 | Drug Resistance | **19,21** | **4,263785614** |
| DHFR | Dihydrofolate Reductase | Drug Metabolism | **26,6110444** | **4,733953228** |
| ABCC5 | ATP-binding cassette, sub-family C (MDR/TAP), member 5 | Drug Resistance | **38,18152012** | **5,254802637** |
| MYC | V-myc myelocytomatosis viral oncogene homolog (avian) | Transcription Factors | **48,03486946** | **5,586010162** |
| TP53 | Tumor Protein P53 | Drug Resistance | **66,70823351** | **6,059792933** |
| BCL2L1 | BCL2 Like 1 | Drug Resistance | **82,25697903** | **6,362066183** |
| CYP2B6 | Cytochrome P450 Family 2 Subfamily B Member 6 | Drug Metabolism | **82,25697903** | **6,362066183** |
| ERBB3 | V-erb-b2 erythroblastic leukemia viral oncogene homolog 3 (avian) | Growth Factor Receptors | **179,0674808** | **7,484359553** |
| BLMH | Bleomycin Hydrolase | Drug Metabolism | **192,2875116** | **7,587121258** |

| | | | | |
|---|---|---|---|---|
| SOD1 | Superoxide dismutase 1, soluble | Drug Metabolism | **311,0007633** | **8,280774311** |
| MSH2 | MutS homolog 2, colon cancer, nonpolyposis type 1 (E. coli) | DNA Damage and Repair | **506,1907132** | **8,983537229** |
| ABCC3 | ATP-binding cassette, sub-family C (MDR/TAP), member 3 | Drug Resistance | **587,72** | **9,198985184** |

**Summary of gene expression analysis following RT-qPCR using the cancer drug resistance RT² Profiler PCR Array. Results display an overall upregulation of thirty-seven genes involved in cancer drug resistance following hypoxia-induced EMT with only three genes being downregulated. Cells were colored according to fold change and $Log_2$ fold change (control/hypoxia-induced EMT MCF-7 cells) with the intensity of color corresponding to the degree of fold change.*

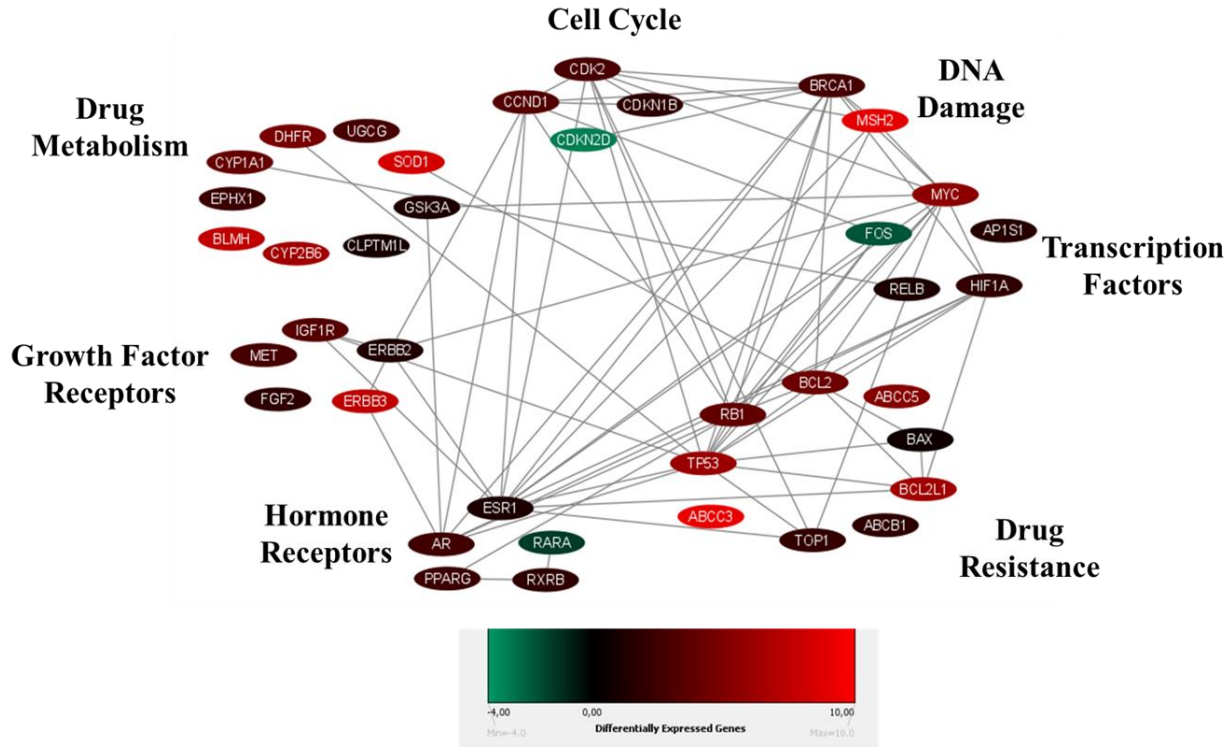



**Figure 4.7: Network map of genes involved in cancer drug resistance pathways following hypoxia-induced EMT**

*A network map of genes involved in cancer drug resistance post-hypoxia induced EMT was created using Cytoscape. Nodes (genes) were colored according to $Log_2$ fold change (control/hypoxia-induced EMT MCF-7 cells) with the intensity of color corresponding to the degree of fold change. Potential gene interactions (links; coloured in grey) were generated using OmicsNet and visualized in Cytoscape. Genes were grouped according to the pathway they act in, demonstrating several intra-pathway and inter-pathway interactions.*

## 4.8. Delineating the link between hypoxia-induced EMT and cholesterol in MCF-7 cells

Incipient scientific evidence exists, elucidating cholesterol dyshomeostasis as a key requirement for cancer initiation, progression as well as drug resistance. In an attempt to understand how cellular cholesterol levels were affected following EMT-induction, a range of cholesterol staining assays were complete. Seeing that exposure to the aforementioned hypoxic conditions resulted in a stable EMT phenotype, cells that were grown under normoxic conditions will be referred to as pre-EMT cells and cells that were exposed to hypoxic conditions will be referred to as post-EMT cells for the remainder of the dissertation. Results corresponding to each of the cholesterol assays conducted will be further elaborated on below.

### *4.8.1. Filipin Staining*

To delineate how hypoxia induced-EMT would affect free cellular cholesterol levels, filipin staining was completed. Filipin is known to form a tight complex with sterols possessing a planar steroid nucleus, an unesterified 3β hydroxyl group, as well as an apolar side chain at the C-17 position. This UV-excitable dye, when excited by light of a specific wavelength (360 nm) will emit light of a wavelength (480 nm) corresponding to blue fluorescence. This will consequently facilitate the quantification of free cholesterol in cells. It is evident that free cholesterol increases by 10.36% (ns) following hypoxia-induced EMT in MCF-7 cells as indicated by the increased fluorescence intensity *(Figure 4.8A)*. Treatment with MβCD proved more effective in lowering cellular cholesterol in the pre-EMT (48.93%) state relative to post-EMT (40.68%) *(Figure 4.8B)*. Importantly, free cholesterol was significantly reduced following treatment with KS-01 (63.34%) or Simvastatin (80.50%) in MCF-7 cells with the effect for both being more prominent in the post-EMT state *(Figure 4.8C and D)*.

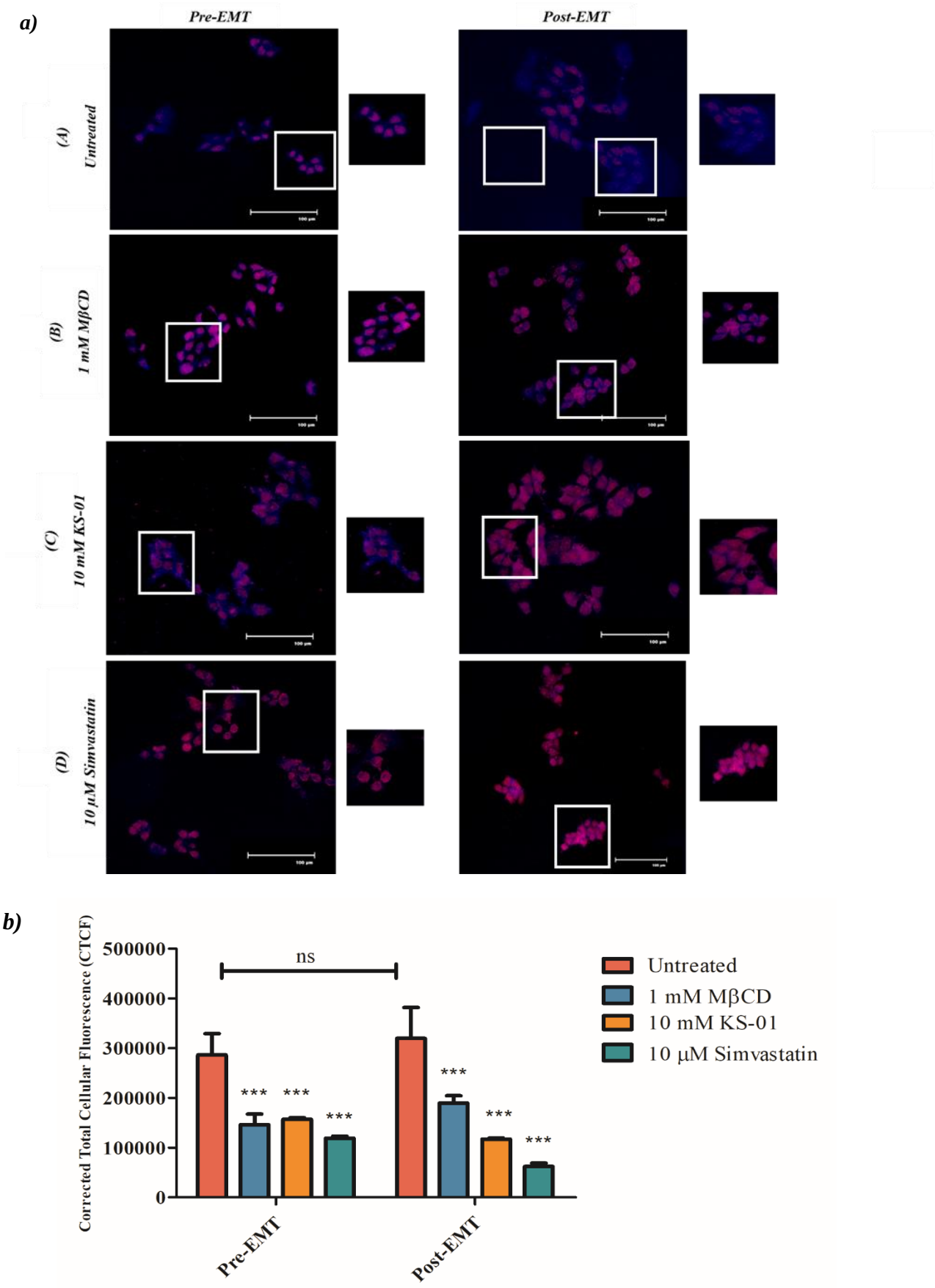


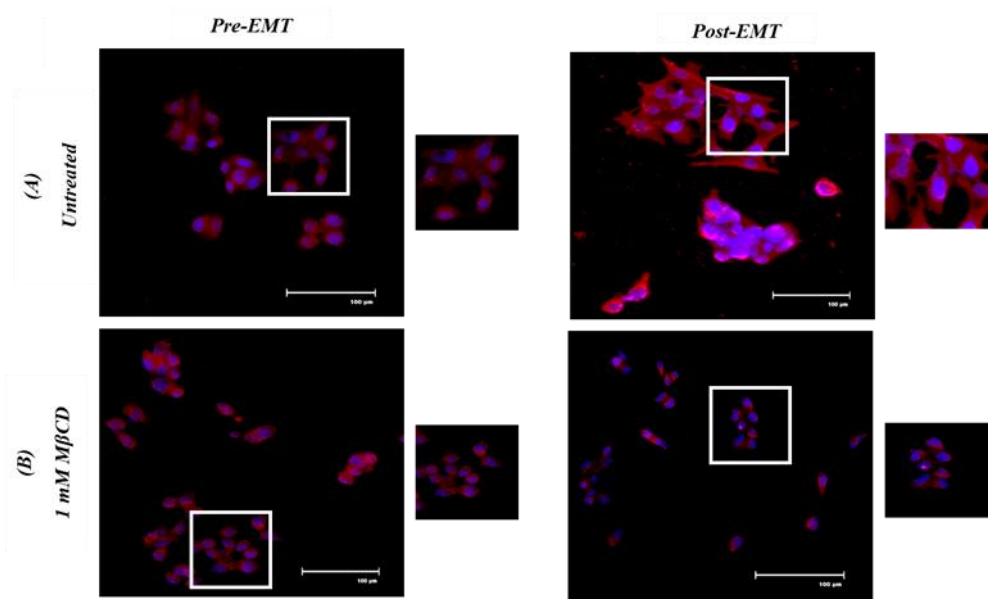

**Figure 4.8: Quantifying free cholesterol levels following cholesterol depletion in MCF-7 cells pre- and post-EMT induction**

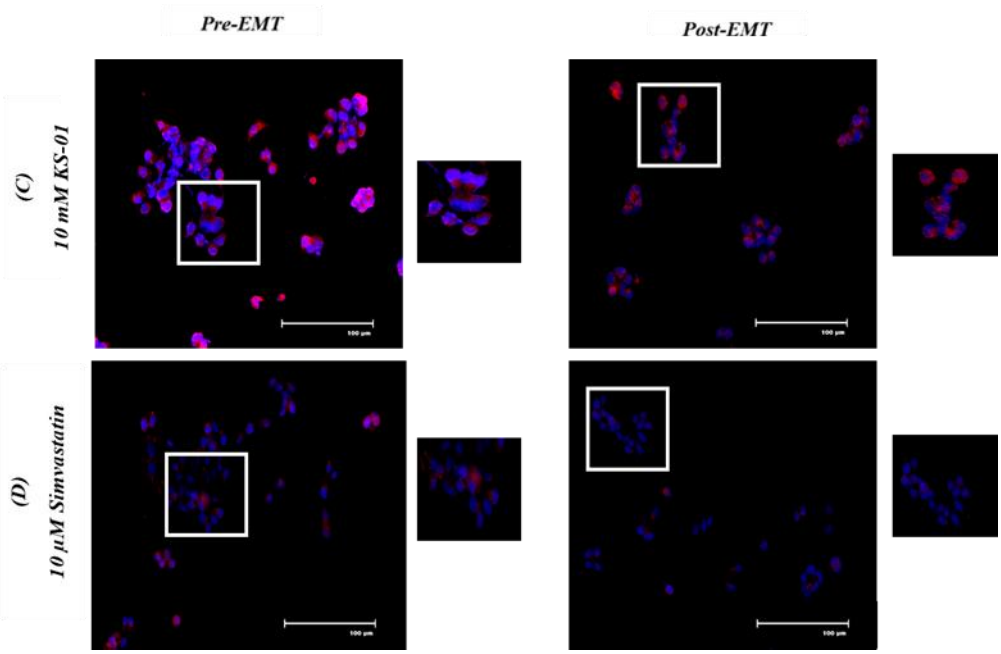
***(a)*** *Visual Representation indicating the levels of free cholesterol following treatment with various cholesterol targeting agents in MCF-7 cells pre- and post-EMT induction. Cellular cholesterol level is indicated by Filipin staining (blue) while nuclei are stained with NucRed™ Dead (red).* ***(b)*** *Representative graph indicating the CTCF which serves as a direct indication of cellular cholesterol content in MCF-7 cells following treatment with cholesterol targeting agents pre- and post-EMT induction. Images were captured using the Floid™ Cell Imaging System followed by analysis using the Image J software. The scale bar on each of the images represents 100 µm. A two-way ANOVA was performed for statistical analysis. A Bonferroni post-hoc test was employed for pairwise analysis comparing treated groups to untreated groups in pre- and post-EMT cells. Data represent the mean ± standard deviation. n=3. *P < 0.05, ** P < 0.01, *** P < 0.001.*

### *4.8.2. Vybrant Alexa Fluor® Lipid Raft Labelling*

Vybrant lipid raft labelling was completed to further quantify the effects of hypoxia-induced EMT on membrane cholesterol levels. The cholera toxin subunit B (CT-B) recognizes and binds to the pentasaccharide chain of plasma membrane ganglioside $G_{M1}$. By conjugating a fluorescent probe to the antibody directed against CT-B, selective localization, and visualization of lipid raft cholesterol content in cells is mediated. Similar to free cholesterol levels, a significant increase (30.66%; p=0.0115) in lipid raft cholesterol content post-EMT induction is documented in MCF-7 cells *(Figure 4.9)*. Importantly, a significant decrease in lipid raft cholesterol content was observed by employing membrane cholesterol depletion through treatment with MβCD (78.82%) and KS-01 (85.06%) as well as cholesterol synthesis inhibition through Simvastatin administration (86.84%) *(Figure 4.9)*. In all instances, a reduction of lipid raft content following compound administration proved more effective in the post-EMT state *(Figure 4.9)*.

***a)***






***b)***

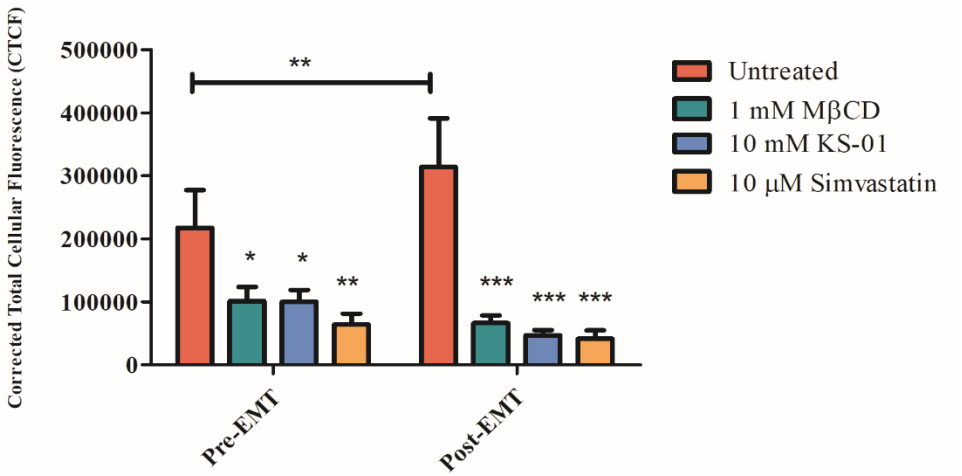



**Figure 4.9: Quantifying membrane cholesterol levels following cholesterol depletion in MCF-7 cells pre- and post-EMT induction**

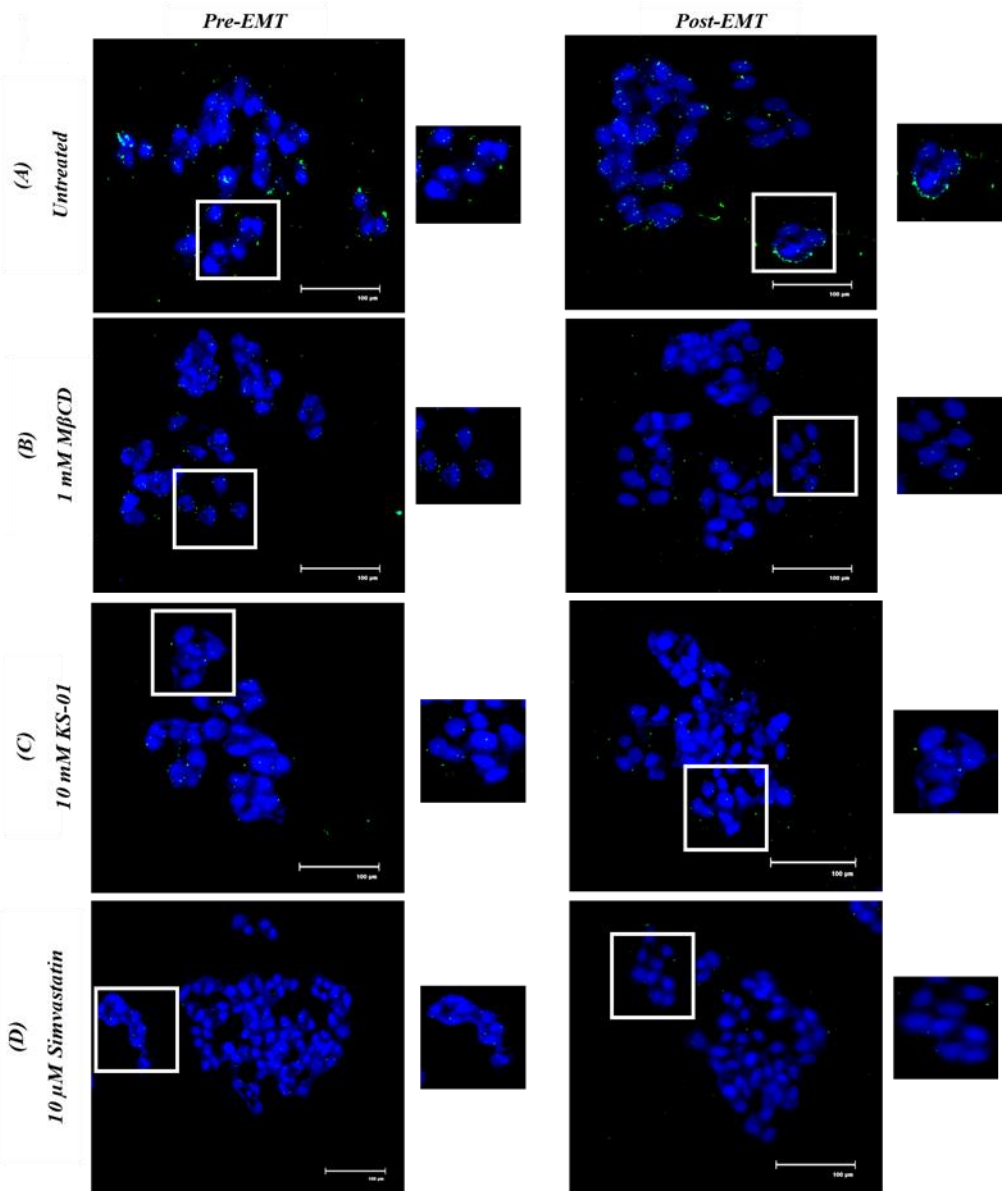
***(a)*** *Visual Representation indicating the levels of membrane cholesterol following treatment with various cholesterol targeting agents in MCF-7 cells pre- and post-EMT induction. Membrane cholesterol level is indicated by Alexa Fluor 594 staining (red) while nuclei are stained with DAPI (blue).* ***(b)*** *Representative graphs indicating the CTCF which serves as a direct indication of membrane cholesterol content in MCF-7 cells following treatment with cholesterol targeting agents pre- and post-EMT induction. Images were captured using the Floid™ Cell Imaging System followed by analysis using the Image J software. The scale bar on each of the images represents 100 µm. A two-way ANOVA was performed for statistical analysis. A Bonferroni post-hoc test was employed for pairwise analysis comparing treated groups to untreated groups in pre- and post-EMT cells. Data represent the mean ± standard deviation. n=3. *P < 0.05, ** P < 0.01, *** P < 0.001.*

.

### *4.8.3. BODIPY Staining*

In an attempt to quantify how lipid droplet CE content changes following hypoxia-induced EMT, BODIPY staining was completed. The non-polar nature of this neutral lipophilic fluorophore allows for efficient diffusion into neutral lipid droplets and subsequent conjugation to C-24 of the sterol ring. When excited by light of a wavelength corresponding to 493 nm, the fluorophore emits a bright green fluorescence. Hypoxia-induced EMT resulted in a significant increase (31.89%; p=0.0051) in CE content in MCF-7 cells *(Figure 4.10)*. While a significant decrease in CE content was observed following treatment with either MβCD (81.42%), KS-01 (85.20%) or Simvastatin (92.19%), with the reduction proving more effective in the post-EMT state *(Figure 4.10)*.

***a)***



***b)***

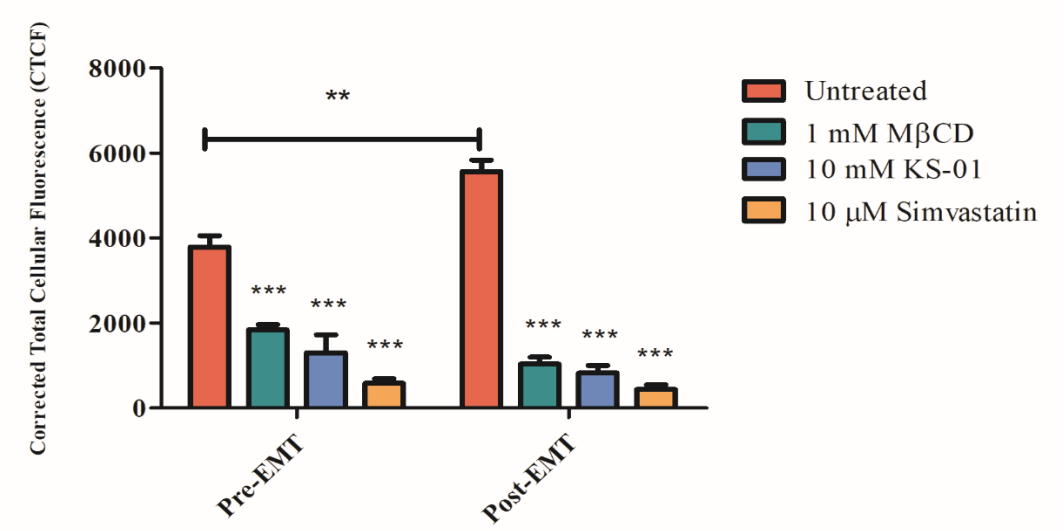



**Figure 4.10: Quantifying cholesteryl ester levels in lipid droplets following cholesterol depletion in MCF-7 cells pre- and post-EMT induction**

***(a)*** *Visual Representation indicating the levels of lipid droplet cholesteryl esters following treatment with various cholesterol targeting agents in MCF-7 cells pre- and post-EMT induction. Lipid droplet cholesteryl ester levels is indicated by BODIPY staining (green) while nuclei are stained with DAPI (blue).* ***(b)*** *Representative graphs indicating the CTCF which serves as a direct indication of cholesteryl ester content in MCF-7 cells following treatment with cholesterol targeting agents pre- and post-EMT induction. Images were captured using the Floid™ Cell Imaging System followed by analysis using the Image J software. The scale bar on each of the images represents 100 µm. A two-way ANOVA was performed for statistical analysis. A Bonferroni post-hoc test was employed for pairwise analysis comparing treated groups to untreated groups in pre- and post-EMT cells. Data represent the mean ± standard deviation. n=3. *P < 0.05, ** P < 0.01, *** P < 0.001.*

### *4.8.4. Analyzing the Effect of Targeting Cellular Cholesterol in EMT*

Based on the observation that cells post-EMT induction presented with increased levels of free cholesterol, membrane lipid raft cholesterol as well as CEs together with scientific evidence implicating cholesterol in regulating EMT-related signalling pathways, we consequently sought to elucidate the effect of targeting cellular cholesterol on EMT state in MCF-7 cells by studying the protein expression of EMT molecular markers E-cadherin and vimentin following cholesterol synthesis inhibition/depletion. Importantly, employing cholesterol synthesis inhibition/depletion in post-EMT cells lead to a significant increase in E-cadherin and decreased expression of vimentin (*Figure 4.11 and 4.12*). It can thus be postulated that targeting cellular cholesterol in post-EMT cells helps promote restoration of an epithelial phenotype.

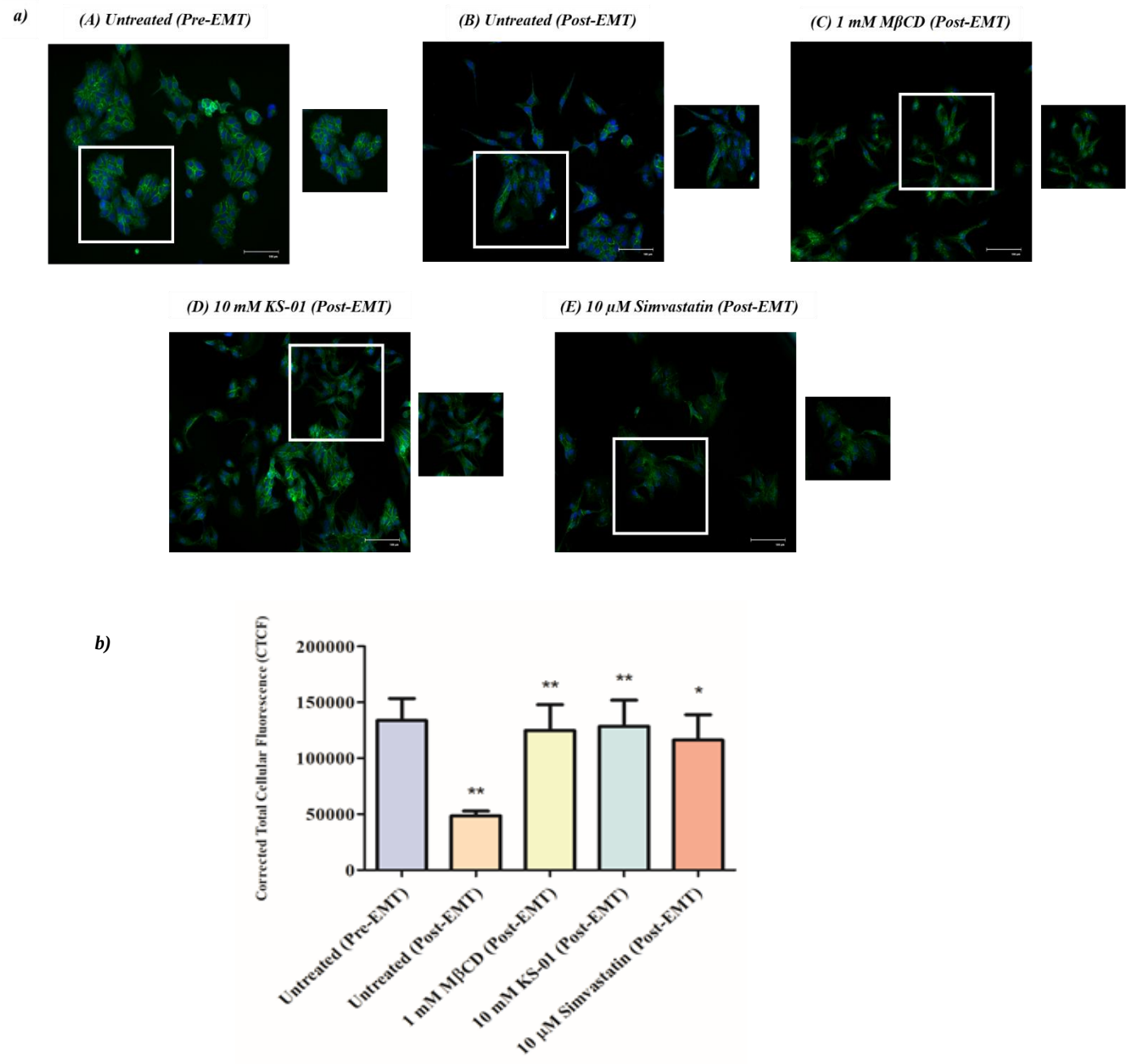



**Figure 4.11: Quantifying E-cadherin expression in MCF-7 cells following treatment with cholesterol targeting agents**

***(a)*** *Visual Representation indicating the protein expression of E-cadherin following treatment with various cholesterol targeting agents in MCF-7 cells pre- and post-EMT induction. E-cadherin expression is indicated by Alexa Fluor 488 staining (green) while nuclei are stained with DAPI (blue).* ***(b)*** *It is evident that treatment with cholesterol targeting agents leads to an increase in the expression of E-cadherin with the effect being significant in post-EMT cells. Images were captured using the Floid™ Cell Imaging System followed by analysis using the Image J software. The scale bar on each of the images represents 100 µm. A one-way ANOVA as well as the Bonferroni post-hoc test was employed for statistical analysis where data represent the mean ± standard deviation. n=3. * P < 0.05, ** P < 0.01, *** P < 0.001.*

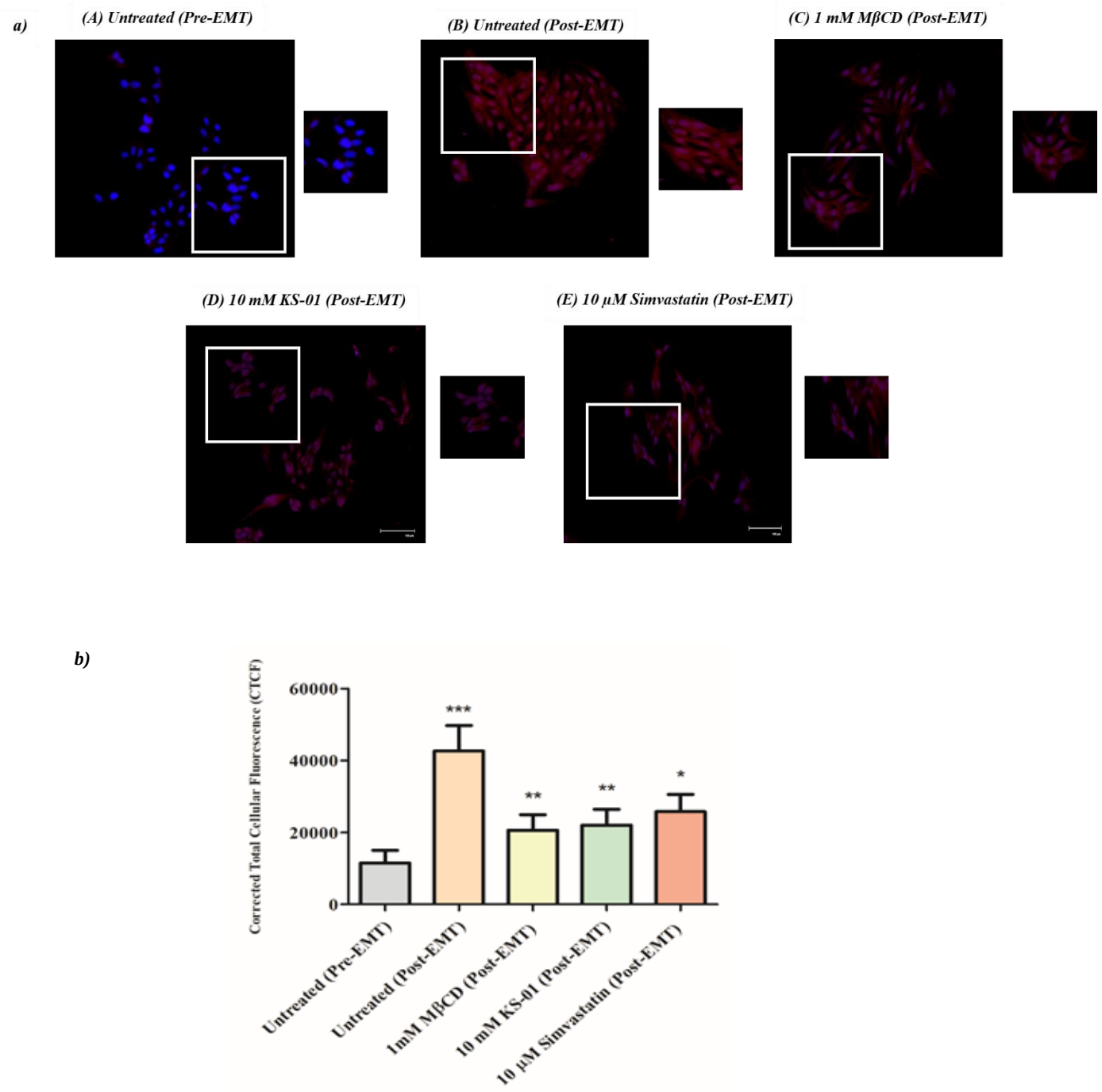



**Figure 4.12: Quantifying vimentin expression in MCF-7 cells following treatment with cholesterol targeting agents**

***(a)*** *Visual Representation indicating the protein expression of vimentin following treatment with various cholesterol targeting agents in MCF-7 cells pre- and post-EMT induction. Vimentin expression is indicated by Texas Red staining (red) while nuclei are stained with DAPI (blue).* ***(b)*** *It is evident that treatment with cholesterol targeting agents lead to a decrease in the expression of vimentin with the effect being significant in post-EMT cells. Images were captured using the Floid™ Cell Imaging System followed by analysis using the Image J software. The scale bar on each of the images represents 100 µm. A one-way ANOVA as well as the Bonferroni post-hoc test was employed for statistical analysis where data represent the mean ± standard deviation. n=3. * P < 0.05, ** P < 0.01, *** P < 0.001.*

## 4.9. Assessing the invasive potential of MCF-7 cells post-EMT induction following treatment with cholesterol targeting agents

Seeing that cholesterol synthesis inhibition/depletion in post-EMT cells lead to a significant increase in E-cadherin and decreased expression of vimentin, we consequently sought to investigate the resulting effect on invasive potential following cholesterol synthesis inhibition/depletion. When comparing the untreated groups pre- and post-EMT it is evident that post-EMT cells display a highly significant increase (85.15%) in invasive potential. Importantly, treating post-EMT cells with cholesterol targeting agents led to a significant decrease in invasive potential, with a documented 70.31% decrease following treatment with 1 mM MβCD, 66.86% decrease following treatment with 10 mM KS-01 and an 80.2% decrease following treatment with 10 µM Simvastatin *(Figure 4.13)*.

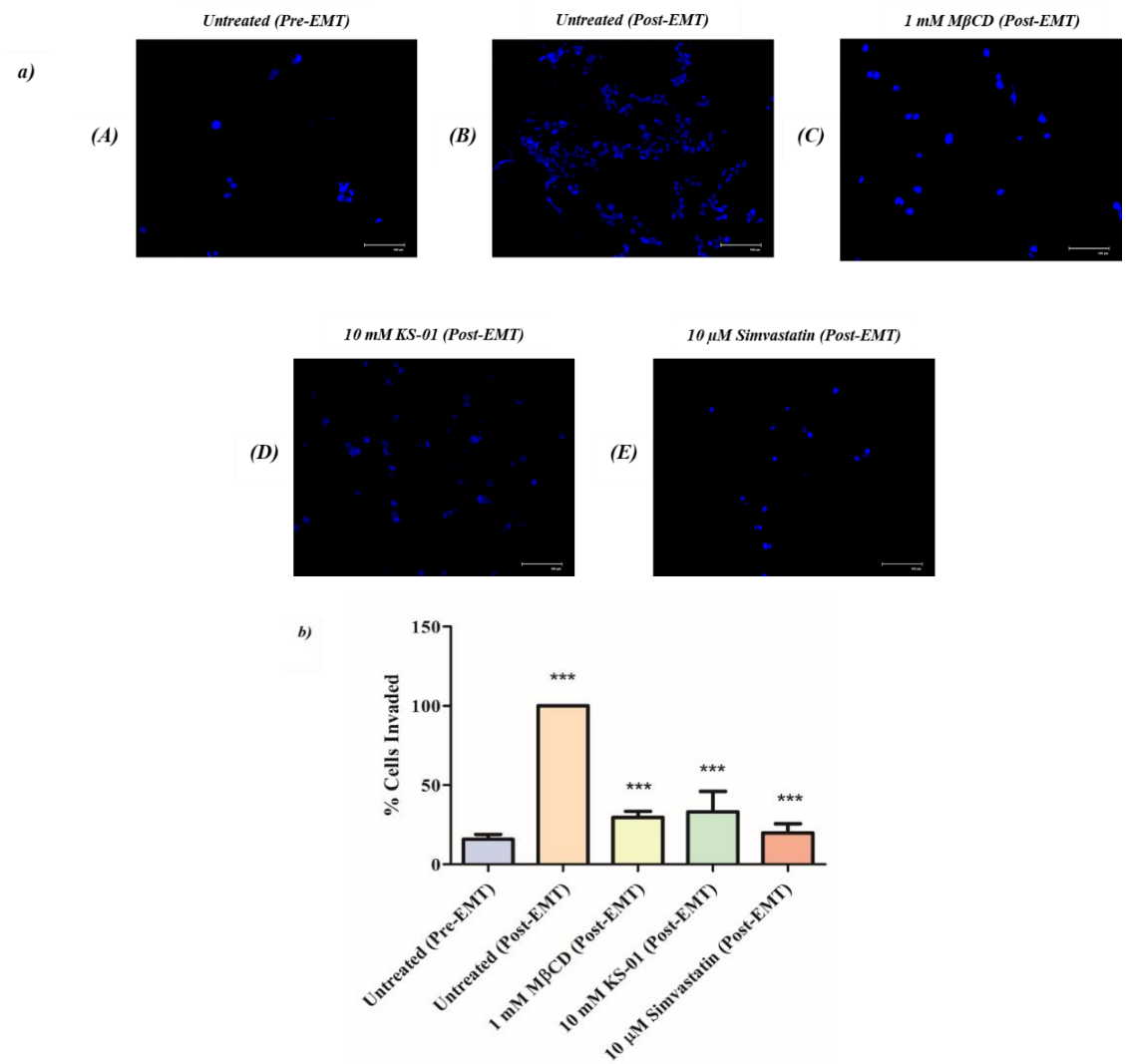



**Figure 4.13: Assessing the invasive potential of MCF-7 cells following treatment with cholesterol targeting agents**

***(a)*** *Visual Representation indicating the number of cells that have invaded following treatment with various cholesterol targeting agents in MCF-7 cells pre- and post-EMT induction. Nuclei staining with DAPI (blue) facilitates visualization.* ***(b)*** *It is evident that hypoxia-induced EMT lead to a significant increase in invasive potential of MCF-7 cells. Treatment with cholesterol targeting agents decreased the invasive potential of post-EMT cells. Images were captured using the Floid™ Cell Imaging System followed by analysis using the Image J software. The scale bar on each of the images represents 100 µm. A one-way ANOVA as well as a Bonferroni post-hoc test was employed for statistical analysis where data represent the mean ± standard deviation. n=3 * P < 0.05, ** P < 0.01, *** P < 0.001.*

## 4.10. Analysing the drug resistant potential of MCF-7 cells post-EMT induction following treatment with cholesterol targeting agents

Hypoxic induction and enhanced MDR potential is a well-documented link in cancer. Importantly, cholesterol plays a multi-faceted role in modulating the expression as well as the activity of MDR transporters including MDR1. To assess the functionality of the key drug transporter MDR1 following cholesterol synthesis inhibition/depletion the intracellular retention of fluorescent calcein (metabolized MDR1 substrate) was measured. Seeing that MCF-7 cells without hypoxic induction do not express the MDR1, intracellular retention of calcein was set to 100%. Hypoxia-induced EMT led to a significant increase in MDR potential as evidenced by the 47.13% decrease in calcein retention. Importantly, treating post-EMT cells with cholesterol targeting agents led to a significant decrease in MDR potential, as evidenced by the increase in calcein retention following treatment with 1 mM MβCD (45.01%), 10 mM KS-01 (41,27%) and 10 µM Simvastatin (35.31%) (*Figure 4.14*).

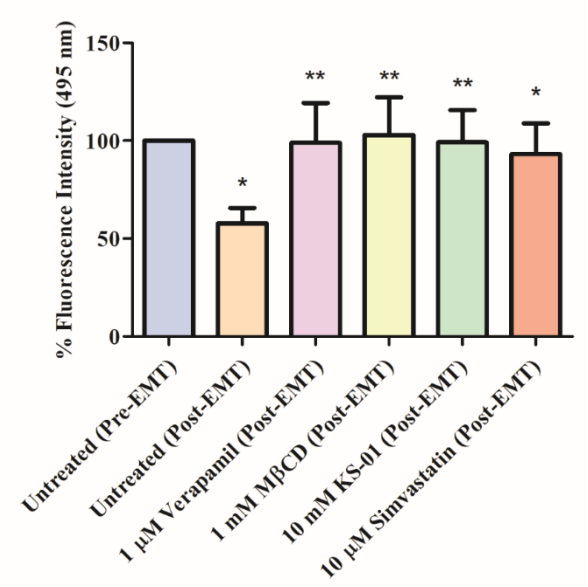



**Figure 4.14: Evaluating the effect of targeting cholesterol on the functionality of the MDR1 transporter**

*Intracellular retention of fluorescent calcein in MCF-7 cells was significantly increased following treatment with cholesterol targeting agents post-EMT, therefore potentiating treatment with cholesterol targeting agents as suitable means to abrogate MDR potential. Fluorescence intensity (RFU) was quantified using the Victor Nivo multi-mode microplate reader (Perkin Elmer, USA) with the excitation maximum set to 494 nm and the emission maximum set to 517 nm. A one-way ANOVA as well as a Bonferroni post-hoc test was employed for statistical analysis where data represent the mean ± standard deviation. n=3 * P < 0.05, ** P < 0.01, *** P < 0.*

## 5. Discussion:

Based on the pleotropic role of cholesterol in the cell, it is not surprising that cancer cells have evolved several mechanisms to facilitate cholesterol dyshomoestasis to meet their increased metabolic demands. Additionally, an increase in cholesterol content corresponds to an increase in lipid raft presence. Seeing that lipid rafts house several cell signalling proteins, alteration to lipid raft domains may therefore influence cell signalling pathways that ultimately augment neoplastic transformation (Zalba and ten Hagen, 2017). These rafts in turn regulate crucial processes that cancer cells subvert such as proliferation, migration, invasion, and apoptosis. Importantly, activation of the cellular EMT program is crucial to mediating tumorigenesis. Interestingly, incipient scientific evidence exists documenting that cellular cholesterol availability is crucial to regulating the activity of protein intermediates in EMT-related signalling pathways. Seeing that the link between cholesterol dyshomeostasis and EMT is a relatively novel field that has not been well explored, the present study sought to delineate how the cellular cholesterol profile of the MCF-7 breast adenocarcinoma cell line is altered following hypoxia-induced EMT. This was completed with the intention of proposing whether targeting cellular cholesterol in these cells might serve as a novel means of combatting aggressive cancer phenotypes while mediating drug sensitivity restoration.

### 5.1. $CoCl_2$ mediated induction of HIF-1α – Mechanism of action and resulting implications on the expression of downstream target proteins

During tumorigenesis, the rate of cell proliferation exceeds that of neo-angiogenesis which leads to a mismatch in oxygen consumption versus supply (Qiu et al., 2017a). In response to hypoxia, complex cellular mechanisms are activated which is principally mediated by the HIF family of proteins. This heterodimeric transcription factor consists of an oxygen sensitive α subunit as well as a constitutively expressed β subunit (Choudhry and Harris, 2018). Under normoxic conditions, hydroxylation of proline and arginine residues of HIF-1α, mediated by the prolyl hydroxylases (PHD) as well as factor inhibiting hypoxia (FIH) respectively, creates an interface which mediates the interaction with the von Hippel Lindau tumour suppressor protein (Nurwidya et al., 2012). This consequently results in the recruitment of the E3 ubiquitin ligase complex, polyubiquitination and subsequent degradation of the protein. Conversely, exposure to hypoxic conditions impedes hydroxylation on HIF-1α leading to increased stability of HIF-1α, dimerization with HIF-1β and subsequent translocation to the nucleus and binding to hypoxia response elements at target gene promoters (Hapke and Haake, 2020). In this study,

hypoxic conditions were mimicked by treating MCF-7 cells with the hypoxia mimetic $CoCl_2$. In general, hypoxia mimetics simulate a hypoxic environment by increasing cellular availability of HIF-1α. The mechanism for $CoCl_2$ mediated stabilisation of HIF-1α is explained by the substitution of $Co^{2+}$ for $Fe^{2+}$ in the active site of the PHD enzymes consequently impeding activity (Pavlacky and Polak, 2020b). Additionally, evidence exists implicating $CoCl_2$ in repressing the expression of FIH (Ke et al., 2005). This is achieved through the cobalt ion induced depletion of ascorbate, thereby leading to increased stability of HIF-1α (Hirsilä et al., 2005). The conditions seen to work best in stimulating HIF-1α induction for MCF-7 cells was demonstrated by the intense fluorescent staining and nuclear localisation of HIF-1α following a 48-hour incubation with 150 µM $CoCl_2$. This condition corresponds well to previous studies conducted in MCF-7 cells, justifying the increased stability of HIF-1α following $CoCl_2$ treatment (Li et al., 2018, Chen et al., 2010).

To further corroborate that the afore-mentioned conditions induced HIF-1α expression and was associated with an increase in transcriptional activity, the expression of a downstream target protein VEGF was evaluated. Hypoxia-mediated induction of VEGF is seen to facilitate neoangiogenesis to compensate for the decreased oxygen tension in tissues. While this process is crucial to supporting persistence of the parental tumour, angiogenesis further mediates metastatic dissemination (Gilkes and Semenza, 2013).

An increase in the expression of VEGF following $CoCl_2$ treatment also corresponds with findings reported in other studies (Li et al., 2015a, Rana et al., 2019). This result is justified by scientific evidence indicating that HIF-1 serves as a master stimulator of VEGF expression, by directly binding to specific HRE located at nucleotide positions –947 to –939 (5′-TACGTG-3′) relative to the common transcription start site (Olenyuk et al., 2004). While binding of HIF-1 to the promoter is well documented, several studies conducted also implicate STAT3 in mediating HIF-1-induced expression of VEGF (Jahangiri et al., 2018). STAT3 is seen to increase the stability of HIF-1α and further enhances its transcriptional capability by forming a complex with the transcriptional co-activator CBP/p300 (Carbajo-Pescador et al., 2013). Recent evidence indicates that binding of both TFs to VEGF promoters leads to maximal expression (Jahangiri et al., 2018). Moreover, VEGF is a principal angiogenesis inducer and is known to increase the expression of various other proangiogenic factors that bind to cellular receptors to mediate neoangiogenesis (Zimna and Kurpisz, 2015). Consequently, both direct and indirect regulation of proangiogenic factors thus implicates HIF-1 in the regulation of every step of angiogenesis (Zimna and Kurpisz, 2015).

Besides angiogenesis, evidence exists implicating VEGF in cancer aggressiveness through its EMT modulatory effects. Studies conducted in nasopharyngeal carcinoma implicate VEGF in regulating the expression of EMT markers and matrix metalloproteinases (MMPs) in an autocrine manner to promote metastasis (Chen et al., 2020). Similarly, studies conducted in prostate cancer identify that the expression of VEGF confers cells with features characteristic of EMT and further enhances TGF-β1 signalling (Gonzalez-Moreno et al., 2010). The increased VEGF stimulates an autocrine loop which enhances migration and invasive potential of cells. In BC, VEGF is seen to induce the expression of Snail, by impeding the activity of the established Snail inhibitor Glycogen synthase kinase-3 (GSK3) and in this way mediates EMT (Wanami et al., 2008). Similarly, VEGF-mediated activation of Vascular Endothelial Growth Factor Receptor 1 (VEGFR1) was shown to increase the nuclear expression of the TFs Snail, Slug and Twist consequently mediating EMT and potentiating pancreatic cancer aggressiveness (Yang et al., 2006).

It is important to emphasise, even though HIF-1α is the main regulator of VEGF expression, other mechanisms may also contribute to its expression in tumorigenic cells (Ferrara, 2004). This could account for the expression of VEGF in MCF-7 cells that were cultured under control conditions. One of the mechanisms is illustrated in a study conducted by Fuji *et al.*, where authors implicate the mTOR pathway in regulating the expression of VEGF in MCF-7 cells (Fujii et al., 2016).

### 5.2. Effect of $CoCl_2$ on cell viability and proliferation

In terms of the effect of $CoCl_2$ treatment on cell viability, maintaining the afore-mentioned treatment conditions for 3 days did not significantly affect the viability of MCF-7 cells. This contrasts with treatment with 200 µM which significantly affected the viability of cells. This result also corresponds with previous studies conducted in MCF-7 cells, where cells displayed maximal proliferation following treatment with 150 µM $CoCl_2$ and any further increases in the concentration resulted in a gradual decrease in the proliferation rate (Rana et al., 2019, Zhang et al., 2018b). This result was further recapitulated in other cell lines indicating that treatment with $CoCl_2$ at doses below 200 µM for a duration of 24 -72 hours did not significantly affect cell viability (Kong et al., 2015, Zhang et al., 2017b). Studies identify that treating cells with concentrations exceeding 200 µM results in oxidative DNA damage due to the accumulation of reactive oxygen species (ROS) together with abrogation of DNA repair which ultimately results in cell death (Lison et al., 2001, Simonsen et al., 2012).

To further validate the effect of hypoxia-induced EMT on cell viability, the expression and localisation of the cell proliferation antigen Ki-67 was analysed. Ki-67 is constitutively expressed in actively dividing cells (Sobecki et al., 2016). Interestingly, MCF-7 cells cultured under hypoxic conditions displayed decreased expression of Ki-67 relative to control cells. While this observation appears to contradict the results obtained through cell counts, this observation can be justified. Studies conducted by Sobecki *et al.* document that Ki-67 expression varies throughout the cell cycle, where the highest expression is detected in G2 and M-phase indicating that Ki-67 is a late marker of cell cycle entry (Sobecki et al., 2016). Conversely, cells that have recently entered the cell cycle or following cell cycle exit display low levels of Ki-67 (Sobecki et al., 2016). Depending on the cell cycle stage cells were in when fixed, this would directly affect the expression of Ki-67 detected in cells and consequently justifies the reduced expression in cells post-EMT induction. Furthermore, Ki-67 expression is also dependent on CDK2 activity, where cells with low CDK2 activity display a continuous decay of Ki-67 and cells with increased CDK2 activity present with an accumulation of Ki-67 (Miller et al., 2018). Importantly, hypoxia is seen to negatively affect CDK2 activity, by upregulating the expression of cyclin-dependent kinase inhibitor p27 and further suppresses expression of the *CDC25A* phosphatase that is required for activation of cyclin E-CDK2 complex (Druker et al., 2021, Hasvold et al., 2016). Additionally, evidence exists indicating that the lack of CDK2 activity in hypoxic cells is not attributed to decreased CDK2 protein level or decreased expression of cyclin binding proteins but rather due to inhibitory phosphorylation on the tyrosine 15 residue which results in unproductive binding of ATP (substrate) hence impeding the catalytic activity of CDK2 (Malumbres, 2014).

Furthermore, recent studies indicate that CDK2 temporally controls the activity of PHDs through phosphorylation on specific amino acid residues. This consequently contributes to increased activity of the PHD enzymes thereby facilitating PHD-mediated degradation of HIF-1α. Additionally, CDK2 when complexed with Cyclin E further promotes HIF-1α degradation through autophagy (Druker et al., 2021). The decreased activity of CDK2 can hence be justified as an adaptation of MCF-7 cells to hypoxic conditions. On this basis, it can be proposed that due to the decreased CDK2 activity in hypoxic cells, Ki-67 is more susceptible to degradation and hence cells present with decreased expression post-EMT.

### 5.3. Alterations to Cellular Morphology and Resulting Implications following Hypoxia-Induced EMT

The EMT is classified as a cell plasticity program. Previously thought to operate as a binary switch, current experimental evidence highlights a significant degree of plasticity where instead of transitioning between full epithelial to full mesenchymal phenotype, cells traverse through a spectrum of intermediate states along the epithelial-mesenchymal axis expressing varying levels of epithelial and mesenchymal markers (Nieto et al., 2016). Interestingly, the existence in a hybrid state occurs more frequently than expected conferring upon cancer cells dynamic cellular plasticity leading to poor clinical outcome.

In this study, the effect of hypoxia on EMT induction was investigated. Following $CoCl_2$ treatment, MCF-7 cells altered cell morphology from the characteristic cobble stone-like morphology of an epithelial cell to adopt an elongated spindle-like appearance possessing abundant cellular protrusions, features characteristic of a mesenchymal cell phenotype. Moreover, a significant decrease in the expression of the epithelial protein E-cadherin was observed, with a concomitant increase in the expression of the mesenchymal marker vimentin which often serves as a hallmark event in EMT induction. E-cadherin is classified as an adherens junctional protein which mediates epithelial cell attachment (Bhatt et al., 2013) forming intercellular adhesive complexes including tight junctions and desmosomes which confers epithelial cells with the characteristic property of apico-basal polarity and further contributes to the maintenance of epithelial tissue architecture (Bhatt et al., 2013). On this basis, disruption of cell-cell and cell-ECM interactions is seen to mediate altered cell-adhesion signalling leading to a loss of epithelial-cell integrity (Yu et al., 2019).

Furthermore, MCF-7 cells display cytoskeletal compositional changes, possessing increased levels of the type III intermediate filament, vimentin. Vimentin is known to influence cytoskeletal architecture through its interactions with microfilaments and microtubules present within cells (Liu et al., 2015). Linking of actin cytoskeleton with microtubules is facilitated by vimentin, which consequently confers upon vimentin a crucial role in the regulation of cytoskeletal structure. The altered cytoskeletal structure facilitates mechanical force stability. This is elucidated by studies conducted highlighting that the expression of vimentin in epithelial cells results in epithelial cell flattening allowing the cell to adapt to and resist compression and deformation forces that cells are susceptible to as they navigate from primary tumours to secondary sites (Mendez et al., 2010). One of the ways it achieves this is by

increasing cytoplasmic stiffness which enhances stability of cellular organelles (Lowery et al., 2015). In like manner, vimentin mechanically cushions the cell nucleus protecting it from compressive forces, consequently impeding nuclear rupture by forming a stiff shell surrounding the nucleus, when cells are placed in highly confined spaces during cell migration (Leggett et al., 2021).

Equally important, the expression of vimentin also facilitates microtubule polarisation to mediate cell-directional migration (Liu et al., 2015). Interestingly, vimentin serves as a template for the creation of new microtubule networks, with the templating function seen to stabilise cell polarity and facilitate directional migration (Gan et al., 2016). Alterations to the cytoskeleton lead to altered cell polarity, where cells transition from apical-basal polarity to adopt a front-rear polarity (Wesseling et al., 2018). The front side of the cell possesses Cdc42 and Rac1 (members of the Rho family of GTP-binding proteins) that promote the polarisation of actin and further facilitates the establishment of membrane protrusions, consequently forming the leading edge of the cell (Wesseling et al., 2018). The rear-side of the cell harbours RhoA which mediates actomyosin contractility and retraction. Consequently, adopting the front-rear polarity confers cells with crucial traits required for cancer cell motility (Wesseling et al., 2018).

### 5.4. Molecular Mechanisms facilitating Hypoxia-induced EMT

Intratumoral hypoxia serves as a strong selective pressure that confers cells with specific traits to exacerbate malignant potential while overcoming low oxygen conditions and impeding apoptotic induction (Gilkes and Semenza, 2013). Molecular mechanisms employed by cancer cells in response to low cellular oxygen tension, potentiates increased stability of the HIFs, which when expressed modulates epithelial to mesenchymal plasticity (Gilkes and Semenza, 2013). The two main mechanisms, *(i)* directly activating EMT master TFs and *(ii)* activation of EMT-related signalling pathways are further elaborated on below and justifies the increased expression of mesenchymal markers and the observed phenotype following hypoxic induction in MCF-7 cells.

Hypoxia induced signalling of HIF, mediates either a direct or indirect induction of cellular EMT. Notably, several studies conducted implicate hypoxia-induced expression of HIF-1α in the direct activation of EMT master TF's. Hypoxia-induced stabilisation of HIF-1α is also seen to promote SNAIL expression, as proposed by the identification of two HRE's in the promoter

region (Zhang et al., 2013a). Studies conducted by Yang *et al*., document that HIF-1α directly regulates the expression of TWIST1, which is attributed to the presence of a HRE in the proximal promoter region of TWIST1 (Yang et al., 2008). Additionally, studies report HIF-1α mediated regulation of ZEB1 by binding to HRE3 in the proximal promoter region (Zhang et al., 2015b). In all the afore-mentioned studies, HIF-1α-induced expression of EMT master TFs induced a significant decrease in the expression of epithelial markers with a concomitant gain in mesenchymal markers leading to enhanced migratory and invasive potential (Yang et al., 2017, Joseph et al., 2015).

Indirect mediation of hypoxia-induced EMT is documented by studies elucidating the modulatory effect of HIF-1α on the expression and activity of intermediates in various EMT-related signalling pathways.

Focusing on TGF-β, hypoxia is documented to stimulate the production of TGF-β in cancer cells which consequently implies that TGF-β-induced EMT signalling is potentiated by hypoxia (Furuta et al., 2015). This is justified by the observation of TGF-β-mediated Smad-3 dependent transcription of Snail, Slug and Twist. Consequently, targeting Smad3 abrogates TGF-β1 mediated EMT induction (Jo et al., 2015). Hypoxia is also seen to facilitate autocrine TGF-β/TGF-βR1 signalling, consequently increasing the expression of Twist and Zeb1 leading to EMT induction (Matsuoka et al., 2013). Conversely, TGF-β is also seen to decrease the expression of PHD2 through the Smad signalling pathway, leading to impaired prolyl hydroxylation of HIF-1α and increased stability (McMahon et al., 2006). This observation points to the existence of a positive feedback loop between these two signalling pathways.

Experimental evidence also exists, implicating hypoxia in regulating Wnt-induced EMT. Studies conducted in lung cancer identify that hypoxia mediated induction of *SNAIL* and *SLUG* decreased E-cadherin expression which consequently promoted nuclear translocation of β-catenin (Liu et al., 2018). Subsequent activation of β-catenin was pivotal in mediating EMT as evidenced by the increased expression of MMP-2, MMP-9, vimentin and fibronectin (Liu et al., 2018). Additionally, studies conducted by Hong *et al.* implicate hypoxia in increasing the stability of β-catenin through post-translational modifications and consequently enhancing Wnt signalling (Hong et al., 2017). Interestingly, studies conducted in hepatocellular carcinoma document the direct interaction between β-catenin and HIF-1α, which facilitates enhanced transcriptional activity of HIF-1α and further augments hypoxia-induced EMT (Zhang et al., 2013b). In prostate cancer, the Wnt signalling pathway is crucial for hypoxia-induced EMT,

where knockdown of β-catenin leads to EMT reversal consequently abrogating invasive potential of prostate cancer cells (Zhao et al., 2011). Furthermore, HIF-1α is implicated in transcriptional regulation of an essential Wnt/β-catenin co-activator Bcl9, by binding to HRE-B and HRE-C in the promoter region. Bcl9 is crucial in hypoxia mediated induction of the Wnt/β-catenin pathway (Xu et al., 2017).

In summary, it is clearly evident that hypoxia plays a crucial role in the mediating cellular EMT induction, conferring cancer cells with cellular traits that facilitates a more aggressive cancer phenotype.

### 5.5. Hypoxia-induced EMT potentiates drug resistance in MCF-7 cells

Even though scientific advances in cancer research continue to provide renewed hope to cancer patients with major improvements documented in surgery, MDR constitutes a major hurdle leading to therapy failure and ultimately mortality contributing to over 90% of cancer patients' deaths (Bukowski et al., 2020). Intrinsic drug resistance occurs when the tumour cell mass present with resistant mechanisms prior to therapy administration, while acquired resistance describes a condition where cells that were initially sensitive to therapy develop mechanisms that confer them with survival traits during therapy (Haider et al., 2020). Multiple mechanisms implicated in conferring drug resistance to cancer cells have been documented in literature which include but is not limited to: enhanced drug efflux capability, mutations to the drug targets, increased metabolism of xenobiotics leading to drug detoxification and concomitant inactivation, hyperactivation of survival pathways coupled with inactivation of apoptotic pathways as well as the induction of the epithelial-mesenchymal transition (EMT) (Bukowski et al., 2020, Haider et al., 2020, Ke and Shen, 2017, Housman et al., 2014, Du and Shim, 2016). Importantly, the acquisition of resistance is dictated by inherent genetic instability, mutagenicity of tumour cells as well as the influence of cells in the tumour microenvironment (Haider et al., 2020).

In terms of drug efflux pumps, exposing MCF-7 cells to hypoxic conditions led to an upregulation of *ABCB1* expression. This observation is justified by the presence HIF-1α binding site in the MDR1 gene, where inhibition of HIF-1 expression resulted in significant inhibition of hypoxia-inducible MDR1 expression and a nearly complete loss of basal MDR1 expression (Comerford et al., 2002). Furthermore, cells cultured under hypoxic conditions also presented with a significant increase in the expression of *ABCC3* and *ABCC5*. While evidence

does exist implicating hypoxia in the induction of *ABCC3* expression, other studies show that the master EMT TFs upregulate expression of both transporters by enhancing the promoter activity (Sakulterdkiat et al., 2012, Wang et al., 2019). It can thus be postulated that both hypoxia as well as hypoxia-induced activation of master EMT TFs is crucial to conferring MDR potential to cancer cells. Interestingly, studies also exist identifying a crucial role for *ABCC3* in facilitating the expression of stemness genes in TNBC and maintenance of the BC stem cell phenotype (Balaji et al., 2016).

Another mechanism that cells employ to mediate resistance, is the induction of gene products encoding enzymes that facilitate drug detoxification and concomitant inactivation (Bukowski et al., 2020). Importantly, culturing cells under hypoxic conditions led to a significant increase in all genes involved in drug metabolism. Bleomycin utilized primarily as an antineoplastic agent, exerts its anti-neoplastic effects by employing a sequence specific iron-dependent oxidative cleavage of DNA leading to apoptosis induction (Chen et al., 2012). Importantly, overexpression or hyperactivation of the enzyme bleomycin hydrolase leads to drug detoxification thereby limiting bleomycin toxicity in tumour tissue (Delou et al., 2019). Interestingly, studies conducted in MCF-7 cells indicate that knockdown of bleomycin hydrolase can restore sensitivity to other chemotherapeutic agents as well including topoisomerase inhibitors, platinum-based compounds as well as nucleoside analogs, further highlighting the detrimental outcome associated with overexpression of this enzyme (Chen et al., 2017). In terms of the cytochrome p450 enzymes, culturing MCF-7 cells under hypoxic conditions led to a significant increase in the expression of *CYP1A1* and *CYP2B6*. Previous studies conducted indicated that increased expression of *CYP1A1* may serve as a protective mechanism in MCF-7 cells that have acquired doxorubicin-resistance (AbuHammad and Zihlif, 2013). Additionally, *CYP1A1* is seen to promote BC proliferation and survival by repressing AMPK signalling and knockdown of *CYP1A1* impedes cell cycle progression, consequently decreasing rate of proliferation and further mediating apoptotic induction (Rodriguez and Potter, 2013). Scientific evidence also exists implicating *CYP1A1* in maintaining BC stem cell integrity through its modulation on the β-catenin and PI3K/Akt signalling pathways (Al-Dhfyan et al., 2017). In terms of CYP2B6, this enzyme in conjunction with other enzymes is seen to metabolise several BC prodrugs including camptothecin, tegafur as well as tamoxifen (Sneha et al., 2021). The increased expression post hypoxic induction may point to potential increased sensitivity of hypoxic MCF-7 cells to these chemotherapeutics agents and requires further experimental validation. Furthermore, *DHFR* gene was also

significantly increased following hypoxic treatment in MCF-7 cells. This gene encodes for a crucial enzyme involved in folate metabolism. *DHFR* catalyses the formation of tetrahydrofolate an essential co-factor required for the biosynthesis of purines and thymidylate consequently promoting cell growth and proliferation (Rana et al., 2020). Importantly, evidence exists documenting overexpression of *DHFR* in cells that have adopted a cancer stem-like state and further associate overexpression with poor patient prognosis (Lee et al., 2017, Liu et al., 2019). In terms of *SOD1* expression, exposing MCF-7 cells to hypoxic conditions led to a significant increase in expression. *SOD1* encodes for superoxide dismutase 1 which converts harmful superoxide radicals to molecular oxygen and hydrogen peroxide (Che et al., 2016). The increased expression post hypoxic exposure is justified by the observation of a superoxide burst in cells that are exposed to acute hypoxic conditions which further facilitates HIF-1 activation through inhibiting the activity of PHD (Hernansanz-Agustín et al., 2014). Importantly, the hydrogen peroxide produced can function as a secondary messenger to regulate several cellular processes including EMT, conferring cells with crucial traits required to mediate cancer aggressiveness (Azimi et al., 2017, Li et al., 2015b). Conversely, excessive induction of ROS can lead to altered expression of EMT markers that will impede cell motility and invasion (Das et al., 2014), hence indicating the crucial role of SOD1 in maintaining the mesenchymal phenotype.

Apoptosis impediment is a crucial mechanism that cancer cells employ which contributes to the development of MDR. Cancer cells achieve this by upregulating the expression of anti-apoptotic proteins such as Bcl-2 and Bcl-xL and decreasing the expression of the pro-apoptotic proteins namely, Bax, Bak, Bad and Bim. Survival of cancer cells and sensitivity to apoptosis is thus dictated by the intricate balance between the expression of these pro- and anti-apoptotic proteins. Even though hypoxic conditions led to an increase in both pro-apoptotic Bax and anti-apoptotic Bcl-2 and BCL2L1/Bcl-xL, the increase in the expression of anti-apoptotic genes displayed a greater folder change hence pointing to a compensatory mechanism in response to the increase in Bax expression in attempt to evade apoptosis. This observation further supports the results obtained through cell counts conducted post-hypoxic induction. Similar findings are reported in hepatocellular carcinoma, where cells cultured under hypoxic conditions present with increased expression of anti-apoptotic proteins Mcl-1 and Bcl-xL, whereas the expression of Bax was decreased (Meyenberg Cunha-de Padua et al., 2019). A role for HIF-1α in the regulation of Bcl-xL expression is justified by the presence of a HRE in the promoter region of Bcl-xL (Chen et al., 2009). Additional roles for these proteins are elucidated where a recent

study identified that hypoxia enhanced the interaction between Bcl-2 and Twist 1 which subsequently translocated to the nucleus to activate transcription of downstream target genes required for EMT induction (Duan et al., 2017). Conversely, overexpression of Bcl-2 was also seen to enhance stability of HIF-1α by impeding ubiquitin-mediated degradation and further facilitated a proangiogenic effect of Bcl-2 on HIF-1/VEGF axis (Trisciuoglio et al., 2010). This points to dual regulation, where hypoxia is seen to increase expression of Bcl-2 and the overexpression of Bcl-2 is implicated in further enhancing the stability of HIF-1α.

The p53 protein encoded by the TP53 gene is known to play an important role in regulating apoptosis, cell cycle as well as DNA damage and repair. Based on its function as the guardian of the genome it is not surprising that this gene is the most frequently mutated gene in human tumours (Feroz and Sheikh, 2020). Following hypoxic exposure, MCF-7 cells presented with an increase in the expression of TP53. This observation is supported by studies which indicate that hypoxia can induce p53 through either HIF-dependent or independent pathways (Zhang et al., 2021). Interestingly, studies conducted indicate that the hypoxia induced p53 is transcriptionally inactive due to the oxygen dependent conformational change to a mutant form under low oxygen conditions (Gogna et al., 2012). This would explain the fact that even though TP53 is expressed, apoptosis is not induced under hypoxic conditions. It is important to emphasise, even though a close interplay between hypoxia and TP53 is documented, cellular response to hypoxia is influenced by several factors including the severity and duration of hypoxic exposure, as well as the cell type (Zhang et al., 2021). In addition to TP53, another tumour suppressor that is deregulated following hypoxia-induced EMT includes *RB1*, the gene which encodes for the RB transcriptional corepressor 1 protein. This protein's conventional role includes negative regulation of the cell cycle however during hypoxia it is implicated in promoting biochemical alterations that facilitate the acquisition of an invasive phenotype (Labrecque et al., 2014).

While HIF-1α displayed an increase in expression, the oncogene MYC also presented with increased expression in MCF-7 cells following hypoxic exposure. It is important to point out the interplay between HIF-1α and MYC, where overexpression of MYC is seen to stabilise HIF-1α, and in cases where MYC is overexpressed, HIF-1α is only able to suppress MYC during short periods of hypoxia, whereas the increased expression of MYC is still able to mediate proliferation (Zwaans and Lombard, 2014). Interestingly emerging experimental evidence also points to a role for MYC in facilitating EMT induction by regulating the expression of master EMT TFs (Meškytė et al., 2020).

Sustained proliferative signalling is an important trait cancer cells acquire to mediate tumorigenesis. The ER in response to estrogen stimulation, functions as a TF to control the expression of various genes involved in cell cycle, proliferation, and survival. Seeing that ERα is expressed in 75% of BC, employing endocrine therapy as a means to combat cancer progression seems like a reasonable approach, however the efficacy of these compounds in combatting BC progression is often limited due to evolutionary mechanisms adopted thereby conferring cells with drug resistant potential in the pursuance of cancer cell survival. The existence of complex molecular crosstalk between ER signalling and other growth factor signalling pathways is further implicated in contributing to drug resistance in BC. This is illustrated by studies showing that the overexpression of HER2 in ER+ cancers can confer resistance to TAM (Viedma-Rodríguez et al., 2014). Additionally, tumours that display amplification of HER2 results in tumour growth promotion by conferring TAM with estrogen agonist function (Rani et al., 2019). Interestingly, cells rendered resistant to TAM due to HER2 amplification displayed increased sensitivity to TAM following downregulation of ERBB3, consequently implicating ERBB3 in TAM resistance. Importantly, evidence exists pointing to heterodimer formation between ERBB2 and ERBB3 which represents the most pro-tumorigenic form of all ERBB complexes implicating this complex in mediating cell survival and impeding apoptosis through its potent PI3K/Akt activating ability (Wang et al., 2010). Additionally, interdependence between IGF-IR and ERα has also been documented in BC where studies conducted identify that targeting the IGF-IR proved effective in decreasing the growth of tamoxifen resistant BC cells (Viedma-Rodríguez et al., 2014). Seeing that exposure to hypoxic conditions led to an increase in the expression of ER as well as the growth factor receptors that contribute to drug resistance, it can be stated that hypoxic conditions exacerbate endocrine resistance in BC cells.

The cell cycle can be described as a highly organized process that is well orchestrated in cells to ensure accurate duplication of genetic material and cell division (Otto and Sicinski, 2017). Progression through the cell cycle is mediated by the cyclin dependent kinases that function in the presence of the appropriate binding partner proteins termed cyclins (Druker et al., 2021). Seeing that the cell cycle is an increasingly demanding and energy-driven process, it is not surprising that the oxygen-sensing system of the cell can directly affect cell cycle progression (Druker et al., 2021). In the case of cyclin D1, exposure to hypoxic conditions led to an increase in expression. This observation is supported by evidence indicating that hypoxia can mediate transcriptional activation of cyclin D1 inducing Jak2/STAT signalling in BC (Joung et al.,

2005). Additionally, protein-protein interaction between HIF-1 and AKT is also documented to increase the expression of Cyclin D1 (Zhang et al., 2018a). Furthermore, hypoxia mediated activation of NFκβ signalling may also contribute to the observed increase in expression (Druker et al., 2021). Interestingly culturing MCF-7 cells under hypoxic conditions further upregulated the expression of CDK2. This CDK when complexed with cyclin E is crucial to facilitating S phase entry by modulating Rb to facilitate progression past the restriction point in G1/S (Ding et al., 2020). Subsequent association with cyclin A is further necessary for S-phase termination and entry into G2. Furthermore, culturing cells under hypoxic conditions also led to an increase in the expression of *CCND1* which encodes for p27, a cyclin dependent kinase inhibitor (Ding et al., 2020). Seeing that cell proliferation was not significantly affected by culturing cells under hypoxic conditions, the increase in the expression of p27 points to a probable oncogenic role of p27 in the cell. This statement can be justified by studies implicating phosphorylated p27 in the induction of EMT, by binding to JAK2, facilitating STAT3 activation which led to increased expression of TWIST1 (Zhao et al., 2015). Furthermore, studies show that phosphorylated p27 can also associate with c-Jun and are both co-recruited to chromatin to mediate activation of transcription programs that facilitate EMT, cell motility and metastasis (Yoon et al., 2019). Additionally, p27 is also seen to directly regulate invadopodia formation and mediates cell invasion by binding to cortactin (a monomeric scaffold protein) known to play a key role in the formation of actin protrusive structures (Jeannot et al., 2017). On this basis, it can be hypothesised that the increased expression of p27 in MCF-7 cells post hypoxic induction facilitates EMT induction and confers cells with traits that enhance metastatic potential. In terms of *CDKN2D*, exposing MCF-7 cells to hypoxic conditions led to a decrease in the expression of this gene which encodes for the cyclin dependent kinase inhibitor p19. Seeing that CDK4/6 is negatively regulated by p19, decreased expression of this negative regulator will facilitate cell cycle progression by promoting progression through G1 phase of the cell cycle (Ding et al., 2020). Consequently, scientific evidence exists indicating that p19-deficient carcinomas display increased levels of benign tumour growth. Interestingly, together with increased benign growth, loss of p19 exacerbated benign to malign conversion and also mediated metastatic dissemination of epithelial tumours (Kelly-Spratt et al., 2004). Consequently, decreased levels of p19 following hypoxic induction could facilitate cancer growth and may potentiate increased metastatic capacity.

The acquisition of drug resistance is strongly linked with aberrant expression and regulation of DNA damage response mechanisms which confers cancer cells with the ability to repair

damaged DNA and continue proliferating in response to genotoxic insults (Assaraf et al., 2019). Interestingly, exposing cells to hypoxic conditions led to an increase in the expression of genes involved in DNA damage and repair. The breast cancer type 1 susceptibility protein encoded by BRCA1 plays a crucial role in mediating precise and efficient repair of DNA double stranded breaks (Liu and Lu, 2020). Additionally, MutS Homolog 2 (MSH2) is an important protein known to play a role in mismatch repair, which functions to correct erroneous bases that occur during the process of DNA replication and recombination (Tang et al., 2021). It is important to note, even though both genes are upregulated, exposure to hypoxic conditions is seen to induce mutations to these genes thereby decreasing the efficiency of DNA repair leading to unchecked cell cycle arrest, which consequently promotes increased chromosomal and genetic instability thereby facilitating tumorigenesis (Hassan Venkatesh et al., 2020).

### 5.6. Hypoxia-induced EMT increases cellular cholesterol content potentiating an aggressive disease phenotype

Despite evidence indicating that cholesterol directly regulates signalling pathways related to EMT, no publication to date has attempted to delineate the effect of EMT induction on the cellular cholesterol profile in cancer. This study aimed to shed light on the dynamics of cholesterol in the relationship between hypoxia and EMT. Interestingly, free cholesterol, lipid raft cholesterol and CE content was increased following hypoxia-induced EMT.

Evidence exists implicating hypoxia in the regulation of cholesterol biosynthesis through HIF-1α dependent and independent pathways (Riscal et al., 2019). Indeed, studies document hypoxia mediated translocation of SREBP2 to the nucleus thereby enhancing the expression as well as the activity of HMGCR (Pallottini et al., 2008). This is supported by studies highlighting increased levels of cholesterol in cells exposed to hypoxic conditions (Danza et al., 2013). Moreover, a study implicated the hypoxic tumour microenvironment in promoting SREBP transcriptional activity thereby enhancing the expression of downstream target genes that are crucial to mediating cancer cell survival and tumorigenesis (Lewis et al., 2015). Alternatively, hypoxia-induced cholesterol accumulation is also potentiated by decreased cholesterol catabolism and reverse cholesterol transport (Cao et al., 2014). This finding further validates the observation made in this study of reduced ABCA1 expression in MCF-7 cells following hypoxia-induced EMT (Supplementary Data- Figure S1.1).

Based on the fact that cholesterol is crucial to supporting the activity of several EMT-related protein intermediates, together with the observation of increased cholesterol following hypoxic

induction, it can be proposed, that hypoxia-induced EMT facilitates increased cellular cholesterol abundance by mediating both cholesterol synthesis and also abrogating cholesterol catabolism and efflux.

While the documented increase in free cholesterol was not significant (10.36%) both lipid raft (30.68%) and CE (31.89%) content displayed a significant increase following hypoxia-induced EMT. The slight increase in free cholesterol can be principally attributed to the observation that excess free cholesterol proves toxic to the cancer cell (Riscal et al., 2019). Since free cholesterol is toxic to the cells, cancer cells have developed mechanisms that compensate for the increased free cholesterol by increasing the expression of ACAT-1, responsible for catalysing esterification of cholesterol to a more stable state termed CEs which are stored in lipid droplets (Mayengbam et al., 2021). Importantly, scientific evidence exists implicating cellular stresses such as hypoxia in facilitating aberrant lipid droplet accumulation (Bång-Rudenstam et al., 2019). This mechanism consequently justifies the significant increase in CE content following hypoxia-induced EMT. Indeed, the increase in CE lipid droplet content is also emerging as a common mechanism employed by advanced cancers to fuel cancer aggressiveness (Morandi et al., 2017). By maintaining low levels of free cholesterol, cancer cells are able to induce constitutive activity of SREBP (Yue et al., 2014). This consequently mediates transcription of genes involved in cholesterol biosynthesis and uptake potentiating increased cellular cholesterol availability to satisfy the energetic requirements of cancer cells (Riscal et al., 2019). Importantly, the increased CE content is seen to promote unrestrained proliferation and growth and is further linked with increased cancer cell migration and invasion corresponding with enhanced metastatic potential (de Gonzalo-Calvo et al., 2015, Li et al., 2016, Peck and Schulze, 2014). This is justified by evidence implicating CEs in mediating regulation of the WNT/β-catenin signalling pathway (Lee et al., 2018). In terms of clinicopathological findings, a direct association between intratumoral CE levels and higher histologic grade, Ki-67 and tumour necrosis is documented substantiating the poor clinical outcome in BC patients with CE accumulation (de Gonzalo-Calvo et al., 2015).

Studies now show that exposing cancer cells to hypoxic conditions promotes the coalescence of lipid rafts leading to the formation of large liquid-ordered domains that facilitate compartmentalization of several proteins promoting activation of EMT-related signalling pathways (Danza et al., 2013). The heterogenous and dynamic nature of lipid rafts together with the ability to compartmentalise cellular processes, makes them crucial signalling modules in cancer (de Oliveira Andrade, 2016). Increased lipid raft cholesterol content is justified by

the crucial role these rafts play in mediating cancer cell signalling that subsequently modulates cellular function. Indeed, evidence exists implicating increased cholesterol content in tumorigenic progression by modulating signal transduction through its effects on lipid rafts (Alikhani et al., 2013). This is evidenced by studies indicating that tumour promoting molecules such as osteopontin interact with integrin αVβ3 as well as CD44 receptors located in lipid raft domains to mediate activation of several signalling pathways including MAPK, PI3K/Akt as well as NFκβ to induce expression of EMT-related genes (Li et al., 2019). Additionally, lipid raft localisation of podoplanin facilitates recruitment and subsequent activation of the Ezrin family leading to EMT induction thereby promoting invadopodia formation. Furthermore, lipid raft localised caveolin-1 enhances EMT induction by promoting expression of the EMT master TF Slug through PI3K/Akt activation. On this basis it can be stated that inhibiting cholesterol synthesis, or depleting membrane cholesterol destroys lipid raft structure thereby counteracting the pro-tumorigenic effect of cholesterol (Li et al., 2019).

Interestingly, emerging scientific evidence documents a link between plasma membrane composition including membrane cholesterol content which consequently dictates biophysical properties and maintenance of a mesenchymal state (Morandi et al., 2017). In cells undergoing EMT, together with an increase in membrane cholesterol, a reduction in the ceramide pool synergistically contributes to enhanced membrane fluidity (Morandi et al., 2017). The increased membrane fluidity is emerging as a crucial requirement of cancer cells to facilitate metastatic dissemination (Morandi et al., 2017). The increase in lipid raft cholesterol following hypoxia-induced EMT is hence clearly justified, implicating cholesterol in not only directly modulating EMT associated signalling intermediates but also modifying the physical properties of the membrane to support EMT.

Findings from the present study document that cancer cells that have undergone EMT display increased sensitivity to cholesterol targeting agents. Interestingly, this result corresponded to a significant increase in the expression of E-cadherin with an accompanying decrease in Vimentin expression following the administration of cholesterol targeting agents. Furthermore, post-EMT cells treated with cholesterol targeting agents display a significant decrease in invasive potential which also supports the results obtained from immunofluorescence. This can be corroborated with findings in other studies that elucidate the beneficial outcome associated with employing cholesterol targeting agents to reduce the metastatic potential of cells by decreasing the migratory and invasive potential of cells.

This is evidenced by studies reporting that the disruption of lipid raft integrity (by administering Simvastatin or MβCD) facilitates the shedding of the key cell surface receptor, CD44 that is overtly expressed by cancer cells. This receptor is crucial for conferring an aggressive disease phenotype as it mediates cancer cell migration, invasion and metastasis (Murai et al., 2011).

Cholesterol targeting agents are also seen to affect EMT-related signalling intermediates to combat metastasis. Guerra *et al.* identified that post-administration of MβCD, MDA-MB-231 cells displayed significantly reduced membrane protrusions relative to the control group which exhibited the presence of ruffled membranes and lamellipodia and increased migratory potential (Guerra et al., 2016). Further investigation by this group implicated the non-canonical Wnt pathway in the inhibition of cell migration following administration of MβCD (Guerra *et al*., 2016). Similar findings are also reported in a study conducted by Badana *et al.* where authors found that treatment with MβCD inhibited the migration of MDA-MB-231 and MDA-MB-468 cells (Badana et al., 2018). Upon further investigation, mRNA and protein analysis identified the downregulation of several anti-apoptotic proteins as well as decreased expression of LRP6 and β-catenin (Badana et al., 2018). Seeing that LRP6 and β-catenin (both key proteins in the Wnt pathway) displayed decreased expression, it can be postulated that MβCD plays an important role in preventing Wnt signalling thereby reducing the aggressive potential of TNBC to metastasise. In terms of HPβCD, a recent study demonstrated that treatment with HPβCD prevented EMT by inhibiting the TGFβ/Smad signalling pathway which consequently activates ER stress in MDA-MB-231 cell line. Following the administration of HPβCD, TβR1 expression significantly decreased leading authors to postulate that treating cells with HPβCD probably affected the distribution of TβR1 in lipid rafts (Wu et al., 2020).

With regards to statins, studies conducted indicate that Simvastatin mediated suppression of Smad 2 and 3 phosphorylation attenuates TGF-β1 induced EMT and consequently impedes cell migration (Yang et al., 2013). Additionally, Simvastatin mediated suppression of the PI3K/Akt/GK3β as well as MAPK/ERK signalling pathways is also seen to inhibit EMT and suppress cell migration (Wang et al., 2016). Furthermore, inactivation of the Hippo/YAP/RhoA pathway has also been documented following Simvastatin administration consequently impairing metastatic potential (Kato et al., 2018). Interestingly, evidence exists implicating Atorvastatin (belonging to the same class as Simvastatin) in impeding EMT by attenuating the levels of HIF-1α and β-catenin (Du et al., 2018). One can thus postulate that Simvastatin may also work in a similar way to impede EMT induction.

Accordingly, targeting cellular cholesterol enhanced levels of key epithelial markers namely E-cadherin and Keratin 19 while simultaneously decreasing the expression of characteristic mesenchymal markers namely Vimentin and N-cadherin (Deezagi and Safari, 2020, Sharma et al., 2019, Wu et al., 2020). Both Zeb-1 and Zeb-2 also displayed decreased expression relative to the untreated cells (Sharma et al., 2019). These findings subsequently account for the reduced migratory and invasive capabilities of these cells post-treatment.

Based on the above findings it can be stated that treatment with cholesterol targeting agents proves effective in reducing metastatic potential of cells by decreasing the migratory and invasive potential of cells. This can be attributed to the disruption in lipid raft integrity which facilitates the shedding of key cell surface receptor that cancer cells depend on for conferring an aggressive disease phenotype. Furthermore, several EMT related pathways are also inhibited. This facilitates an increased expression of key epithelial markers while reducing the expression of mesenchymal markers. As a result of this, employing cholesterol targeting agents effectively combats EMT and metastasis and prevents the acquisition of an aggressive disease phenotype.

### 5.7. Hypoxia mediated MDR potential is efficiently combatted by targeting cholesterol

Scientific evidence exists consolidating the link between hypoxic induction and enhanced MDR potential in cancer cells. This is predominantly achieved by the transcription and activation of several drug transporter proteins promoting chemoresistance (Jing et al., 2019). MDR1 is the most well-characterised MDR transporter associated with cancer therapy resistance (Robinson and Tiriveedhi, 2020).

Seeing that exposure to hypoxic conditions induces expression of the MDR1 transporter coupled with the observation that high levels of cholesterol is crucial to supporting the activity of MDR1, we sought to elucidate the effect on MDR1 pump functionality following administration of cholesterol targeting agents post-EMT. As expected, cells post-hypoxia induced EMT displayed increased MDR potential as evidenced by the 47.13% decrease in retention of fluorescent calcein (metabolised substrate of MDR1) in the cytosol of MCF-7 cells.

Importantly, treatment with cholesterol targeting agents combatted hypoxia-induced increase in MDR potential as evidence by the increased retention of fluorescent calcein following treatment. Interestingly, membrane cholesterol depletion proved more effective in restoring sensitivity when compared with cholesterol synthesis inhibition. This observation can be

justified by studies reporting that treatment with membrane cholesterol depletors abrogates expression of the MDR1 transporter whereas treatment with statins affects the activity (Glodkowska-Mrowka et al., 2014, Kim et al., 2018b). By repressing the expression of these transporters, retention of substrate will be more efficiently achieved as opposed to reduced activity. Furthermore, seeing that these transporters are housed in membrane lipid rafts, depleting lipid raft cholesterol is seen to impair the efflux activity of MDR1 (Subramanian et al., 2016). This can be attributed to alterations in lipid-raft membrane structure which affects basal ATPase activity (Celestino et al., 2015). Studies indicate that membrane cholesterol depletion results in translocation of MDR1 to detergent soluble fractions leading to a loss of activity (Ferreira et al., 2015). Additionally, evidence exists implicating MβCD in directly modulating ATPase activity independently from its ability to facilitate membrane cholesterol depletion hence justifying the result obtained in the present study.

## 6. Conclusions and Future Perspectives

Administering 150 µM of $CoCl_2$ to MCF-7 cells for 48-hours mediated the induction of EMT without significantly affecting cell viability. Following hypoxia-induced EMT, cells alter their molecular profile to facilitate a resistant state. This is evidenced by the increased expression of genes involved in drug metabolism and efflux, DNA damage and repair as well as apoptotic evasion. Interestingly, this is the first study documenting alterations to the cellular cholesterol profile following hypoxia-induced EMT indicating increased levels of free cholesterol, lipid raft cholesterol as well as CEs. The abundance of cholesterol in addition to directly regulating protein intermediates, promotes an increase in the presence of lipid rafts which serve as key signalling hubs crucial for EMT induction. Seeing that the induction of EMT is associated with increased drug resistant potential, it can be inferred that cholesterol through its EMT-modulatory effects promotes increased drug resistance potential. Additionally, deregulated cholesterol metabolism is also seen to directly contribute to drug resistance by directly regulating the activity of the MDR transporters conferring cells with chemoresistant traits. This therefore points to the multifaceted role of cholesterol in promoting EMT and mediating cancer drug resistance (Figure 5).

Consequently, attempts made at targeting cellular cholesterol by employing cholesterol synthesis inhibition/depletion to restore sensitivity was exploited. In this study, treatment with

cholesterol targeting agents proved more effective in the post-EMT particularly in the case of cholesterol depletion as opposed to cholesterol synthesis inhibition. This finding is beneficial based on the debilitating side effects associated with statin therapy which is seen as a major limitation in a clinical setting. This could be attributed to the long-term impediment of cholesterol synthesis in cells where cholesterol plays an integral role in regulating essential cellular processes. Consequently, the discovery of cholesterol depletory agents is pivotal to combat drug resistance. Based on the crucial role of altered cholesterol metabolism in drug resistance, screening additional compounds that either as single agents or in combination with anti-cancer therapies will restore drug sensitivity, seems like a promising avenue to pursue. Additionally, further insight is required to delineate the precise role that cholesterol plays in influencing the major components of the tumour microenvironment. This consequently highlights the incipient need to develop models that more closely mimic human immune response and the human tumour microenvironment in general.

Given the importance of cholesterol dyshomeostasis in cancer progression and drug resistance, as well as the observation of increased cellular cholesterol in cells following EMT induction, targeting cellular cholesterol to combat BC pathogenesis seems to be a promising direction to pursue in the search for novel anticancer therapeutics (*Figure 5*).

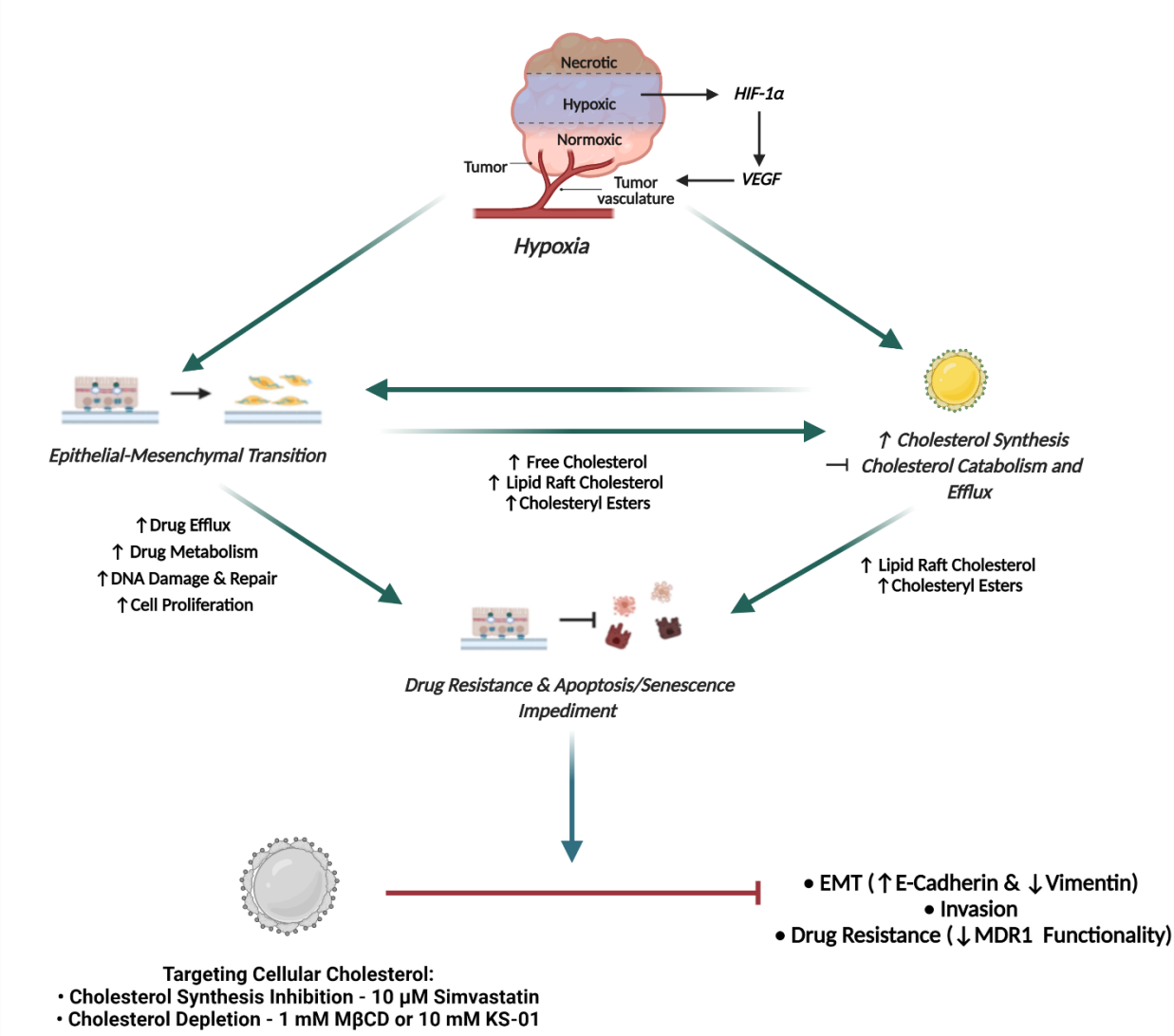



**Figure 5: Visual Representation Summarising the Role of Cholesterol in Hypoxia-induced EMT**

*The hypoxic tumour microenvironment facilitates EMT induction and promotes increased cellular cholesterol availability by enhancing mechanisms associated with cholesterol synthesis and impeding cholesterol catabolism and efflux. While increased cholesterol content is seen to fuel EMT, findings from this study elucidate that hypoxia-induced EMT increases cellular cholesterol content (free cholesterol, cholesteryl esters and lipid raft cholesterol). Importantly, both EMT and increased cholesterol content is seen to enhance drug resistance and impede apoptotic and senescence induction. Findings from this study indicate that targeting cellular cholesterol, either through cholesterol synthesis inhibition or depletion, efficiently combats EMT, decreases the invasive potential of cells and may also restore sensitivity to conventional chemotherapeutic agents by decreasing the functionality of the MDR1 pump. Consequently, targeting cellular cholesterol to combat breast cancer pathogenesis seems to be a promising direction to pursue in the search for novel anticancer therapeutics.*

## 7. Successes and Limitations of the Study

The design of this study makes it quite novel as it is the first study to document alterations to the cellular cholesterol profile in MCF-7 cells following hypoxia-induced EMT and the downstream implications this has on cellular characteristics that promote metastasis and drug resistance. Immunofluorescent as well as cholesterol staining facilitates both localisation and quantification of protein and cholesterol content as opposed to western blotting and cholesterol-based assays that only provide a quantitative result.

In terms of the limitations of the study, only one cell line was utilised to study the effects of hypoxia-induced EMT on the cellular cholesterol profile. It would be interesting to consider what the outcome would be in the MCF-10A non-malignant breast epithelial cell line. Additionally, based on the costly nature of the $RT^2$ PCR Profiler Arrays, other arrays such as lipoprotein signaling and cholesterol metabolism could not be employed. Additionally, expression levels of genes will not necessarily parallel protein expression, hence it cannot be stated with absolute certainty that hypoxia-induced EMT results in the afore-mentioned changes in drug resistance, yet it provides substantial clues into the pathway dynamics under the tested conditions. Future studies will therefore seek to address this by studying the protein expression following hypoxia-induced EMT. Lastly, the study was conducted *in-vitro.* While *in-vitro* studies are crucial to facilitating a basic understanding of molecular mechanisms governing cancer progression, these studies often present with limitations by not considering the influence of the tumour microenvironment as well as the inter- and intra-tumour heterogeneity. This heterogeneity serves as a platform for the selection and outgrowth of well adapted tumour subtypes consequently promoting metastatic dissemination and relapse, a feature that is not compensated for in *in-vitro* models. Nevertheless, findings from the current study provides us with insightful and novel information potentiating the design of future studies aimed at validating these findings *in-vivo.*

## 8. Supplementary Data

A bioinformatics approach was employed by carrying out transcription factor binding site (TFBS) analysis on a list of 84 cholesterol-related genes ($RT^2$ Profiler™ PCR Array Human Lipoprotein Signalling and Cholesterol Metabolism: PAHS-080Z). This list was submitted to the TFBS enrichment webtool oPOSSUM-3 (http://opossum.cisreg.ca/oPOSSUM3/) to detect the over-represented conserved TFBS's in a set of genes. The following parameters were set: conservation cutoff = 0.40, matrix score threshold = 85%, region for upstream and downstream sequences = 1000 bp and 200 bp, respectively. Results were selected based on the Z-score (>=10) and Fischer score (>=7). This resulted in a list of 52 genes out of a total of 84 genes had TFBs for ZEB1. These 52 genes were subsequently matched to a previous study which analyzed all ZEB1 related genes in TNBC (Maturi et al., 2018).

To delineate a possible mechanism that cancer cells employ to increase cellular cholesterol content post-EMT, protein expression analysis of the cholesterol efflux protein ABCA1 was completed. This protein was chosen based on bioinformatics analysis conducted which predicted a transcription factor binding site for ZEB1 in the ABCA1 gene. Following hypoxia-induced EMT, MCF-7 cells presented with decreased levels of the ABCA1 protein (40.66%) as evidenced by the reduced fluorescence intensity in $CoCl_2$ treated cells relative to untreated cells *(Figure 4.11)*. This result consequently supports results obtained through cholesterol staining indicating increased levels of cholesterol post-EMT induction.

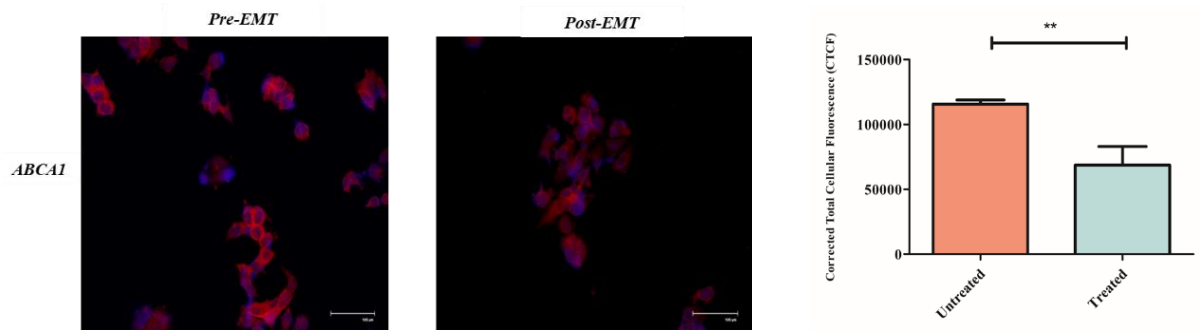
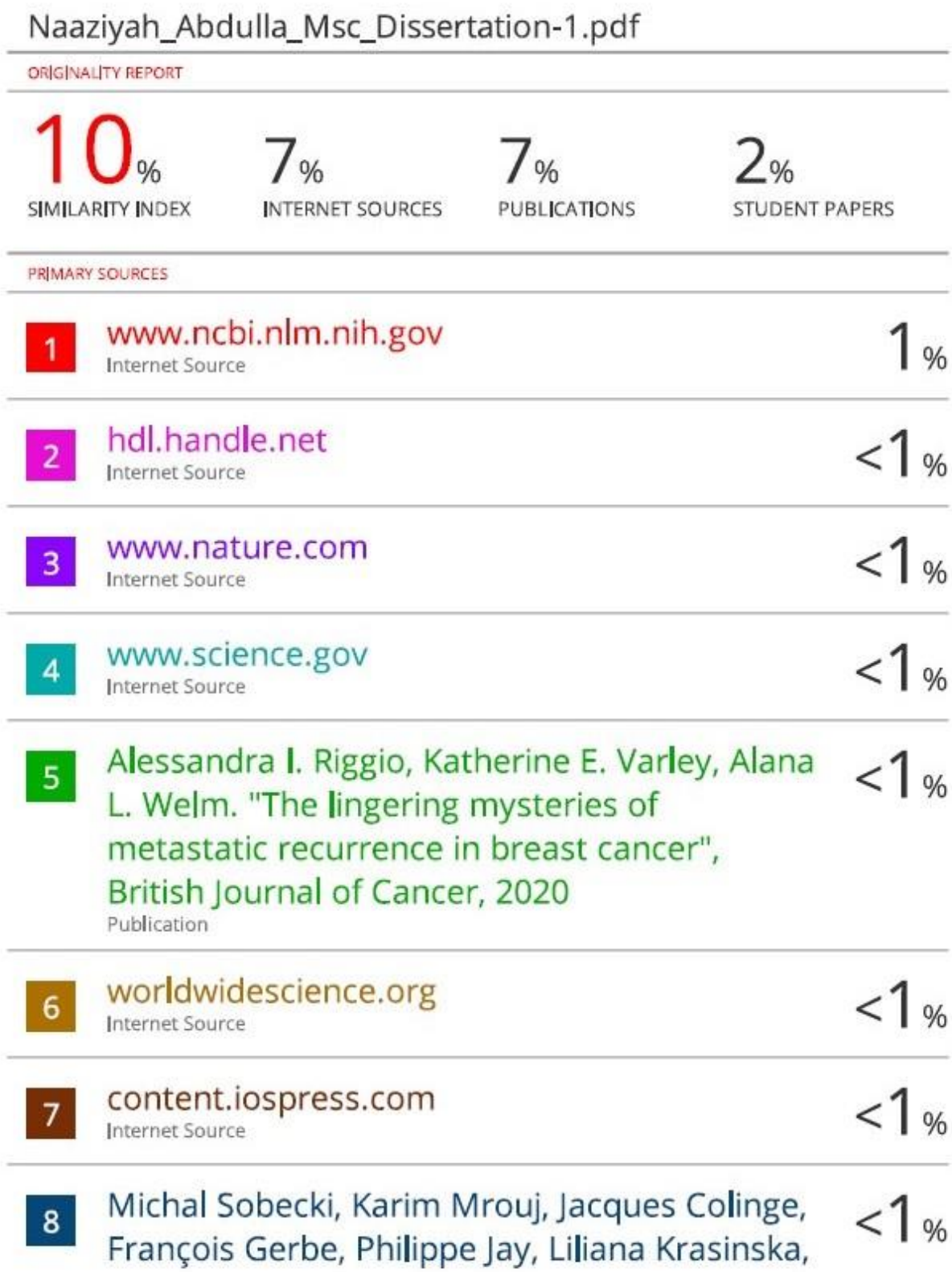



**Figure S1.1: Effect of $CoCl_2$ on the expression of cholesterol efflux protein ABCA1**

*Protein expression of ABCA1 in untreated and $CoCl_2$ treated MCF-7 cells for a duration of 48 hours was detected by employing immunofluorescence microscopy. (a) ABCA1 expression is indicated by Alexa Fluor 594 staining (red). It is evident that ABCA1 is significantly decreased following treatment with $CoCl_2$ where further analysis by Image J, document a 40.66% decrease in ABCA1 expression of $CoCl_2$ treated cells relative to untreated cells. Images were captured using the Floid™ Cell Imaging System followed by analysis using the Image J software. The scale bar on each of the images represents 100 µm. A paired two-tailed t-test was employed for statistical analysis where data represent the mean ± standard deviation. n=3. * P < 0.05, ** P < 0.01, *** P < 0.001*

## 9. Turnitin Summary Plagiarism Report



Naaziyah_Abdulla_Msc_Dissertation-1.pdf

ORIGINALITY REPORT

| 10% | 7% | 7% | 2% |
|---|---|---|---|
| SIMILARITY INDEX | INTERNET SOURCES | PUBLICATIONS | STUDENT PAPERS |

PRIMARY SOURCES

| | | |
|---|---|---|
| 1 | www.ncbi.nlm.nih.gov<br>Internet Source | 1% |
| 2 | hdl.handle.net<br>Internet Source | <1% |
| 3 | www.nature.com<br>Internet Source | <1% |
| 4 | www.science.gov<br>Internet Source | <1% |
| 5 | Alessandra I. Riggio, Katherine E. Varley, Alana L. Welm. "The lingering mysteries of metastatic recurrence in breast cancer", British Journal of Cancer, 2020<br>Publication | <1% |
| 6 | worldwidescience.org<br>Internet Source | <1% |
| 7 | content.iospress.com<br>Internet Source | <1% |
| 8 | Michal Sobecki, Karim Mrouj, Jacques Colinge, François Gerbe, Philippe Jay, Liliana Krasinska, | <1% |

## 10. References


ABBA, M. L., PATIL, N., LEUPOLD, J. H. & ALLGAYER, H. 2016. MicroRNA Regulation of Epithelial to Mesenchymal Transition. *Journal of Clinical Medicine,* 5**,** 8.

ABUHAMMAD, S. & ZIHLIF, M. 2013. Gene expression alterations in doxorubicin resistant MCF7 breast cancer cell line. *Genomics,* 101**,** 213-220.

AHMADI, M., AMIRI, S., PECIC, S., MACHAJ, F., ROSIK, J., ŁOS, M. J., ALIZADEH, J., MAHDIAN, R., DA SILVA ROSA, S. C., SCHAAFSMA, D., SHOJAEI, S., MADRAKIAN, T., ZEKI, A. A. & GHAVAMI, S. 2020. Pleiotropic effects of statins: A focus on cancer. *Biochimica et Biophysica Acta (BBA) - Molecular Basis of Disease,* 1866**,** 165968.

AL-DHFYAN, A., ALHOSHANI, A. & KORASHY, H. M. 2017. Aryl hydrocarbon receptor/cytochrome P450 1A1 pathway mediates breast cancer stem cells expansion through PTEN inhibition and β-Catenin and Akt activation. *Molecular Cancer,* 16**,** 14-14.

ALAM, A., KOWAL, J., BROUDE, E., RONINSON, I. & LOCHER, K. P. 2019. Structural insight into substrate and inhibitor discrimination by human P-glycoprotein. *Science,* 363**,** 753-756.

ALBERTS, B., JOHNSON, A., LEWIS, J., RAFF, M., ROBERTS, K. & WALTER, P. 2002. Molecular Biology of the Cell. 4th ed. New York: Garland Science.

ALFAKEEH, A. & BREZDEN-MASLEY, C. 2018. Overcoming endocrine resistance in hormone receptor-positive breast cancer. *Current oncology (Toronto, Ont.),* 25**,** S18-S27.

ALIKHANI, N., FERGUSON, R. D., NOVOSYADLYY, R., GALLAGHER, E. J., SCHEINMAN, E. J., YAKAR, S. & LEROITH, D. 2013. Mammary tumor growth and pulmonary metastasis are enhanced in a hyperlipidemic mouse model. *Oncogene,* 32**,** 961-967.

AN, K.-C. 2016. Selective Estrogen Receptor Modulators. *Asian spine journal,* 10**,** 787-791.

ASSARAF, Y. G., BROZOVIC, A., GONÇALVES, A. C., JURKOVICOVA, D., LINĒ, A., MACHUQUEIRO, M., SAPONARA, S., SARMENTO-RIBEIRO, A. B., XAVIER, C. P. R. & VASCONCELOS, M. H. 2019. The multi-factorial nature of clinical multidrug resistance in cancer. *Drug Resistance Updates,* 46**,** 100645.

AZIMI, I., PETERSEN, R. M., THOMPSON, E. W., ROBERTS-THOMSON, S. J. & MONTEITH, G. R. 2017. Hypoxia-induced reactive oxygen species mediate N-cadherin and SERPINE1 expression, EGFR signalling and motility in MDA-MB-468 breast cancer cells. *Scientific Reports,* 7**,** 15140.

BADANA, A. K., CHINTALA, M., GAVARA, M. M., NAIK, S., KUMARI, S., KAPPALA, V. R., ISKA, B. R. & MALLA, R. R. 2018. Lipid rafts disruption induces apoptosis by attenuating expression of LRP6 and survivin in triple negative breast cancer. *Biomedicine & Pharmacotherapy,* 97**,** 359-368.

BALAJI, S. A., UDUPA, N., CHAMALLAMUDI, M. R., GUPTA, V. & RANGARAJAN, A. 2016. Role of the Drug Transporter ABCC3 in Breast Cancer Chemoresistance. *PLOS ONE,* 11**,** e0155013.

BÅNG-RUDENSTAM, A., CEREZO-MAGAÑA, M. & BELTING, M. 2019. Pro-metastatic functions of lipoproteins and extracellular vesicles in the acidic tumor microenvironment. *Cancer and Metastasis Reviews,* 38**,** 79-92.

BAO, B., AZMI, A. S., ALI, S., AHMAD, A., LI, Y., BANERJEE, S., KONG, D. & SARKAR, F. H. 2012. The biological kinship of hypoxia with CSC and EMT and their relationship with deregulated expression of miRNAs and tumor aggressiveness. *Biochimica et biophysica acta,* 1826**,** 272-296.

BASKAR, R., DAI, J., WENLONG, N., YEO, R. & YEOH, K.-W. 2014. Biological response of cancer cells to radiation treatment. *Frontiers in Molecular Biosciences,* 1**,** 24-24.

BATLLE, E., SANCHO, E., FRANCÍ, C., DOMÍNGUEZ, D., MONFAR, M., BAULIDA, J. & GARCÍA DE HERREROS, A. 2000. The transcription factor Snail is a repressor of E-cadherin gene expression in epithelial tumour cells. *Nature Cell Biology,* 2**,** 84-89.

BHATT, T., RIZVI, A., BATTA, S. P. R., KATARIA, S. & JAMORA, C. 2013. Signaling and Mechanical Roles of E-cadherin. *Cell Communication & Adhesion,* 20**,** 189-199.

BIDET, M., JOUBERT, O., LACOMBE, B., CIANTAR, M., NEHMÉ, R., MOLLAT, P., BRÉTILLON, L., FAURE, H., BITTMAN, R., RUAT, M. & MUS-VETEAU, I. 2011. The hedgehog receptor patched is involved in cholesterol transport. *PloS one,* 6**,** e23834-e23834.

BINDELS, S., MESTDAGT, M., VANDEWALLE, C., JACOBS, N., VOLDERS, L., NOËL, A., ROY, F. V., BERX, G., FOIDART, J. M. & GILLES, C. 2006. Regulation of vimentin by SIP1 in human epithelial breast tumor cells. *Oncogene,* 25**,** 4975-4985.

BLASSBERG, R. & JACOB, J. 2017. Lipid metabolism fattens up hedgehog signaling. *BMC Biology,* 15**,** 95.

BRAY, F., FERLAY, J., SOERJOMATARAM, I., SIEGEL, R. L., TORRE, L. A. & JEMAL, A. 2018. Global cancer statistics 2018: GLOBOCAN estimates of incidence and mortality worldwide for 36 cancers in 185 countries. *CA:A cancer journal for clinicians,* 68**,** 394-424.

BUKOWSKI, K., KCIUK, M. & KONTEK, R. 2020. Mechanisms of Multidrug Resistance in Cancer Chemotherapy. *International journal of Molecular Sciences,* 21**,** 3233.

BUTTURINI, E., CARCERERI DE PRATI, A., BORIERO, D. & MARIOTTO, S. 2019. Tumor Dormancy and Interplay with Hypoxic Tumor Microenvironment. *International journal of Molecular Sciences,* 20**,** 4305.

CALLAHAN, B. P. & WANG, C. 2015. Hedgehog Cholesterolysis: Specialized Gatekeeper to Oncogenic Signaling. *Cancers (Basel),* 7**,** 2037-2053.

CANO, A., PÉREZ-MORENO, M. A., RODRIGO, I., LOCASCIO, A., BLANCO, M. J., DEL BARRIO, M. G., PORTILLO, F. & NIETO, M. A. 2000. The transcription factor Snail controls

epithelial–mesenchymal transitions by repressing E-cadherin expression. *Nature Cell Biology,* 2**,** 76-83.

CAO, R., ZHAO, X., LI, S., ZHOU, H., CHEN, W., REN, L., ZHOU, X., ZHANG, H. & SHI, R. 2014. Hypoxia Induces Dysregulation of Lipid Metabolism in HepG2 Cells via Activation of HIF-2α. *Cellular Physiology and Biochemistry,* 34**,** 1427-1441.

CARBAJO-PESCADOR, S., ORDOÑEZ, R., BENET, M., JOVER, R., GARCÍA-PALOMO, A., MAURIZ, J. L. & GONZÁLEZ-GALLEGO, J. 2013. Inhibition of VEGF expression through blockade of Hif1α and STAT3 signalling mediates the anti-angiogenic effect of melatonin in HepG2 liver cancer cells. *British Journal of Cancer,* 109**,** 83-91.

CASTANON, I. & BAYLIES, M. K. 2002. A Twist in fate: evolutionary comparison of Twist structure and function. *Gene,* 287**,** 11-22.

CELESTINO, A. T., LEVY, D., MARIA RUIZ, J. L. & BYDLOWSKI, S. P. 2015. ABCB1, ABCC1, and LRP gene expressions are altered by LDL, HDL, and serum deprivation in a human doxorubicin-resistant uterine sarcoma cell line. *Biochemical and Biophysical Research Communications,* 457**,** 664-668.

CHALLAPALLI, A., CARROLL, L. & ABOAGYE, E. O. 2017. Molecular mechanisms of hypoxia in cancer. *Clinical and Translational Imaging,* 5**,** 225-253.

CHAUDHURI, A. & ANAND, D. 2017. Cholesterol: Revisiting its fluorescent journey on 200th anniversary of Chevruel's "cholesterine". *Biomedical Spectroscopy and Imaging,* 6**,** 1-24.

CHE, M., WANG, R., LI, X., WANG, H.-Y. & ZHENG, X. F. S. 2016. Expanding roles of superoxide dismutases in cell regulation and cancer. *Drug Discovery Today,* 21**,** 143-149.

CHEE, N. T., LOHSE, I. & BROTHERS, S. P. 2019. mRNA-to-protein translation in hypoxia. *Molecular Cancer,* 18**,** 49.

CHEN, C.-L., CHU, J.-S., SU, W.-C., HUANG, S.-C. & LEE, W.-Y. 2010. Hypoxia and metabolic phenotypes during breast carcinogenesis: expression of HIF-1α, GLUT1, and CAIX. *Virchows Archiv,* 457**,** 53-61.

CHEN, J., CHEN, Y. & HE, Q. 2012. Action of bleomycin is affected by bleomycin hydrolase but not by caveolin-1. *International Journal of Oncology,* 41**,** 2245-2252.

CHEN, J., DING, Z., PENG, Y., PAN, F., LI, J., ZOU, L., ZHANG, Y. & LIANG, H. 2014. HIF-1α Inhibition Reverses Multidrug Resistance in Colon Cancer Cells via Downregulation of MDR1/P-Glycoprotein. *PLOS ONE,* 9**,** e98882.

CHEN, L., LIN, G., CHEN, K., LIANG, R., WAN, F., ZHANG, C., TIAN, G. & ZHU, X. 2020. VEGF promotes migration and invasion by regulating EMT and MMPs in nasopharyngeal carcinoma. *Journal of Cancer,* 11**,** 7291-7301.

CHEN, N., CHEN, X., HUANG, R., ZENG, H., GONG, J., MENG, W., LU, Y., ZHAO, F., WANG, L. & ZHOU, Q. 2009. BCL-xL Is a Target Gene Regulated by Hypoxia-inducible Factor-1-α; *. *Journal of Biological Chemistry,* 284**,** 10004-10012.

CHEN, Y., ZHANG, H. & HE, Q. 2017. Involvement of bleomycin hydrolase and poly(ADP-ribose) polymerase-1 in Ubc9-mediated resistance to chemotherapy agents. *International Journal of Oncology,* 50**,** 223-231.

CHO, E. S., KANG, H. E., KIM, N. H. & YOOK, J. I. 2019. Therapeutic implications of cancer epithelial-mesenchymal transition (EMT). *Archives of Pharmacal Research,* 42**,** 14-24.

CHOUDHRY, H. & HARRIS, A. L. 2018. Advances in Hypoxia-Inducible Factor Biology. *Cell Metabolism,* 27**,** 281-298.

CLOUSER, A. F., ALAM, Y. H. & ATKINS, W. M. 2021. Cholesterol Asymmetrically Modulates the Conformational Ensemble of the Nucleotide-Binding Domains of P-Glycoprotein in Lipid Nanodiscs. *Biochemistry,* 60**,** 85-94.

COISNE, C., TILLOY, S., MONFLIER, E., WILS, D., FENART, L. & GOSSELET, F. 2016. Cyclodextrins as Emerging Therapeutic Tools in the Treatment of Cholesterol-Associated Vascular and Neurodegenerative Diseases. *Molecules (Basel, Switzerland),* 21**,** 1748.

COMERFORD, K. M., WALLACE, T. J., KARHAUSEN, J., LOUIS, N. A., MONTALTO, M. C. & COLGAN, S. P. 2002. Hypoxia-inducible Factor-1-dependent Regulation of the Multidrug Resistance (MDR1) Gene. *Cancer Research,* 62**,** 3387-3394.

CRONIN-FENTON, D. P., DAMKIER, P. & LASH, T. L. 2014. Metabolism and transport of tamoxifen in relation to its effectiveness: new perspectives on an ongoing controversy. *Future oncology (London, England),* 10**,** 107-122.

DANZA, G., DI SERIO, C., AMBROSIO, M. R., STURLI, N., LONETTO, G., ROSATI, F., ROCCA, B. J., VENTIMIGLIA, G., DEL VECCHIO, M. T., PRUDOVSKY, I., MARCHIONNI, N. & TARANTINI, F. 2013. Notch3 is activated by chronic hypoxia and contributes to the progression of human prostate cancer. *International Journal of Cancer,* 133**,** 2577-2586.

DAS, T. P., SUMAN, S. & DAMODARAN, C. 2014. Induction of reactive oxygen species generation inhibits epithelial–mesenchymal transition and promotes growth arrest in prostate cancer cells. *Molecular Carcinogenesis* 53**,** 537-547.

DE GONZALO-CALVO, D., LÓPEZ-VILARÓ, L., NASARRE, L., PEREZ-OLABARRIA, M., VÁZQUEZ, T., ESCUIN, D., BADIMON, L., BARNADAS, A., LERMA, E. & LLORENTE-CORTÉS, V. 2015. Intratumor cholesteryl ester accumulation is associated with human breast cancer proliferation and aggressive potential: a molecular and clinicopathological study. *BMC Cancer,* 15**,** 460.

DE MARCHI, T., LIU, N. Q., STINGL, C., TIMMERMANS, M. A., SMID, M., LOOK, M. P., TJOA, M., BRAAKMAN, R. B. H., OPDAM, M., LINN, S. C., SWEEP, F. C. G. J., SPAN, P. N., KLIFFEN, M., LUIDER, T. M., FOEKENS, J. A., MARTENS, J. W. M. & UMAR, A. 2016. 4-protein signature predicting tamoxifen treatment outcome in recurrent breast cancer. *Molecular Oncology,* 10**,** 24-39.

DE OLIVEIRA ANDRADE, L. 2016. Understanding the role of cholesterol in cellular biomechanics and regulation of vesicular trafficking: The power of imaging. *Biomedical Spectroscopy and Imaging,* 5**,** S101-S117.

DEEZAGI, A. & SAFARI, N. 2020. Rosuvastatin inhibit spheroid formation and epithelial–mesenchymal transition (EMT) in prostate cancer PC-3 cell line. *Molecular Biology Reports,* 47**,** 8727-8737.

DELOU, J. M. A., SOUZA, A. S. O., SOUZA, L. C. M. & BORGES, H. L. 2019. Highlights in Resistance Mechanism Pathways for Combination Therapy. *Cells,* 8**,** 1013.

DERYNCK, R. & BUDI, E. H. 2019. Specificity, versatility, and control of TGF-β family signaling. *Science Signaling,* 12**,** eaav5183.

DERYNCK, R. & WEINBERG, R. A. 2019. EMT and Cancer: More Than Meets the Eye. *Developmental Cell,* 49**,** 313-316.

DING, L., CAO, J., LIN, W., CHEN, H., XIONG, X., AO, H., YU, M., LIN, J. & CUI, Q. 2020. The Roles of Cyclin-Dependent Kinases in Cell-Cycle Progression and Therapeutic Strategies in Human Breast Cancer. *International journal of Molecular Sciences,* 21**,** 1960.

DONALDSON, J. G. 2015. Immunofluorescence Staining. *Current Protocols in Cell Biology,* 69**,** 4.3.1-4.3.6.

DONG, C., WU, Y., YAO, J., WANG, Y., YU, Y., RYCHAHOU, P. G., EVERS, B. M. & ZHOU, B. P. 2012. G9a interacts with Snail and is critical for Snail-mediated E-cadherin repression in human breast cancer. *The Journal of Clinical Investigation,* 122**,** 1469-1486.

DONGRE, A. & WEINBERG, R. A. 2019. New insights into the mechanisms of epithelial–mesenchymal transition and implications for cancer. *Nature Reviews Molecular Cell Biology,* 20**,** 69-84.

DRUKER, J., WILSON, J. W., CHILD, F., SHAKIR, D., FASANYA, T. & ROCHA, S. 2021. Role of Hypoxia in the Control of the Cell Cycle. *International Journal of Molecular Science,*22**,** 4874.

DU, B. & SHIM, J. S. 2016. Targeting Epithelial-Mesenchymal Transition (EMT) to Overcome Drug Resistance in Cancer. *Molecules (Basel, Switzerland),* 21**,** 965.

DU, J., ZHU, Y., MENG, X., XIE, H., WANG, J., ZHOU, Z. & WANG, R. 2018. Atorvastatin attenuates paraquat poisoning-induced epithelial-mesenchymal transition via downregulating hypoxia-inducible factor-1 alpha. *Life Sciences,* 213**,** 126-133.

DUAN, Y., HE, Q., YUE, K., SI, H., WANG, J., ZHOU, X. & WANG, X. 2017. Hypoxia induced Bcl-2/Twist1 complex promotes tumor cell invasion in oral squamous cell carcinoma. *Oncotarget,* 8**,** 7729-7739.

DUCHARTRE, Y., KIM, Y.-M. & KAHN, M. 2016. The Wnt signaling pathway in cancer. *Critical Reviews in Oncology/Hematology,* 99**,** 141-149.

ESLAMI-S, Z., CORTÉS-HERNÁNDEZ, L. E. & ALIX-PANABIÈRES, C. 2020. The Metastatic Cascade as the Basis for Liquid Biopsy Development. *Frontiers in Oncology,*10.

FENG, Y., SPEZIA, M., HUANG, S., YUAN, C., ZENG, Z., ZHANG, L., JI, X., LIU, W., HUANG, B., LUO, W., LIU, B., LEI, Y., DU, S., VUPPALAPATI, A., LUU, H. H., HAYDON, R. C., HE, T.-C. & REN, G. 2018. Breast cancer development and progression: Risk factors, cancer stem cells, signaling pathways, genomics, and molecular pathogenesis. *Genes & Diseases,* 5**,** 77-106.

FEROZ, W. & SHEIKH, A. M. A. 2020. Exploring the multiple roles of guardian of the genome: P53. *Egyptian Journal of Medical Human Genetics,* 21**,** 49.

FERRARA, N. 2004. Vascular Endothelial Growth Factor: Basic Science and Clinical Progress. *Endocrine Reviews,* 25**,** 581-611.

FERREIRA, R. J., SANTOS, D. J. D. & FERREIRA, M.-J. U. 2015. P-glycoprotein and membrane roles in multidrug resistance. *Future Medicinal Chmeistry,*7**,** 929-946.

FRANCO, H. L., CASASNOVAS, J., RODRÍGUEZ-MEDINA, J. R. & CADILLA, C. L. 2010. Redundant or separate entities?—roles of Twist1 and Twist2 as molecular switches during gene transcription. *Nucleic Acids Research,* 39**,** 1177-1186.

FU, J., QIN, L., HE, T., QIN, J., HONG, J., WONG, J., LIAO, L. & XU, J. 2011. The TWIST/Mi2/NuRD protein complex and its essential role in cancer metastasis. *Cell Research,* 21**,** 275-289.

FUENTES, N. & SILVEYRA, P. 2019. Estrogen receptor signaling mechanisms. *Advances in Protein Chemistry and Structural Biology,* 116**,** 135-170.

FUJII, T., YAJIMA, R., TATSUKI, H., OOSONE, K. & KUWANO, H. 2016. Anticancer effect of rapamycin on MCF-7 via downregulation of VEGF expression. *In Vitro Cellular & Developmental Biology - Animal,* 52**,** 45-48.

FURUTA, C., MIYAMOTO, T., TAKAGI, T., NOGUCHI, Y., KANEKO, J., ITOH, S., WATANABE, T. & ITOH, F. 2015. Transforming growth factor-β signaling enhancement by long-term exposure to hypoxia in a tumor microenvironment composed of Lewis lung carcinoma cells. *Cancer Science,*106**,** 1524-1533.

FUXE, J., VINCENT, T. & GARCIA DE HERREROS, A. 2010. Transcriptional crosstalk between TGFβ and stem cell pathways in tumor cell invasion: Role of EMT promoting Smad complexes. *Cell Cycle,* 9**,** 2363-2374.

GAN, Z., DING, L., BURCKHARDT, CHRISTOPH J., LOWERY, J., ZARITSKY, A., SITTERLEY, K., MOTA, A., COSTIGLIOLA, N., STARKER, COLBY G., VOYTAS, DANIEL F., TYTELL, J., GOLDMAN, ROBERT D. & DANUSER, G. 2016. Vimentin Intermediate Filaments Template Microtubule Networks to Enhance Persistence in Cell Polarity and Directed Migration. *Cell Systems,* 3**,** 252-263.e8.

GANDHI, V., O'BRIEN, M. H. & YADAV, S. 2020. High-Quality and High-Yield RNA Extraction Method From Whole Human Saliva. *Biomark Insights,*15**,** 1177271920929705.

GEORGAKOPOULOS-SOARES, I., CHARTOUMPEKIS, D. V., KYRIAZOPOULOU, V. & ZARAVINOS, A. 2020. EMT Factors and Metabolic Pathways in Cancer. *Frontiers in Oncology,* 10**,** 499-499.

GILKES, D. M. & SEMENZA, G. L. 2013. Role of hypoxia-inducible factors in breast cancer metastasis. *Future oncology (London, England),* 9**,** 1623-1636.

GLODKOWSKA-MROWKA, E., MROWKA, P., BASAK, G. W., NIESIOBEDZKA-KREZEL, J., SEFERYNSKA, I., WLODARSKI, P. K., JAKOBISIAK, M. & STOKLOSA, T. 2014. Statins inhibit ABCB1 and ABCG2 drug transporter activity in chronic myeloid leukemia cells and potentiate antileukemic effects of imatinib. *Experimental Hematology,* 42**,** 439-447.

GOGNA, R., MADAN, E., KUPPUSAMY, P. & PATI, U. 2012. Re-oxygenation causes hypoxic tumor regression through restoration of p53 wild-type conformation and post-translational modifications. *Cell Death & Disease,* 3**,** e286-e286.

GONZALEZ-MORENO, O., LECANDA, J., GREEN, J. E., SEGURA, V., CATENA, R., SERRANO, D. & CALVO, A. 2010. VEGF elicits epithelial-mesenchymal transition (EMT) in prostate intraepithelial neoplasia (PIN)-like cells via an autocrine loop. *Experimental Cell Research,* 316**,** 554-567.

GU, L., SAHA, S. T., THOMAS, J. & KAUR, M. 2019. Targeting cellular cholesterol for anticancer therapy. *FEBS Journal,* 286**,** 4192-4208.

GU, W., XU, W., SUN, X., ZENG, B., WANG, S., DONG, N., ZHANG, X., CHEN, C., YANG, L., CHEN, G., XIN, A., NI, Z., WANG, J. & YANG, J. 2017. Anordrin Eliminates Tamoxifen Side Effects without Changing Its Antitumor Activity. *Scientific Reports,* 7**,** 43940.

GUERRA, F. S., SAMPAIO, L. D. S., KONIG, S., BONAMINO, M., ROSSI, M. I. D., COSTA, M. L., FERNANDES, P. & MERMELSTEIN, C. 2016. Membrane cholesterol depletion reduces breast tumor cell migration by a mechanism that involves non-canonical Wnt signaling and IL-10 secretion. *Translational Medicine Communications,* 1.

GUPTA, K., MADAN, E., SAYYID, M., ARIAS-PULIDO, H., MORENO, E., KUPPUSAMY, P. & GOGNA, R. 2014. Oxygen regulates molecular mechanisms of cancer progression and metastasis. *Cancer and Metastasis Reviews,* 33**,** 183-215.

HAIDER, T., PANDEY, V., BANJARE, N., GUPTA, P. N. & SONI, V. 2020. Drug resistance in cancer: mechanisms and tackling strategies. *Pharmacological Reports,* 72**,** 1125-1151.

HAJRA, K. M., CHEN, D. Y.-S. & FEARON, E. R. 2002. The SLUG Zinc-Finger Protein Represses E-Cadherin in Breast Cancer. *Cancer Research,* 62**,** 1613-1618.

HAMPTON, R. Y. 2002. ER-associated degradation in protein quality control and cellular regulation. *Current Opinion in Cell Biology,* 14**,** 476-482.

HAPKE, R. Y. & HAAKE, S. M. 2020. Hypoxia-induced epithelial to mesenchymal transition in cancer. *Cancer Letters,* 487**,** 10-20.

HASSAN VENKATESH, G., BRAVO, P., SHAABAN MOUSTAFA ELSAYED, W., AMIRTHARAJ, F., WOJTAS, B., ABOU KHOUZAM, R., HUSSEIN NAWAFLEH, H., MALLYA, S., SATYAMOORTHY, K., DESSEN, P., ROSSELLI, F., THIERY, J. & CHOUAIB, S. 2020. Hypoxia increases mutational load of breast cancer cells through frameshift mutations. *Oncoimmunology,* 9**,** 1750750-1750750.

HASVOLD, G., LUND-ANDERSEN, C., LANDO, M., PATZKE, S., HAUGE, S., SUO, Z., LYNG, H. & SYLJUÅSEN, R. G. 2016. Hypoxia-induced alterations of G2 checkpoint regulators. *Molecular Oncology,* 10**,** 764-773.

HEGEDÜS, C., TELBISZ, Á., HEGEDŰS, T., SARKADI, B. & ÖZVEGY-LACZKA, C. 2015. Chapter Four - Lipid Regulation of the ABCB1 and ABCG2 Multidrug Transporters. *In:* SCHUETZ, J. D. & ISHIKAWA, T. (eds.) *Advances in Cancer Research.* Academic Press.

HELDIN, C.-H. & MOUSTAKAS, A. 2016. Signaling Receptors for TGF-β Family Members. 8.

HELDIN, C.-H., VANLANDEWIJCK, M. & MOUSTAKAS, A. 2012. Regulation of EMT by TGFβ in cancer. *FEBS Letters,* 586**,** 1959-1970.

HERNANSANZ-AGUSTÍN, P., IZQUIERDO-ÁLVAREZ, A., SÁNCHEZ-GÓMEZ, F. J., RAMOS, E., VILLA-PIÑA, T., LAMAS, S., BOGDANOVA, A. & MARTÍNEZ-RUIZ, A. 2014. Acute hypoxia produces a superoxide burst in cells. *Free Radical Biology and Medicine,* 71**,** 146-156.

HERRANZ, N., PASINI, D., DÍAZ, V. M., FRANCÍ, C., GUTIERREZ, A., DAVE, N., ESCRIVÀ, M., HERNANDEZ-MUÑOZ, I., DI CROCE, L., HELIN, K., GARCÍA DE HERREROS, A. & PEIRÓ, S. 2008. Polycomb complex 2 is required for E-cadherin repression by the Snail1 transcription factor. *Molecular and Cellular Biology,* 28**,** 4772-4781.

HIRSILÄ, M., KOIVUNEN, P., XU, L., SEELEY, T., KIVIRIKKO, K. I. & MYLLYHARJU, J. 2005. Effect of desferrioxamine and metals on the hydroxylases in the oxygen sensing pathway. *FASEB Journal,*19**,** 1308-1310.

HONG, C.-F., CHEN, W.-Y. & WU, C.-W. 2017. Upregulation of Wnt signaling under hypoxia promotes lung cancer progression. *Oncology Reports,* 38**,** 1706-1714.

HOU, Z., PENG, H., AYYANATHAN, K., YAN, K.-P., LANGER, E. M., LONGMORE, G. D. & RAUSCHER, F. J., 3RD 2008. The LIM protein AJUBA recruits protein arginine methyltransferase 5 to mediate SNAIL-dependent transcriptional repression. *Molecular and Cellular Biology,* 28**,** 3198-3207.

HOUSMAN, G., BYLER, S., HEERBOTH, S., LAPINSKA, K., LONGACRE, M., SNYDER, N. & SARKAR, S. 2014. Drug Resistance in Cancer: an overview. *Cancers,* 6**,** 1769-1792.

IKENOUCHI, J., MATSUDA, M., FURUSE, M. & TSUKITA, S. 2003. Regulation of tight junctions during the epithelium-mesenchyme transition: direct repression of the gene expression of claudins/occludin by Snail. *Journal of Cell Science,* 116**,** 1959.

IM, K., MARENINOV, S., DIAZ, M. F. P. & YONG, W. H. 2019. An Introduction to Performing Immunofluorescence Staining. *Methods in Molecular Biology (Clifton, N.J.),* 1897**,** 299-311.

IREKA, Y., AGUSTINA, H., AZIZ, A., HERNOWO, B. S. & SURYANTI, S. 2019. Comparison of Fixation Methods for Preservation Cytology Specimens of Cell Block Preparation Using 10% Neutral Buffer Formalin and 96% Alcohol Fixation in E-cadherin and Ki-67 Immunohistochemical Examination. *Open access Macedonian Journal of Medical Sciences,* 7**,** 3139-3144.

IZEM, L. & MORTON, R. E. 2007. Possible Role for Intracellular Cholesteryl Ester Transfer Protein in Adipocyte Lipid Metabolism and Storage. *The Journal of Biological Chemistry,* 282**,** 21856-21865.

JAHANGIRI, A., DADMANESH, M. & GHORBAN, K. 2018. Suppression of STAT3 by S31-201 to reduce the production of immunoinhibitory cytokines in a HIF1-α-dependent manner: a study on the MCF-7 cell line. *In Vitro Cellular & Developmental Biology - Animal,* 54**,** 743-748.

JEANNOT, P., NOWOSAD, A., PERCHEY, R. T., CALLOT, C., BENNANA, E., KATSUBE, T., MAYEUX, P., GUILLONNEAU, F., MANENTI, S. & BESSON, A. 2017. p27(Kip1) promotes invadopodia turnover and invasion through the regulation of the PAK1/Cortactin pathway. *eLife,* 6**,** e22207.

JETHWA, P., NAQVI, M., HARDY, R. G., HOTCHIN, N.-A., ROBERTS, S., SPYCHAL, R. & TSELEPIS, C. 2008. Overexpression of Slug is associated with malignant progression of esophageal adenocarcinoma. *World Journal of Gastroenterology,* 14**,** 1044-1052.

JIAO, M. & NAN, K.-J. 2012. Activation of PI3 kinase/Akt/HIF-1α pathway contributes to hypoxia-induced epithelial-mesenchymal transition and chemoresistance in hepatocellular carcinoma. *International Journal of Oncology,* 40**,** 461-468.

JING, X., YANG, F., SHAO, C., WEI, K., XIE, M., SHEN, H. & SHU, Y. 2019. Role of hypoxia in cancer therapy by regulating the tumor microenvironment. *Molecular Cancer,* 18**,** 157.

JO, E., PARK, S. J., CHOI, Y. S., JEON, W.-K. & KIM, B.-C. 2015. Kaempferol Suppresses Transforming Growth Factor-β1–Induced Epithelial-to-Mesenchymal Transition and Migration of A549 Lung Cancer Cells by Inhibiting Akt1-Mediated Phosphorylation of Smad3 at Threonine-179. *Neoplasia,* 17**,** 525-537.

JOSEPH, J. V., CONROY, S., PAVLOV, K., SONTAKKE, P., TOMAR, T., EGGENS-MEIJER, E., BALASUBRAMANIYAN, V., WAGEMAKERS, M., DEN DUNNEN, W. F. A. & KRUYT, F. A. E. 2015. Hypoxia enhances migration and invasion in glioblastoma by promoting a mesenchymal shift mediated by the HIF1α–ZEB1 axis. *Cancer Letters,* 359**,** 107-116.

JOUNG, Y. H., LIM, E. J., LEE, M. Y., PARK, J. H., YE, S. K., PARK, E. U., KIM, S. Y., ZHANG, Z., LEE, K. J., PARK, D. K., PARK, T., MOON, W. K. & YANG, Y. M. 2005. Hypoxia activates the cyclin D1 promoter via the Jak2/STAT5b pathway in breast cancer cells. *Experimental and Molecular Medicine* 37.

KATO, S., LIBERONA, M. F., CERDA-INFANTE, J., SÁNCHEZ, M., HENRÍQUEZ, J., BIZAMA, C., BRAVO, M. L., GONZALEZ, P., GEJMAN, R., BRAÑES, J., GARCÍA, K., IBAÑEZ, C.,

OWEN, G. I., ROA, J. C., MONTECINOS, V. & CUELLO, M. A. 2018. Simvastatin interferes with cancer 'stem-cell' plasticity reducing metastasis in ovarian cancer *Endocrine-Related Cancer*. 25**,** 821-836.

KE, Q., KLUZ, T. & COSTA, M. 2005. Down-regulation of the expression of the FIH-1 and ARD-1 genes at the transcriptional level by nickel and cobalt in the human lung adenocarcinoma A549 cell line. *International Journal of Environmental Research and Public Health,* 2**,** 10-13.

KE, X. & SHEN, L. 2017. Molecular targeted therapy of cancer: The progress and future prospect. *Frontiers in Laboratory Medicine,* 1**,** 69-75.

KELLY-SPRATT, K. S., GURLEY, K. E., YASUI, Y. & KEMP, C. J. 2004. p19 Arf Suppresses Growth, Progression, and Metastasis of Hras-Driven Carcinomas through p53-Dependent and -Independent Pathways. *PLOS Biology,* 2**,** e242.

KIM, M.-C., HWANG, S.-H., KIM, N.-Y., LEE, H.-S., JI, S., YANG, Y. & KIM, Y. 2018a. Hypoxia promotes acquisition of aggressive phenotypes in human malignant mesothelioma. *BMC Cancer,* 18**,** 819.

KIM, S., LEE, M., DHANASEKARAN, D. N. & SONG, Y. S. 2018b. Activation of LXRα/β by cholesterol in malignant ascites promotes chemoresistance in ovarian cancer. *BMC cancer,* 18**,** 1232-1232.

KONG, D., ZHANG, F., SHAO, J., WU, L., ZHANG, X., CHEN, L., LU, Y. & ZHENG, S. 2015. Curcumin inhibits cobalt chloride-induced epithelial-to-mesenchymal transition associated with interference with TGF-β/Smad signaling in hepatocytes. *Laboratory Investigation,* 95**,** 1234-1245.

KOPECKA, J., TROUILLAS, P., GAŠPAROVIĆ, A. Č., GAZZANO, E., ASSARAF, Y. G. & RIGANTI, C. 2020. Phospholipids and cholesterol: Inducers of cancer multidrug resistance and therapeutic targets. *Drug Resistance Updates,* 49**,** 100670.

KRAUSS, K. & STICKELER, E. 2020. Endocrine Therapy in Early Breast Cancer. *Breast Care,* 15**,** 337-346.

KRZYWINSKA, E. & STOCKMANN, C. 2018. Hypoxia, Metabolism and Immune Cell Function. *Biomedicines,* 6**,** 56.

KUO, T.-T., HUANG, Y.-B. & HSIEH, C.-J. 2020. Consumption and market share of cholesterol-lowering drugs in high-risk patients before and after the release of the 2013 ACC/AHA cholesterol guidelines: a retrospective observational study. *BMJ Open,* 10**,** e036769.

KUŞOĞLU, A. & BIRAY AVCı, Ç. 2019. Cancer stem cells: A brief review of the current status. *Gene,* 681**,** 80-85.

KUZU, O. F., NOORY, M. A. & ROBERTSON, G. P. 2016. The Role of Cholesterol in Cancer. *Cancer Research,* 76**,** 2063-2070.

LABRECQUE, M. P., TAKHAR, M. K., JAGDEO, J. M., TAM, K. J., CHIU, C., WANG, T.-Y., PREFONTAINE, G. G., COX, M. E. & BEISCHLAG, T. V. 2014. A TRIP230-Retinoblastoma

Protein Complex Regulates Hypoxia-Inducible Factor-1α-Mediated Transcription and Cancer Cell Invasion. *PLOS ONE,* 9**,** e99214.

LAMBERT, A. W., PATTABIRAMAN, D. R. & WEINBERG, R. A. 2017. Emerging Biological Principles of Metastasis. *Cell,* 168**,** 670-691.

LAMOUILLE, S., XU, J. & DERYNCK, R. 2014. Molecular mechanisms of epithelial–mesenchymal transition. *Nature Reviews Molecular Cell Biology,* 15**,** 178-196.

LEE, H. J., LI, J., VICKMAN, R. E., LI, J., LIU, R., DURKES, A. C., ELZEY, B. D., YUE, S., LIU, X., RATLIFF, T. L. & CHENG, J.-X. 2018. Cholesterol Esterification Inhibition Suppresses Prostate Cancer Metastasis by Impairing the Wnt/β-catenin Pathway. *Molecular Cancer Research,* 16**,** 974-985.

LEE, Y.-H., YANG, H.-W., YANG, L.-C., LU, M.-Y., TSAI, L.-L., YANG, S.-F., HUANG, Y.-F., CHOU, M.-Y., YU, C.-C. & HU, F.-W. 2017. DHFR and MDR1 upregulation is associated with chemoresistance in osteosarcoma stem-like cells. *Oncology letters,* 14**,** 171-179.

LEGGETT, S. E., HRUSKA, A. M., GUO, M. & WONG, I. Y. 2021. The epithelial-mesenchymal transition and the cytoskeleton in bioengineered systems. *Cell Communication and Signaling,* 19**,** 32.

LEWIS, C. A., BRAULT, C., PECK, B., BENSAAD, K., GRIFFITHS, B., MITTER, R., CHAKRAVARTY, P., EAST, P., DANKWORTH, B., ALIBHAI, D., HARRIS, A. L. & SCHULZE, A. 2015. SREBP maintains lipid biosynthesis and viability of cancer cells under lipid- and oxygen-deprived conditions and defines a gene signature associated with poor survival in glioblastoma multiforme. *Oncogene,* 34**,** 5128-5140.

LI, H., FENG, Z. & HE, M.-L. 2020. Lipid metabolism alteration contributes to and maintains the properties of cancer stem cells. *Theranostics,* 10**,** 7053-7069.

LI, J., GU, D., LEE, S. S. Y., SONG, B., BANDYOPADHYAY, S., CHEN, S., KONIECZNY, S. F., RATLIFF, T. L., LIU, X., XIE, J. & CHENG, J. X. 2016. Abrogating cholesterol esterification suppresses growth and metastasis of pancreatic cancer. *Oncogene,* 35**,** 6378-6388.

LI, M., BU, X., CAI, B., LIANG, P., LI, K., QU, X. & SHEN, L. 2019. Biological role of metabolic reprogramming of cancer cells during epithelial-mesenchymal transition (Review). *Oncol Rep,* 41**,** 727-741.

LI, Q., MA, R. & ZHANG, M. 2018. CoCl(2) increases the expression of hypoxic markers HIF-1α, VEGF and CXCR4 in breast cancer MCF-7 cells. *Oncology letters,* 15**,** 1119-1124.

LI, S., ZHANG, J., YANG, H., WU, C., DANG, X. & LIU, Y. 2015a. Copper depletion inhibits CoCl2-induced aggressive phenotype of MCF-7 cells via downregulation of HIF-1 and inhibition of Snail/Twist-mediated epithelial-mesenchymal transition. *Scientific Reports,* 5**,** 12410.

LI, W., CAO, L., HAN, L., XU, Q. & MA, Q. 2015b. Superoxide dismutase promotes the epithelial-mesenchymal transition of pancreatic cancer cells via activation of the H2O2/ERK/NF-κB axis. *International Journal of Oncology,* 46**,** 2613-2620.

LIAO, T.-T. & YANG, M.-H. 2020. Hybrid Epithelial/Mesenchymal State in Cancer Metastasis: Clinical Significance and Regulatory Mechanisms. *Cells,* 9**,** 623.

LIN, Y., WU, Y., LI, J., DONG, C., YE, X., CHI, Y.-I., EVERS, B. M. & ZHOU, B. P. 2010. The SNAG domain of Snail1 functions as a molecular hook for recruiting lysine-specific demethylase 1. *The EMBO journal,* 29**,** 1803-1816.

LISON, D., DE BOECK, M., VEROUGSTRAETE, V. & KIRSCH-VOLDERS, M. 2001. Update on the genotoxicity and carcinogenicity of cobalt compounds. *Occupational and Environmental Medicine,* 58**,** 619-625.

LIU, C.-Y., LIN, H.-H., TANG, M.-J. & WANG, Y.-K. 2015. Vimentin contributes to epithelial-mesenchymal transition cancer cell mechanics by mediating cytoskeletal organization and focal adhesion maturation. *Oncotarget,* 6**,** 15966-15983.

LIU, H., QIN, Y., ZHAI, D., ZHANG, Q., GU, J., TANG, Y., YANG, J., LI, K., YANG, L., CHEN, S., ZHONG, W., MENG, J., LIU, Y., SUN, T. & YANG, C. 2019. Antimalarial Drug Pyrimethamine Plays a Dual Role in Antitumor Proliferation and Metastasis through Targeting DHFR and TP. *Molecular Cancer Therapy,*18**,** 541-555.

LIU, K.-H., TSAI, Y.-T., CHIN, S.-Y., LEE, W.-R., CHEN, Y.-C. & SHEN, S.-C. 2018. Hypoxia Stimulates the Epithelial–to–Mesenchymal Transition in Lung Cancer Cells Through Accumulation of Nuclear β-Catenin. *Anticancer Research,* 38**,** 6299-6308.

LIU, Y. & LU, L.-Y. 2020. BRCA1 and homologous recombination: implications from mouse embryonic development. *Cell & Bioscience,* 10**,** 49.

LONGO, J., VAN LEEUWEN, J. E., ELBAZ, M., BRANCHARD, E. & PENN, L. Z. 2020. Statins as Anticancer Agents in the Era of Precision Medicine. *Clinical Cancer Research,* 26**,** 5791-5800.

LOWERY, J., KUCZMARSKI, E. R., HERRMANN, H. & GOLDMAN, R. D. 2015. Intermediate Filaments Play a Pivotal Role in Regulating Cell Architecture and Function*. *Journal of Biological Chemistry,* 290**,** 17145-17153.

LUCHETTI, G., SIRCAR, R., KONG, J. H., NACHTERGAELE, S., SAGNER, A., BYRNE, E. F., COVEY, D. F., SIEBOLD, C. & ROHATGI, R. 2016. Cholesterol activates the G-protein coupled receptor Smoothened to promote Hedgehog signaling. *eLife,* 5**,** e20304.

LUU, W., SHARPE, L., GELISSEN, I. & BROWN, A. 2013a. The role of signalling in cellular cholesterol homeostasis. *IUBMB Life,* 65**,** 675-684.

LUU, W., SHARPE, L. J., GELISSEN, I. C. & BROWN, A. J. 2013b. The role of signalling in cellular cholesterol homeostasis. *IUBMB Life,* 65**,** 675-684.

MALUMBRES, M. 2014. Cyclin-dependent kinases. *Genome Biology,* 15**,** 122.

MANDAL, C. C. & RAHMAN, M. M. 2014. Targeting Intracellular Cholesterol is a Novel Therapeutic Strategy for Cancer Treatment. *Journal of Cancer Science & Therapy,* 6**,** 510-513.

MARTÍNEZ-ESTRADA, O. M., CULLERÉS, A., SORIANO, F. X., PEINADO, H., BOLÓS, V., MARTÍNEZ, F. O., REINA, M., CANO, A., FABRE, M. & VILARÓ, S. 2006. The

transcription factors Slug and Snail act as repressors of Claudin-1 expression in epithelial cells. *The Biochemical Journal,* 394**,** 449-457.

MATSUOKA, J., YASHIRO, M., DOI, Y., FUYUHIRO, Y., KATO, Y., SHINTO, O., NODA, S., KASHIWAGI, S., AOMATSU, N., HIRAKAWA, T., HASEGAWA, T., SHIMIZU, K., SHIMIZU, T., MIWA, A., YAMADA, N., SAWADA, T. & HIRAKAWA, K. 2013. Hypoxia stimulates the EMT of gastric cancer cells through autocrine TGFβ signaling. *PloS one,* 8**,** e62310-e62310.

MATURI, V., ENROTH, S., HELDIN, C.-H. & MOUSTAKAS, A. 2018. Genome-wide binding of transcription factor ZEB1 in triple-negative breast cancer cells. *Journal of Cellular Physiology,* 233**,** 7113-7127.

MATUSEWICZ, L., CZOGALLA, A. & SIKORSKI, A. F. 2020. Attempts to use statins in cancer therapy: An update. *Tumour Biology,* 42**,** 1010428320941760.

MAXFIELD, F. R. & WÜSTNER, D. 2012. Chapter 17 - Analysis of Cholesterol Trafficking with Fluorescent Probes. *In:* DI PAOLO, G. & WENK, M. R. (eds.) *Methods in Cell Biology.* Academic Press.

MAYENGBAM, S. S., SINGH, A., PILLAI, A. D. & BHAT, M. K. 2021. Influence of cholesterol on cancer progression and therapy. *Translational Oncology,* 14**,** 101043.

MCMAHON, S., CHARBONNEAU, M., GRANDMONT, S., RICHARD, D. E. & DUBOIS, C. M. 2006. Transforming Growth Factor-β Induces Hypoxia-inducible Factor-1 Stabilization through Selective Inhibition of PHD2 Expression *. *Journal of Biological Chemistry,* 281**,** 24171-24181.

MENDEZ, M. G., KOJIMA, S.-I. & GOLDMAN, R. D. 2010. Vimentin induces changes in cell shape, motility, and adhesion during the epithelial to mesenchymal transition. *FASEB journal : official publication of the Federation of American Societies for Experimental Biology,* 24**,** 1838-1851.

MENG, J., CHEN, S., HAN, J.-X., QIAN, B., WANG, X.-R., ZHONG, W.-L., QIN, Y., ZHANG, H., GAO, W.-F., LEI, Y.-Y., YANG, W., YANG, L., ZHANG, C., LIU, H.-J., LIU, Y.-R., ZHOU, H.-G., SUN, T. & YANG, C. 2018. Twist1 Regulates Vimentin through Cul2 Circular RNA to Promote EMT in Hepatocellular Carcinoma. *Cancer Research,* 78**,** 4150.

MEŠKYTĖ, E. M., KESKAS, S. & CIRIBILLI, Y. 2020. MYC as a Multifaceted Regulator of Tumor Microenvironment Leading to Metastasis. *International Journal of Molecular Sciences,* 21**,** 7710.

MEYENBERG CUNHA-DE PADUA, M., NOLETO, G. R., DE OLIVEIRA PETKOWICZ, C. L., CADENA, S. M. S. C., BOST, F., POUYSSÉGUR, J. & MAZURE, N. M. 2019. Hypoxia protects against the cell death triggered by oxovanadium–galactomannan complexes in HepG2 cells. *Cellular & Molecular Biology Letters,* 24**,** 18.

MILLER, I., MIN, M., YANG, C., TIAN, C., GOOKIN, S., CARTER, D. & SPENCER, S. L. 2018. Ki67 is a Graded Rather than a Binary Marker of Proliferation versus Quiescence. *Cell Reports,* 24**,** 1105-1112.e5.

MOHAMMAD, N., MALVI, P., MEENA, A. S., SINGH, S. V., CHAUBE, B., VANNURUSWAMY, G., KULKARNI, M. J. & BHAT, M. K. 2014. Cholesterol depletion by methyl-β-cyclodextrin augments tamoxifen induced cell death by enhancing its uptake in melanoma. *Molecular Cancer,* 13**,** 204-204.

MOLLINEDO, F. & GAJATE, C. 2015. Lipid rafts as major platforms for signaling regulation in cancer. *Advances in Biological Regulation,* 57**,** 130-146.

MORANDI, A., TADDEI, M. L., CHIARUGI, P. & GIANNONI, E. 2017. Targeting the Metabolic Reprogramming That Controls Epithelial-to-Mesenchymal Transition in Aggressive Tumors. *Frontiers in Oncology,* 7.

MUNDHARA, N., MAJUMDER, A. & PANDA, D. 2019. Methyl-β-cyclodextrin, an actin depolymerizer augments the antiproliferative potential of microtubule-targeting agents. *Scientific Reports,* 9**,** 7638.

MUÑOZ-SÁNCHEZ, J. & CHÁNEZ-CÁRDENAS, M. E. 2018. The use of cobalt chloride as a chemical hypoxia model. *Journal of Applied Toxicology,* 39**,** 556–570.

MURAI, T. 2015. Cholesterol Lowering: Role in Cancer Prevention and Treatment. *Biological Chemistry,* 396**,** 1-11.

MURAI, T., MARUYAMA, Y., MIO, K., NISHIYAMA, H., SUGA, M. & SATO, C. 2011. Low Cholesterol Triggers Membrane Microdomain-dependent CD44 Shedding and Suppresses Tumor Cell Migration *. *Journal of Biological Chemistry,* 286**,** 1999-2007.

NAIR, S. & SACHDEVA, G. 2018. Estrogen matters in metastasis. *Steroids,* 138**,** 108-116.

NELSON, E. R., CHANG, C.-Y. & MCDONNELL, D. P. 2014a. Cholesterol and breast cancer pathophysiology. *Trends in Endocrinology and Metabolism: TEM,* 25**,** 649-655.

NIETO, M. A., HUANG, RUBY Y.-J., JACKSON, REBECCA A. & THIERY, JEAN P. 2016. EMT: 2016. *Cell,* 166**,** 21-45.

NURWIDYA, F., TAKAHASHI, F., MINAKATA, K., MURAKAMI, A. & TAKAHASHI, K. 2012. From tumor hypoxia to cancer progression: the implications of hypoxia-inducible factor-1 expression in cancers. *Anatomy & cell biology,* 45**,** 73-78.

OLENYUK, B. Z., ZHANG, G.-J., KLCO, J. M., NICKOLS, N. G., KAELIN, W. G., JR. & DERVAN, P. B. 2004. Inhibition of vascular endothelial growth factor with a sequence-specific hypoxia response element antagonist. *Proceedings of the National Academy of Sciences of the United States of America,* 101**,** 16768-16773.

ONCUL, S. & ERCAN, A. 2017. Discrimination of the Effects of Doxorubicin on Two Different Breast Cancer Cell Lines on Account of Multidrug Resistance and Apoptosis. *Indian Journal of Pharmaceutical Sciences,* 79.

OTTO, T. & SICINSKI, P. 2017. Cell cycle proteins as promising targets in cancer therapy. *Nature reviews. Cancer,* 17**,** 93-115.

PALLOTTINI, V., GUANTARIO, B., MARTINI, C., TOTTA, P., FILIPPI, I., CARRARO, F. & TRENTALANCE, A. 2008. Regulation of HMG-CoA reductase expression by hypoxia. *Journal of Cellular Biochemistry,* 104**,** 701-709.

PALMER, C. P., MAHEN, R., SCHNELL, E., DJAMGOZ, M. B. A. & AYDAR, E. 2007. Sigma-1 Receptors Bind Cholesterol and Remodel Lipid Rafts in Breast Cancer Cell Lines. *Cancer Research,* 67**,** 11166-11175.

PAN, S.-T., LI, Z.-L., HE, Z.-X., QIU, J.-X. & ZHOU, S.-F. 2016. Molecular mechanisms for tumour resistance to chemotherapy. *Clinical and Experimental Pharmacology and Physiology,* 43**,** 723-737.

PASTUSHENKO, I. & BLANPAIN, C. 2019. EMT Transition States during Tumor Progression and Metastasis. *Trends in Cell Biology,* 29**,** 212-226.

PATEL, H. K. & BIHANI, T. 2018. Selective estrogen receptor modulators (SERMs) and selective estrogen receptor degraders (SERDs) in cancer treatment. *Pharmacology & Therapeutics,* 186**,** 1-24.

PAVLACKY, J. & POLAK, J. 2020a. Technical Feasibility and Physiological Relevance of Hypoxic Cell Culture Models. *Frontiers in Endocrinology,* 11.

PAVLACKY, J. & POLAK, J. 2020b. Technical Feasibility and Physiological Relevance of Hypoxic Cell Culture Models. *Frontiers in Endocrinology,*11.

PECK, B. & SCHULZE, A. 2014. Cholesteryl Esters: Fueling the Fury of Prostate Cancer. *Cell Metabolism,* 19**,** 350-352.

PEINADO, H., BALLESTAR, E., ESTELLER, M. & CANO, A. 2004. Snail mediates E-cadherin repression by the recruitment of the Sin3A/histone deacetylase 1 (HDAC1)/HDAC2 complex. *Molecular and Cellular Biology,* 24**,** 306-319.

POIRIER, S., MAYER, G., POUPON, V., MCPHERSON, P. S., DESJARDINS, R., LY, K., ASSELIN, M.-C., DAY, R., DUCLOS, F. J., WITMER, M., PARKER, R., PRAT, A. & SEIDAH, N. G. 2009. Dissection of the endogenous cellular pathways of PCSK9-induced low density lipoprotein receptor degradation: evidence for an intracellular route. *The Journal of Biological Chemistry,* 284**,** 28856-28864.

QIU, G.-Z., JIN, M.-Z., DAI, J.-X., SUN, W., FENG, J.-H. & JIN, W.-L. 2017a. Reprogramming of the Tumor in the Hypoxic Niche: The Emerging Concept and Associated Therapeutic Strategies. *Trends in Pharmacological Sciences,* 38**,** 669-686.

QIU, N., LI, X. & LIU, J. 2017b. Application of cyclodextrins in cancer treatment. *Journal of Inclusion Phenomena and Macrocyclic Chemistry,* 89**,** 229-246.

RANA, N. K., SINGH, P. & KOCH, B. 2019. CoCl(2) simulated hypoxia induce cell proliferation and alter the expression pattern of hypoxia associated genes involved in angiogenesis and apoptosis. *Biological Research,* 52**,** 12-12.

RANA, R. M., RAMPOGU, S., ABID, N. B., ZEB, A., PARATE, S., LEE, G., YOON, S., KIM, Y., KIM, D. & LEE, K. W. 2020. In Silico Study Identified Methotrexate Analog as Potential Inhibitor of Drug Resistant Human Dihydrofolate Reductase for Cancer Therapeutics. *Molecules (Basel, Switzerland),* 25**,** 3510.

RANI, A., STEBBING, J., GIAMAS, G. & MURPHY, J. 2019. Endocrine Resistance in Hormone Receptor Positive Breast Cancer–From Mechanism to Therapy. *Frontiers in Endocrinology (Basel, Switzerland)*10.

RANKIN, E. B., NAM, J.-M. & GIACCIA, A. J. 2016. Hypoxia: Signaling the Metastatic Cascade. *Trends in Cancer,* 2**,** 295-304.

RIGGIO, A. I., VARLEY, K. E. & WELM, A. L. 2021. The lingering mysteries of metastatic recurrence in breast cancer. *British Journal of Cancer,* 124**,** 13-26.

RISCAL, R., SKULI, N. & SIMON, M. C. 2019. Even Cancer Cells Watch Their Cholesterol! *Molecular Cell,* 76**,** 220-231.

ROBINSON, K. & TIRIVEEDHI, V. 2020. Perplexing Role of P-Glycoprotein in Tumor Microenvironment. *Frontiers in Onoclogy,*10.

RODRIGUEZ, M. & POTTER, D. A. 2013. CYP1A1 regulates breast cancer proliferation and survival. *Molecular cancer research : MCR,* 11**,** 780-792.

SAGAR, S., ESAU, L., MOOSA, B., KHASHAB, N. M., BAJIC, V. B. & KAUR, M. 2014. Cytotoxicity and apoptosis induced by a plumbagin derivative in estrogen positive MCF-7 breast cancer cells. *Anti-cancer agents in medicinal chemistry,* 14**,** 170-180.

SAITOH, M. 2018. Involvement of partial EMT in cancer progression. *The Journal of Biochemistry,* 164**,** 257-264.

SAKULTERDKIAT, T., SRISOMSAP, C., UDOMSANGPETCH, R., SVASTI, J. & LIRDPRAPAMONGKOL, K. 2012. Curcumin Resistance Induced by Hypoxia in HepG2 Cells Is Mediated by Multidrug-resistance-associated Proteins. *Anticancer Research,* 32**,** 5337-5342.

SAXENA, K. & JOLLY, M. K. 2019. Acute vs. Chronic vs. Cyclic Hypoxia: Their Differential Dynamics, Molecular Mechanisms, and Effects on Tumor Progression. *Biomolecules,* 9**,** 339.

SEBIO, A., KAHN, M. & LENZ, H.-J. 2014. The potential of targeting Wnt/β-catenin in colon cancer. *Expert Opinion on Therapeutic Targets,* 18**,** 611-615.

SERRANO-GOMEZ, S. J., MAZIVEYI, M. & ALAHARI, S. K. 2016. Regulation of epithelial-mesenchymal transition through epigenetic and post-translational modifications. *Molecular Cancer,* 15**,** 18-18.

SEZGIN, E., AZBAZDAR, Y., NG, X. W., TEH, C., SIMONS, K., WEIDINGER, G., WOHLAND, T., EGGELING, C. & OZHAN, G. 2017. Binding of canonical Wnt ligands to their receptor

complexes occurs in ordered plasma membrane environments. *The FEBS Journal,* 284**,** 2513-2526.

SHANNON, P., MARKIEL, A., OZIER, O., BALIGA, N. S., WANG, J. T., RAMAGE, D., AMIN, N., SCHWIKOWSKI, B. & IDEKER, T. 2003. Cytoscape: a software environment for integrated models of biomolecular interaction networks. *Genome research,* 13**,** 2498-2504.

SHAPIRA, K. E., EHRLICH, M. & HENIS, Y. I. 2018. Cholesterol depletion enhances TGF-β Smad signaling by increasing c-Jun expression through a PKR-dependent mechanism. *Molecular Biology of the Cell,* 29**,** 2494-2507.

SHARMA, A., BANDYOPADHAYAYA, S., CHOWDHURY, K., SHARMA, T., MAHESHWARI, R., DAS, A., CHAKRABARTI, G., KUMAR, V. & MANDAL, C. C. 2019. Metformin exhibited anticancer activity by lowering cellular cholesterol content in breast cancer cells. *PLOS ONE,* 14**,** e0209435.

SHENG, R., KIM, H., LEE, H., XIN, Y., CHEN, Y., TIAN, W., CUI, Y., CHOI, J.-C., DOH, J., HAN, J.-K. & CHO, W. 2014. Cholesterol selectively activates canonical Wnt signalling over non-canonical Wnt signalling. *Nature Communications,* 5**,** 4393.

SHIBUE, T. & WEINBERG, R. A. 2017. EMT, CSCs, and drug resistance: the mechanistic link and clinical implications. *Nature Reviews Clinical Oncology,* 14**,** 611–629.

SILVENTE-POIROT, S. & POIROT, M. 2014. Cholesterol and Cancer, in the Balance. *Science,* 343**,** 1445-1446.

SIMONSEN, L. O., HARBAK, H. & BENNEKOU, P. 2012. Cobalt metabolism and toxicology—A brief update. *Science of The Total Environment,* 432**,** 210-215.

SINGH, M., YELLE, N., VENUGOPAL, C. & SINGH, S. K. 2018. EMT: Mechanisms and therapeutic implications. *Pharmacology & Therapeutics,* 182**,** 80-94.

SNEHA, S., BAKER, S. C., GREEN, A., STORR, S., AIYAPPA, R., MARTIN, S. & PORS, K. 2021. Intratumoural Cytochrome P450 Expression in Breast Cancer: Impact on Standard of Care Treatment and New Efforts to Develop Tumour-Selective Therapies. *Biomedicines,* 9**,** 290.

SOBECKI, M., MROUJ, K., CAMASSES, A., PARISIS, N., NICOLAS, E., LLÈRES, D., GERBE, F., PRIETO, S., KRASINSKA, L., DAVID, A., EGUREN, M., BIRLING, M.-C., URBACH, S., HEM, S., DÉJARDIN, J., MALUMBRES, M., JAY, P., DULIC, V., LAFONTAINE, D. L., FEIL, R. & FISHER, D. 2016. The cell proliferation antigen Ki-67 organises heterochromatin. *eLife,* 5**,** e13722-e13722.

SPRING, L. M., GUPTA, A., REYNOLDS, K. L., GADD, M. A., ELLISEN, L. W., ISAKOFF, S. J., MOY, B. & BARDIA, A. 2016. Neoadjuvant Endocrine Therapy for Estrogen Receptor-Positive Breast Cancer: A Systematic Review and Meta-analysis. *JAMA oncology,* 2**,** 1477-1486.

SUBRAMANIAN, N., SCHUMANN-GILLETT, A., MARK, A. E. & O'MARA, M. L. 2016. Understanding the accumulation of P-glycoprotein substrates within cells: The effect of

cholesterol on membrane partitioning. *Biochimica et Biophysica Acta (BBA) - Biomembranes,* 1858**,** 776-782.

SUNG, H., FERLAY, J., SIEGEL, R. L., LAVERSANNE, M., SOERJOMATARAM, I., JEMAL, A. & BRAY, F. 2021. Global cancer statistics 2020: GLOBOCAN estimates of incidence and mortality worldwide for 36 cancers in 185 countries. *CA: A Cancer Journal for Clinicians,* **,** 1-41.

SZENTE, L. & FENYVESI, É. 2017. Cyclodextrin-Lipid Complexes: Cavity Size Matters. *Structural Chemistry,* 28**,** 479-492.

TANG, M., BOLDERSON, E., O'BYRNE, K. J. & RICHARD, D. J. 2021. Tumor Hypoxia Drives Genomic Instability. *Frontiers in Cell and Devleopmental Biology,* 9.

THANKAMONY, A. P., SAXENA, K., MURALI, R., JOLLY, M. K. & NAIR, R. 2020. Cancer Stem Cell Plasticity – A Deadly Deal. *Frontiers in Molecular Biosciences,* 7.

TIRPE, A. A., GULEI, D., CIORTEA, S. M., CRIVII, C. & BERINDAN-NEAGOE, I. 2019. Hypoxia: Overview on Hypoxia-Mediated Mechanisms with a Focus on the Role of HIF Genes. *International journal of Molecular Sciences,* 20**,** 6140.

TONG, Z. T., CAI, M. Y., WANG, X. G., KONG, L. L., MAI, S. J., LIU, Y. H., ZHANG, H. B., LIAO, Y. J., ZHENG, F., ZHU, W., LIU, T. H., BIAN, X. W., GUAN, X. Y., LIN, M. C., ZENG, M. S., ZENG, Y. X., KUNG, H. F. & XIE, D. 2012. EZH2 supports nasopharyngeal carcinoma cell aggressiveness by forming a co-repressor complex with HDAC1/HDAC2 and Snail to inhibit E-cadherin. *Oncogene,* 31**,** 583-594.

TRABOULSI, T., EL EZZY, M., GLEASON, J. L. & MADER, S. 2017. Antiestrogens: structure-activity relationships and use in breast cancer treatment. *Journal of Molecular Endocrinology*. 58**,** R15.

TRISCIUOGLIO, D., GABELLINI, C., DESIDERI, M., ZIPARO, E., ZUPI, G. & DEL BUFALO, D. 2010. Bcl-2 regulates HIF-1alpha protein stabilization in hypoxic melanoma cells via the molecular chaperone HSP90. *PloS one,* 5**,** e11772-e11772.

TSUJI, K., OJIMA, M., OTABE, K., HORIE, M., KOGA, H., SEKIYA, I. & MUNETA, T. 2017. Effects of Different Cell-Detaching Methods on the Viability and Cell Surface Antigen Expression of Synovial Mesenchymal Stem Cells. *Cell transplantation,* 26**,** 1089-1102.

VIEDMA-RODRÍGUEZ, R., BAIZA-GUTMAN, L., SALAMANCA-GÓMEZ, F., DIAZ-ZARAGOZA, M., MARTÍNEZ-HERNÁNDEZ, G., RUIZ ESPARZA-GARRIDO, R., VELÁZQUEZ-FLORES, M. A. & ARENAS-ARANDA, D. 2014. Mechanisms associated with resistance to tamoxifen in estrogen receptor-positive breast cancer (Review). *Oncology Reports,* 32**,** 3-15.

VORREITER, F., RICHTER, S., PETER, M., BAUMANN, S., VON BERGEN, M. & TOMM, J. M. 2016. Comparison and optimization of methods for the simultaneous extraction of DNA, RNA, proteins, and metabolites. *Analytical Biochemistry,* 508**,** 25-33.

WAKS, A. G. & WINER, E. P. 2019. Breast Cancer Treatment: A Review. *JAMA,* 321**,** 288-300.

WANAMI, L. S., CHEN, H.-Y., PEIRÓ, S., GARCÍA DE HERREROS, A. & BACHELDER, R. E. 2008. Vascular endothelial growth factor-A stimulates Snail expression in breast tumor cells: Implications for tumor progression. *Experimental Cell Research,* 314**,** 2448-2453.

WANG, G., CAO, R., WANG, Y., QIAN, G., DAN, H. C., JIANG, W., JU, L., WU, M., XIAO, Y. & WANG, X. 2016. Simvastatin induces cell cycle arrest and inhibits proliferation of bladder cancer cells via PPARγ signalling pathway. *Scientific Reports,* 6**,** 35783.

WANG, S., HUANG, X., LEE, C. K. & LIU, B. 2010. Elevated expression of erbB3 confers paclitaxel resistance in erbB2-overexpressing breast cancer cells via upregulation of Survivin. *Oncogene,* 29**,** 4225-4236.

WANG, X., ZHANG, H. & CHEN, X. 2019. Drug resistance and combating drug resistance in cancer. *Cancer Drug Resistance,* 2**,** 141-160.

WANG, Z., WADE, P., MANDELL, K. J., AKYILDIZ, A., PARKOS, C. A., MRSNY, R. J. & NUSRAT, A. 2007. Raf 1 represses expression of the tight junction protein occludin via activation of the zinc-finger transcription factor slug. *Oncogene,* 26**,** 1222-1230.

WARD, N. C., WATTS, G. F. & ECKEL, R. H. 2019. Statin Toxicity. 124**,** 328-350.

WESSELING, M., SAKKERS, T. R., DE JAGER, S. C. A., PASTERKAMP, G. & GOUMANS, M. J. 2018. The morphological and molecular mechanisms of epithelial/endothelial-to-mesenchymal transition and its involvement in atherosclerosis. *Vascular Pharmacology,* 106**,** 1-8.

WU, F., ZHANG, Y., SUN, B., MCMAHON, A. P. & WANG, Y. 2017. Hedgehog Signaling: From Basic Biology to Cancer Therapy. *Cell Chemical Biology,* 24**,** 252-280.

WU, Y., ZHAO, Y., HE, X., HE, Z., WANG, T., WAN, L., CHEN, L. & YAN, N. 2020. Hydroxypropyl-β-cyclodextrin attenuates the epithelial-to-mesenchymal transition via endoplasmic reticulum stress in MDA-MB-231 breast cancer cells. *Molecular Medicine Reports,* 21**,** 249-257.

WU, Z.-Q., LI, X.-Y., HU, C. Y., FORD, M., KLEER, C. G. & WEISS, S. J. 2012. Canonical Wnt signaling regulates Slug activity and links epithelial–mesenchymal transition with epigenetic Breast Cancer 1, Early Onset (BRCA1) repression. *Proceedings of the National Academy of Sciences,* 109**,** 16654.

XIE, F., LIU, J., LI, C. & ZHAO, Y. 2016. Simvastatin blocks TGF-β1-induced epithelial-mesenchymal transition in human prostate cancer cells. *Oncology letters,* 11**,** 3377-3383.

XU, W., ZHOU, W., CHENG, M., WANG, J., LIU, Z., HE, S., LUO, X., HUANG, W., CHEN, T., YAN, W. & XIAO, J. 2017. Hypoxia activates Wnt/β-catenin signaling by regulating the expression of BCL9 in human hepatocellular carcinoma. *Scientific reports,* 7**,** 40446-40446.

YANG, A. D., CAMP, E. R., FAN, F., SHEN, L., GRAY, M. J., LIU, W., SOMCIO, R., BAUER, T. W., WU, Y., HICKLIN, D. J. & ELLIS, L. M. 2006. Vascular Endothelial Growth Factor

Receptor-1 Activation Mediates Epithelial to Mesenchymal Transition in Human Pancreatic Carcinoma Cells. *Cancer Research,*66**,** 46-51.

YANG, F., SUN, L., LI, Q., HAN, X., LEI, L., ZHANG, H. & SHANG, Y. 2012. SET8 promotes epithelial–mesenchymal transition and confers TWIST dual transcriptional activities. *The EMBO journal,* 31**,** 110-123.

YANG, J., MANI, S. A., DONAHER, J. L., RAMASWAMY, S., ITZYKSON, R. A., COME, C., SAVAGNER, P., GITELMAN, I., RICHARDSON, A. & WEINBERG, R. A. 2004. Twist, a Master Regulator of Morphogenesis, Plays an Essential Role in Tumor Metastasis. *Cell,* 117**,** 927-939.

YANG, M.-H., WU, M.-Z., CHIOU, S.-H., CHEN, P.-M., CHANG, S.-Y., LIU, C.-J., TENG, S.-C. & WU, K.-J. 2008. Direct regulation of TWIST by HIF-1α promotes metastasis. *Nature Cell Biology,* 10**,** 295-305.

YANG, S.-W., ZHANG, Z.-G., HAO, Y.-X., ZHAO, Y.-L., QIAN, F., SHI, Y., LI, P.-A., LIU, C.-Y. & YU, P.-W. 2017. HIF-1α induces the epithelial-mesenchymal transition in gastric cancer stem cells through the Snail pathway. *Oncotarget,* 8**,** 9535-9545.

YANG, T., CHEN, M. & SUN, T. 2013. Simvastatin Attenuates TGF-β1-Induced Epithelial-Mesenchymal Transition in Human Alveolar Epithelial Cells. *Cellular Physiology and Biochemistry,* 31**,** 863-874.

YEUNG, K. T. & YANG, J. 2017. Epithelial-mesenchymal transition in tumor metastasis. *Molecular Oncology,* 11**,** 28-39.

YOKOO, M., KUBOTA, Y., MOTOYAMA, K., HIGASHI, T., TANIYOSHI, M., TOKUMARU, H., NISHIYAMA, R., TABE, Y., MOCHINAGA, S., SATO, A., SUEOKA-ARAGANE, N., SUEOKA, E., ARIMA, H., IRIE, T. & KIMURA, S. 2015. 2-Hydroxypropyl-β-Cyclodextrin Acts as a Novel Anticancer Agent. *PloS one,* 10**,** e0141946-e0141946.

YOON, H., KIM, M., JANG, K., SHIN, M., BESSER, A., XIAO, X., ZHAO, D., WANDER, S. A., BRIEGEL, K., MOREY, L., MINN, A. & SLINGERLAND, J. M. 2019. p27 transcriptionally coregulates cJun to drive programs of tumor progression. *Proceedings of the National Academy of Science of the United States of America,*116**,** 7005-7014.

YU, W., YANG, L., LI, T. & ZHANG, Y. 2019. Cadherin Signaling in Cancer: Its Functions and Role as a Therapeutic Target. *Frontiers in Oncology,* 9.

YUE, S., LI, J., LEE, S.-Y., LEE, HYEON J., SHAO, T., SONG, B., CHENG, L., MASTERSON, TIMOTHY A., LIU, X., RATLIFF, TIMOTHY L. & CHENG, J.-X. 2014. Cholesteryl Ester Accumulation Induced by PTEN Loss and PI3K/AKT Activation Underlies Human Prostate Cancer Aggressiveness. *Cell Metabolism,* 19**,** 393-406.

ZALBA, S. & TEN HAGEN, T. L. M. 2017. Cell membrane modulation as adjuvant in cancer therapy. *Cancer Treatment Reviews* 52**,** 48–57.

ZHANG, B., LI, Y.-L., ZHAO, J.-L., ZHEN, O., YU, C., YANG, B.-H. & YU, X.-R. 2018a. Hypoxia-inducible factor-1 promotes cancer progression through activating AKT/Cyclin D1 signaling pathway in osteosarcoma. *Biomedicine & Pharmacotherapy,* 105**,** 1-9.

ZHANG, C., LIU, J., WANG, J., ZHANG, T., XU, D., HU, W. & FENG, Z. 2021. The Interplay Between Tumor Suppressor p53 and Hypoxia Signaling Pathways in Cancer. *Frontiers in Cell and Devlelopmental Biology,* 9.

ZHANG, J., LI, Q., WU, Y., WANG, D., XU, L., ZHANG, Y., WANG, S., WANG, T., LIU, F., ZAKY, M. Y., HOU, S., LIU, S., ZOU, K., LEI, H., ZOU, L., ZHANG, Y. & LIU, H. 2019. Cholesterol content in cell membrane maintains surface levels of ErbB2 and confers a therapeutic vulnerability in ErbB2-positive breast cancer. *Cell Communication and Signaling : CCS,* 17**,** 15-15.

ZHANG, J., TIAN, X.-J. & XING, J. 2016. Signal Transduction Pathways of EMT Induced by TGF-β, SHH, and WNT and Their Crosstalks. *Journal of Clinical Medicine,*5**,** 41.

ZHANG, L., HUANG, G., LI, X., ZHANG, Y., JIANG, Y., SHEN, J., LIU, J., WANG, Q., ZHU, J., FENG, X., DONG, J. & QIAN, C. 2013a. Hypoxia induces epithelial-mesenchymal transition via activation of SNAI1 by hypoxia-inducible factor -1α in hepatocellular carcinoma. *BMC Cancer,* 13**,** 108.

ZHANG, M., GAO, C.-E., CHEN, W.-L., TANG, Y.-Y., NIE, J.-Y., SHEN, L.-D., MA, X. & CHEN, D.-D. 2018b. Opposite response to hypoxia by breast cancer cells between cell proliferation and cell migration: A clue from microRNA expression profile. *Oncology letters,* 15**,** 2771-2780.

ZHANG, M., LEI, D., PENG, B., YANG, M., ZHANG, L., CHARLES, M. A., RYE, K.-A., KRAUSS, R. M., JOHNS, D. G. & REN, G. 2017a. Assessing the mechanisms of cholesteryl ester transfer protein inhibitors. *Biochimica et Biophysica Acta (BBA) - Molecular and Cell Biology of Lipids,* 1862**,** 1606-1617.

ZHANG, N., HONG, B., ZHOU, C., DU, X., CHEN, S., DENG, X., DUOERKUN, S., LI, Q., YANG, Y. & GONG, K. 2017b. Cobalt Chloride-induced Hypoxia Induces Epithelial-mesenchymal Transition in Renal Carcinoma Cell Lines. *Annals of Clinical and Laboratory Science,*47**,** 40-46.

ZHANG, P., SUN, Y. & MA, L. 2015a. ZEB1: at the crossroads of epithelial-mesenchymal transition, metastasis and therapy resistance. *Cell cycle (Georgetown, Tex.),* 14**,** 481-487.

ZHANG, Q., BAI, X., CHEN, W., MA, T., HU, Q., LIANG, C., XIE, S., CHEN, C., HU, L., XU, S. & LIANG, T. 2013b. Wnt/β-catenin signaling enhances hypoxia-induced epithelial–mesenchymal transition in hepatocellular carcinoma via crosstalk with hif-1α signaling. *Carcinogenesis,* 34**,** 962-973.

ZHANG, W., SHI, X., PENG, Y., WU, M., ZHANG, P., XIE, R., WU, Y., YAN, Q., LIU, S. & WANG, J. 2015b. HIF-1α Promotes Epithelial-Mesenchymal Transition and Metastasis through Direct Regulation of ZEB1 in Colorectal Cancer. *PLOS ONE,* 10**,** e0129603.

ZHANG, Y. & WEINBERG, R. A. 2018. Epithelial-to-mesenchymal transition in cancer: complexity and opportunities. *Frontiers of Medicine,* 12**,** 361-373.

ZHAO, D., BESSER, A. H., WANDER, S. A., SUN, J., ZHOU, W., WANG, B., INCE, T., DURANTE, M. A., GUO, W., MILLS, G., THEODORESCU, D. & SLINGERLAND, J. 2015. Cytoplasmic p27 promotes epithelial–mesenchymal transition and tumor metastasis via STAT3-mediated Twist1 upregulation. *Oncogene,* 34**,** 5447-5459.

ZHAO, J.-H., LUO, Y., JIANG, Y.-G., HE, D.-L. & WU, C.-T. 2011. Knockdown of β-Catenin Through shRNA Cause a Reversal of EMT and Metastatic Phenotypes Induced by HIF-1α. *Cancer Investigation,* 29**,** 377-382.

ZHAO, Z., HAO, D., WANG, L., LI, J., MENG, Y., LI, P., WANG, Y., ZHANG, C., ZHOU, H., GARDNER, K. & DI, L.-J. 2019. CtBP promotes metastasis of breast cancer through repressing cholesterol and activating TGF-β signaling. *Oncogene,* 38**,** 2076-2091.

ZHONG, Z. & VIRSHUP, D. M. 2020. Wnt Signaling and Drug Resistance in Cancer. *Molecular Pharmacology,* 97**,** 72-89.

ZIDOVETZKI, R. & LEVITAN, I. 2007. Use of cyclodextrins to manipulate plasma membrane cholesterol content: Evidence, misconceptions and control strategies. *Biochimica et Biophysica Acta (BBA) - Biomembranes,* 1768**,** 1311-1324.

ZIMNA, A. & KURPISZ, M. 2015. Hypoxia-Inducible Factor-1 in Physiological and Pathophysiological Angiogenesis: Applications and Therapies. *BioMed Research International,* 2015**,** 549412.

ZUO, W. & CHEN, Y.-G. 2009. Specific activation of mitogen-activated protein kinase by transforming growth factor-beta receptors in lipid rafts is required for epithelial cell plasticity. *Molecular biology of the cell,* 20**,** 1020-1029.

ZWAANS, B. M. M. & LOMBARD, D. B. 2014. Interplay between sirtuins, MYC and hypoxia-inducible factor in cancer-associated metabolic reprogramming. *Disease models & mechanisms,* 7**,** 1023-1032.